



## A total evidence analysis of the phylogeny of hatchet-faced treefrogs (Anura: Hylidae: *Sphaenorhynchus*)

Katyscia Araujo-Vieira<sup>a</sup>, Boris L. Blotto<sup>a,b</sup>, Ulisses Caramaschi<sup>c</sup>,  
Celio F. B. Haddad<sup>d</sup>, Julián Faivovich<sup>a,e,\*</sup>  and Taran Grant<sup>b,\*</sup> 

<sup>a</sup>División Herpetología, Museo Argentino de Ciencias Naturales “Bernardino Rivadavia”-CONICET, Ángel Gallardo 470, Buenos Aires, C1405DJR, Argentina; <sup>b</sup>Departamento de Zoologia, Instituto de Biociências, Universidade de São Paulo, São Paulo, São Paulo, 05508-090, Brazil;

<sup>c</sup>Departamento de Vertebrados, Museu Nacional, Universidade Federal do Rio de Janeiro, Quinta da Boa Vista, São Cristóvão, Rio de Janeiro, Rio de Janeiro, 20940-040, Brazil; <sup>d</sup>Departamento de Zoologia and Centro de Aquicultura (CAUNESP), Instituto de Biociências, Universidade Estadual Paulista, Avenida 24A, 1515, Bela Vista, Rio Claro, São Paulo, 13506-900, Brazil; <sup>e</sup>Departamento de Biodiversidad y Biología Experimental, Facultad de Ciencias Exactas y Naturales, Universidad de Buenos Aires, Buenos Aires, Argentina

Accepted 14 November 2018

### Abstract

The Neotropical hylid genus *Sphaenorhynchus* includes 15 species of small, greenish treefrogs widespread in the Amazon and Orinoco basins, and in the Atlantic Forest of Brazil. Although some studies have addressed the phylogenetic relationships of the genus with other hylids using a few exemplar species, its internal relationships remain poorly understood. In order to test its monophyly and the relationships among its species, we performed a total evidence phylogenetic analysis of sequences of three mitochondrial and three nuclear genes, and 193 phenotypic characters from all species of *Sphaenorhynchus*. Our results support the monophyly of *Sphaenorhynchus* with molecular and phenotypic evidence, with *S. pauloalvini* as the earliest diverging taxon, followed by *S. carneus*, as the sister taxon of all remaining species of the genus. We recognize three species groups in *Sphaenorhynchus* (the *S. lacteus*, *S. planicola* and *S. platycephalus* groups), to facilitate its taxonomic study; only three species (*S. carneus*, *S. pauloalvini* and *S. prasinus*) remain unassigned to any group. Sequence data were not available for only two species (*S. bromelicola* and *S. palustris*) for which we scored phenotypic data; wildcard behaviour was detected only in *S. bromelicola* nested inside the *S. platycephalus* group. On the basis of the resulting phylogenetic hypothesis, we discuss the evolution of oviposition site and a number of phenotypic characters that could be associated with heterochronic events in the evolutionary history of this group.

© The Willi Hennig Society 2018.

### Introduction

Knowledge on the phylogenetic relationships of hylid frogs has increased qualitatively in the last 13 years. There are densely sampled hypotheses for several groups at different taxonomic levels (e.g. Phyllomedusinae, Cophomantini, Hylini, *Osteocephalus*, *Pseudis*; Faivovich et al., 2010; Jungfer et al., 2013; Pinheiro et al., 2019; Faivovich et al., 2018). Nevertheless, the internal relationships of the South American

hatchet-faced treefrogs, *Sphaenorhynchus*, remain poorly known.

*Sphaenorhynchus* comprises 15 species of small, greenish treefrogs. Three species are widespread in the Amazon and Orinoco basins, including *S. carneus*, *S. dorisae* and *S. lacteus*, the last species also occurring in Trinidad (Kenny, 1969; as *Hyla orophila*) and northeastern Brazil (states of Maranhão and Piauí; La Marca et al., 2010; Caramaschi et al., 2009; Benício et al., 2011). The other 12 species occur in the Atlantic Forest of southeastern Brazil, from Pernambuco in the north to northern Rio Grande do Sul in the south, including *S. botocudo*, *S. bromelicola*, *S. cammaeus*,

\*Corresponding authors.

E-mail address: julian@macn.gov.ar; taran.grant@ib.usp.br

*S. canga*, *S. caramaschii*, *S. mirim*, *S. palustris*, *S. pauloalvini*, *S. planicola*, *S. platycephalus*, *S. prasinus* and *S. surdus*. Adults of *Sphaenorhynchus* generally inhabit ponds in open areas and forest edges where males vocalize while perched on the floating vegetation or partially submerged in the water, or more rarely perched on bushes (e.g. Lutz and Lutz, 1938; Bokermann, 1973; Cruz and Peixoto, 1980; C.F.B. Haddad, pers. obs.). *Sphaenorhynchus dorisae*, *S. lacteus*, *S. surdus* and *S. caramaschii* attach their eggs to submerged vegetation (Rodríguez and Duellman, 1994; Toledo et al., 2007), whereas *S. pauloalvini* lays clutches on leaves overhanging water (Bokermann, 1973). *Sphaenorhynchus carneus* has been reported to lay clutches on leaves overhanging water (Bokermann, 1973) or in the water (Crump, 1974; W. Hödl, pers. comm.).

Most tadpoles of *Sphaenorhynchus* swim amid floating vegetation near the water surface, where they are associated with roots and under films of algae (*S. caramaschii*, *S. carneus*, *S. dorisae*, *S. lacteus* and *S. planicola*; Cruz, 1973; Suárez-Mayorga and Lynch, 2001; Araujo-Vieira et al., 2015a). However, larvae of *S. prasinus* and *S. surdus* inhabit darker and deeper places, amidst aquatic vegetation at the bottom of the water bodies (Bokermann, 1973; Caramaschi, 2010).

The remarkable occurrence of sexually mature individuals with larval somatic morphology, such as a long tail, has been reported in *S. bromelicola*, *S. botocudo*, *S. mirim* and *S. palustris* (Bokermann, 1974; Haddad and Prado, 2005; Caramaschi et al., 2009). Larvae of *S. bromelicola* close to metamorphosis with mature oocytes, specimens in metamorphosis and newly metamorphosed males emitting calls and with testicles in spermatogenesis were reported by Bokermann (1974), who explained this shift in the timing of sexual maturity as the result of both accelerated sexual maturation and delayed metamorphosis.

The monophyly of *Sphaenorhynchus* has been universally supported in recent analyses (Faivovich et al., 2005; Wiens et al., 2006, 2010; Pyron and Wiens, 2011; Pyron, 2014; Duellman et al., 2016), and several putative morphological synapomorphies have been suggested for the genus. Duellman and Wiens (1992) studied six species (*S. bromelicola*, *S. carneus*, *S. dorisae*, *S. lacteus*, *S. platycephalus* and *S. planicola*) and suggested 11 putative synapomorphies (mainly osteological), such as the posterior ramus of pterygoid absent and the postorbital process of maxilla reduced, not in contact with quadratojugal. Faivovich et al. (2005) also suggested as putative synapomorphies for *Sphaenorhynchus* the differentiation of the m. *intermandibularis* into a small apical supplementary element (see Tyler, 1971), the extreme development of the m. *interhyoideus*, the deposition of iridophores on

the parietal peritoneum, and myrmecophagous adult diet. Subsequently, Araujo-Vieira et al. (2015a), based on Faivovich et al.'s (2005) comments, proposed the nostril with fleshy flanges and anteriorly directed as additional putative synapomorphies of *Sphaenorhynchus*.

In terms of the position of *Sphaenorhynchus* in Hyliinae, Faivovich et al. (2005) obtained *Sphaenorhynchus* as sister taxon of *Xenohyla* + *Dendropsophus*, with this clade being the sister taxon of *Lysapsus*, *Pseudis*, *Scarthyla* and *Scinax*, together forming the tribe Dendropsophini. Wiens et al. (2006, 2010) obtained *Sphaenorhynchus* as the sister taxon of *Scinax*—with poor support—with this clade being the sister taxon of *Dendropsophus*, *Lysapsus*, *Pseudis*, *Scarthyla* and *Xenohyla*, therefore recovering—again with poor support—the monophyly of Dendropsophini as done by Faivovich et al. (2005). Pyron and Wiens (2011), Pyron (2014) and Duellman et al. (2016) also obtained *Sphaenorhynchus* as the sister taxon of *Scinax* (sensu Faivovich, 2002; Faivovich et al., 2005), with poor support (bootstrap with raxML < 50%; Shimodaira–Hasegawa < 64%), but more distantly related to *Dendropsophus*, *Lysapsus*, *Pseudis*, *Scarthyla* and *Xenohyla*, implying the paraphyly of Dendropsophini.

In a recent reanalysis of hylid GenBank sequences, Duellman et al. (2016), restricted Dendropsophini (as Dendropsophinae) to *Dendropsophus* + *Xenohyla*, resurrected Pseudinae Fitzinger 1843 for *Scarthyla*, *Lysapsus* and *Pseudis*, and erected the new subfamily Scinaxinae for *Scinax* + *Sphaenorhynchus*, a poorly supported clade with 49% bootstrap support in their analysis. In a recent molecular phylogenetic analysis of Hylini, Faivovich et al. (2018) discussed the problem of recognizing a subfamily (Scinaxinae) for a clade with unstable relationships and chose to restrict Scinaxini to *Scinax*, erect the tribe Sphaenorhynchini for *Sphaenorhynchus*, and recognize Dendropsophini for *Dendropsophus* + *Xenohyla*, and Pseudini for *Scarthyla*, *Lysapsus* and *Pseudis*.

Although previous studies have identified putative synapomorphies that support the monophyly of *Sphaenorhynchus*, the taxonomic distribution of these character-states is largely unknown. To date, analyses have included at most three species (*S. dorisae*, *S. lacteus* and *S. platycephalus*; the latter as *S. orophilus*; see Araujo-Vieira et al., 2018), and the relationships of the remaining species have not been studied in a quantitative phylogenetic framework. Given these limitations, in this paper we present a total evidence phylogenetic analysis of *Sphaenorhynchus*, with the goals of (i) testing the monophyly of *Sphaenorhynchus*; (ii) testing the relationships between the species of the genus; and (iii) studying the evolution of some morphological and reproductive biology characters in light of the resulting phylogenetic hypothesis.

## Materials and methods

### Taxon sampling

All known species of *Sphaenorhynchus* were included in the analysis. In order to test the monophyly of *Sphaenorhynchus*, outgroups were selected on the basis of the phylogenetic hypotheses of Faivovich et al. (2005), Wiens et al. (2010), Pyron and Wiens (2011), Pyron (2014) and Duellman et al. (2016), constrained by two criteria: (i) availability of tissues or sequences on GenBank and (ii) availability of specimens for morphological studies. Specifically, our outgroup sample includes *Dendropsophus elegans* (*D. leucophyllatus* group), *D. microps* (*D. parviceps* group), *D. minutus* (*D. minutus* group), *D. sanborni* (*D. microcephalus* group), *Pseudis minuta*, *Scarthyla goinorum*, and *Scinax alter* and *Sci. fuscovarius* (*Sci. ruber* clade), *Sci. catharinae* and *Sci. perpusillus* (*Sci. catharinae* clade), and *Xenohyla truncata*; the trees were rooted with *Phyllodytes luteolus*. Supplemental information Appendices S1 and S2 include a complete list of studied specimens. Institutional collection abbreviations follow Sabaj (2016).

### Molecular character sampling

The mitochondrial DNA sequences used for the phylogenetic analyses include portions of *cytochrome b* (*cytb*, 385 bp), the ribosomal genes *12S*, *tRNA<sup>Val</sup>* and *16S* (~2450 bp), and a fragment including the complete downstream section of the *16S* gene, the intervening *tRNA<sup>Leu</sup>*, *NADH dehydrogenase subunit 1* and *tRNA<sup>Ile</sup>* (~1250 bp), giving a total of ~4085 bp of the mitochondrial genome. The nuclear protein-coding gene sequences include portions of recombination activating gene 1 (*RAG1*, 428 bp), rhodopsin (316 bp) and tyrosinase (532 bp) comprising 1276 bp of the nuclear genome. We complemented our new data with DNA sequences from Faivovich et al. (2005) and Wiens et al. (2006) available on GenBank (see Appendix S1). The final dataset includes ≈ 217 800 bp, with 717–5440 bp ( $\bar{x}$  4033 bp) per terminal.

Tissue samples were unavailable for *Sphaenorhynchus bromelicola* and *S. palustris*. The former is known only from the type locality “Fazenda Santo Onofre, 10 km à l’est de Maracás, Bahia, Brasil” and has not been collected since late 1965 (Bokermann, 1966, 1974). The latter was recently reported from Mucuri, State of Bahia, Brazil, 520 km SSE from the type locality (Lacerda and Moura, 2013); however, sequences of two of these specimens are identical to those of topotypes of *S. botocudo*, and we have been unable to differentiate the adult vouchers from topotypes of this species. As such, we tentatively consider the specimens referred to *S. palustris* by Lacerda and

Moura (2013) to be *S. botocudo* (see Appendix S3 for further discussion).

### Laboratory protocols

Whole cellular DNA was extracted from frozen and ethanol-preserved tissues (liver or muscle) using either phenol-chloroform extraction methods or the Qiagen DNeasy isolation kit. Primers used in PCR amplification and their citations are given in Appendix S4. PCR amplification was carried out in 25- $\mu$ L reactions using 0.2  $\mu$ L Taq (Fermentas). The PCR protocol consisted of an initial denaturation step of 3 min at 94 °C, 35 (for mitochondrial genes) or 45 (for nuclear genes) cycles of 30 s at 94 °C, 40 s at 48–62 °C, and 30–60 s at 72 °C, and a final extension step of 10–15 min at 72 °C. The PCR-amplified products were cleaned with 0.5  $\mu$ L of Exonuclease plus 1  $\mu$ L of alkaline phosphatase per 20  $\mu$ L of reaction. Sequencing was done on an automatic sequencer ABI 3730XL (Applied Biosystems, Waltham, MA, USA) in both directions to check for potential errors and polymorphisms. The chromatograms obtained from the automated sequencer were read and contigs made using the sequence editing software Sequencher v.5.3 (Gene Codes, Ann Arbor, MI, USA) and edited the complete sequences with BioEdit (Hall, 1999). GenBank accession numbers are listed in Appendix S1.

### Phenotypic character sampling

The terminology employed for external morphology follows Duellman (2001); Luna et al. (2018) for nuptial pad morphology; Trueb (1973, 1993) for cranial and postcranial osteology; Fabrezi (1992, 1993) for carpal and tarsal osteology; Trewavas (1933) for laryngeal morphology; Jurgens (1971) for nasal cartilage morphology; Burton (1996, 1998, 2004) and Faivovich (2002) for hand and foot myology; Tyler (1971), Trewavas (1933) and Horton (1982) for submandibular myology; and Altig and McDiarmid (1999) for external larval morphology. The states of characters 72, 74 and 76 for *Scinax catharinae* and *Sci. fuscovarius* were defined following Faivovich (2002, characters 11, 13 and 18). Osteological characters were coded from specimens that were cleared and double-stained with alcian blue and alizarin red (Taylor and Van Dyke, 1985). Larval characters were coded based on information taken from literature when larvae were unavailable for examination. When possible, one specimen of each sex from the type locality or close to it was used to code osteological and myological characters. However, in many cases only one specimen was available for these studies. Only males were examined to code characters of laryngeal morphology due to unavailability of females for most species and some females being

poorly stained with alcian blue. The final phenotypic dataset included 193 characters, 65 multistate, of which 41 were considered additive (see Appendices S5 and S6).

### *Phylogenetic analyses*

*Treatment of molecular and phenotypic characters.* The ribosomal genes (*12S–16S*) and the protein-coding gene (*ND1*) were first broken into contiguous fragments of putative homology (Grant et al., 2006; Wheeler et al., 2006). The fragments were separated by inserting pound signs (#) exclusively in highly conserved regions identified by visualizing a preliminary MAFFT v.7 (Kato and Standley, 2013; default parameters) similarity alignments using BioEdit (Hall, 1999).

Kluge and Grant (2006) argued that by globally minimizing the transformation events required to explain the variation of the character-states of the terminals studied, equally weighted parsimony analysis maximizes explanatory power. Therefore, in this study the molecular and phenotypic characters were treated under equal weights. The relation used to treat indels (insertions and deletions) and all substitutions was 1:1:1 (transition: transversion: unit indels). Matrix edition was done with Mesquite v.3.03 (Maddison and Maddison, 2015).

For total evidence analysis, we treated every specimen sequenced as a separate terminal for each ingroup species. Then, we duplicated the morphological entries for the species for each molecular terminal—that is, each conspecific terminal was given identical entries in the phenotypic matrix, following the arguments of Grant et al. (2006). This process was not extrapolated to the outgroup species; for these, we fused putatively conspecific specimens into a single polymorphic terminal—that is, we combined the morphological entries and different loci from different conspecific specimens into a single terminal (for outgroup sequences, see Appendix S1). Loci not sequenced for particular terminals due to primer failure or unavailability on GenBank were treated as missing data. Multistate characters were considered either as additive or nonadditive; additive characters were coded according to Hawkins et al. (1997) and Strong and Lipscomb (1999). Species-level phenotypic polymorphisms were coded as ambiguities.

*Choice of phylogenetic method.* The optimality criterion used to identify the preferred phylogenetic hypothesis was parsimony, a nonstatistical, nonparametric, evidentially conservative approach to scientific inference that maximizes explanatory power by minimizing both the quantity of evolutionary events and assumptions about the process of character evolution that are

required to explain the evidence (Kluge and Grant, 2006; Grant and Kluge, 2009; for further discussion see Padiál et al., 2014).

On the basis of the arguments of Padiál et al. (2014; see also Kluge and Grant, 2006; Grant and Kluge, 2009), we employed direct optimization (e.g. Sankoff, 1975; Wheeler, 1996; Varón and Wheeler, 2012, 2013) in the program POY v.5.1.1 (Wheeler et al., 2015), which tests hypotheses of nucleotide homology dynamically by optimizing unaligned DNA sequences directly onto alternative topologies (Kluge and Grant, 2006; Wheeler et al., 2006; Grant and Kluge, 2009) while simultaneously optimizing pre-aligned transformation series (e.g. morphology) as standard matrices.

*Data analysis.* We consider the results of the total evidence analysis to be the phylogenetic hypothesis that best explains the evidence, because the analysis of all available evidence maximizes explanatory power (Kluge, 1989; Grant and Kluge, 2003), and all discussion of character evolution and phenotypic synapomorphies is based on the results of total evidence analysis. Nevertheless, to test the effects of including terminals lacking an entire data partition (i.e. terminals scored only for molecular or phenotypic data), we performed independent analyses of three datasets: (i) molecular data only; (ii) phenotypic data only; and (iii) total evidence (molecular and phenotypic data).

The molecular-only dataset (MD) included DNA sequences for 53 terminals (12 outgroup and 41 ingroup; Appendix S1). The phenotypic dataset (PD) included 27 terminals (12 outgroup and 15 ingroup, see Appendices S2 and S5). The total evidence analysis (TE) included 55 terminals, including all 53 MD terminals combined with phenotypic data as described above, plus two PD terminals (*Sphaenorhynchus bromelicola* and *S. palustris*) for which DNA sequences were not available.

The PD matrix was analysed using TNT v.1.5 (Goloboff et al., 2008; Goloboff and Catalano, 2016; equal costs for all transformations). Shortest trees were found by performing either 1000 random addition sequences (RAS), retaining 10 trees per replicate, and then submitting them to a round of tree bisection and reconnection (TBR) branch swapping, or a driven search with the option “New Technology Search.” This search option includes the algorithms Ratchet (Nixon, 1999), Tree Drifting (Goloboff, 1999), Sectorial Searches (Goloboff, 1999) and Tree Fusing (Goloboff, 1999). For this driven search, we used the default options for these algorithms, and the maximum-parsimony trees were requested to be hit 1000 times. The resulting trees were submitted to a round of TBR branch swapping. All searches were done under



the collapsing option “minimum length”, which collapses every node whose minimum length is 0.

Total evidence and molecular-only analyses comprised several steps. First, using the standard direct optimization algorithm (Wheeler, 1996), we ran two 2-h searches using 768 CPUs (=3072 CPU-hours) using the command “search”, which implements a driven search composed of random addition sequence Wagner builds, Subtree Pruning and Regrafting (SPR) and Tree Bisection and Reconnection (TBR), branch swapping (RAS + swapping; Goloboff, 1996), Parsimony Ratcheting (Nixon, 1999) and Tree Fusing (Goloboff, 1999), and alternates between the specified optimization algorithm (standard direct optimization in this case) and static-approximation, which searches using the implied alignment of the best tree in memory. Given the high time complexity of direct optimization (Varón and Wheeler, 2012), a common procedure to accelerate analyses is to treat equal-length sequences as prealigned, static-homology matrices (e.g. Faivovich et al., 2010). Insofar as the resulting speed-up enables a greater tree-space to be explored in a given amount of time, this can result in more parsimonious trees. As such, we analysed the total evidence and molecular-only datasets with *cytb* and nuclear genes treated as both prealigned and unaligned sequences.

Second, we swapped the best trees from the first analyses using the approximate iterative pass algorithm (Wheeler, 2003a) and generated the matrix version of the alignment (i.e. implied alignment; Wheeler, 2003b). Third, to verify the length reported by POY and search for better and/or additional trees given the implied alignment, we performed driven search of the implied alignment in TNT v.1.5 (Goloboff et al., 2008; Goloboff and Catalano, 2016; equal costs for all transformations, gaps treated as fifth state), stopping when the stable consensus was reached 10 times (tnt command: xmult = level 5 chklevel 5 consense 10).

Once we identified the most parsimonious trees (MPTs), we estimated clade support (Grant and Kluge, 2008) for the clades present in the optimal trees by calculating Goodman–Bremer values (GB; Goodman et al., 1982; Bremer, 1988; Grant and Kluge, 2008) in TNT v.1.5 (Goloboff et al., 2008; Goloboff and Catalano, 2016) using the implied alignment and the parameters specified in the bremer.run macro (for details see Goloboff et al., 2008; macro available at <http://www.lillo.org.ar/phylogeny/tnt/>). Although shorter suboptimal trees might be found by calculating the optimal tree-alignment for each visited topology, the time requirements would be prohibitive unless searches were extremely superficial. Further, Padial et al. (2014) found that using the implied alignment to estimate support overestimates GB values less than when GB is calculated using a MAFFT similarity-alignment. Parsimony jackknife absolute frequencies

(Farris et al., 1996) were calculated in TNT v.1.5 (Goloboff et al., 2008; Goloboff and Catalano, 2016) using a MAFFT similarity-alignment and driven search with the option “New Technology Search” requesting 10 hits with driven searches under search level 15, for a total of 1000 replicates.

All POY analyses were run on Ace, a high-performance computing cluster composed of 12 quad-socket AMD Opteron 6376 16-core 2.3-GHz CPU, 16 MB cache, 6.4 GT/s compute nodes (= 768 cores total), eight with 128 GB RAM DDR3 1600 MHz (16 × 8 GB), two with 256 GB (16 × 16 GB), and two with 512 GB (32 × 16 GB) and QDR 4× InfiniBand (32 GB/s) networking. Results were visualized using Mesquite v.3.03 (Maddison and Maddison, 2015). Lists of phenotypic synapomorphies were generated with YBYRÁ (Machado, 2015) using TNT. YBYRÁ categorizes character transformation events from any source of data given all possible optimization schemes in a set of trees. It proceeds by spawning trees and data matrix to TNT to compile synapomorphies using TNT’s command “apo”. Character-state transformations of a node were considered synapomorphies if they (i) were optimized unambiguously (without arbitrary selection of accelerated, ACCTRAN, or delayed optimization, DELTRAN) and (ii) were shared by all dichotomized most parsimonious trees. YBYRÁ generates colour-coded boxes to indicate if a synapomorphic character-state occurs only in the clade in question (nonhomoplastic) or also occurs in other clades (homoplastic), and if it is shared by all terminals of the clade (unique) or is subsequently transformed into one or more different states within the clade (nonunique).

## Results

### *Phylogenetic analyses*

The driven searches of MD performed 39 598 RAS + TBR, 394 867 rounds of tree fusing, and 22 935 rounds of ratcheting when *cytb* and nuclear loci were treated as prealigned; 33 840 RAS + TBR, 320 271 rounds of tree fusing, and 19 720 rounds of ratcheting when all data were subjected to direct optimization; driven searches of TE 37 769 RAS + TBR, 438 830 rounds of tree fusing, and 23 347 rounds of ratcheting when *cytb* and nuclear loci were treated as prealigned; and 31 889 RAS + TBR, 341 268 rounds of tree fusing and 19 920 rounds of ratcheting when all data subjected to direct optimization. Despite performing 14–22% more tree searching operations, trees were consistently longer when *cytb* and nuclear loci were treated as prealigned than when all DNA sequences were analysed under direct optimization, with the best scores being, respectively, 8804 and 8779

steps for MD, and 9601 and 9577 steps for TE. Swapping the best MD and TE trees under iterative pass further reduced the lengths to 8769 steps for MD and 9557 for TE. Driven searches of the implied alignments in TNT did not result in shorter trees, but they did increase the number of most parsimonious trees to four for MD and nine for TE.

The TE parsimony analysis recovered *Sphaenorhynchus* as a well-supported monophyletic group (jackknife support = 100%; GB = 90), sister taxon of *Dendropsophus* + *Xenohyla* (Fig. 1). *Sphaenorhynchus pauloalvini* is the earliest diverging taxon of the genus, followed by *S. carneus*, sister taxon (jackknife support = 100%; GB = 48) of all remaining species of *Sphaenorhynchus*.

The interspecific relationships are well supported in general (jackknife support > 90%; GB 10–48), although the positions of *S. dorisae* + *S. lacteus* and *S. prasinus* (jackknife support < 50%; GB = 10 and 17) and some internal clades of Atlantic Forest species are poorly supported (jackknife support < 65%; GB = 1–3). The conflicts among topologies are restricted to the internal relationship among *S. bromelicola*, *S. canga*, *S. platycephalus*, *S. surdus*, and *S. botocudo* + *S. palustris* (see Fig. 1). The Amazonian species (*S. carneus*, *S. dorisae* and *S. lacteus*) are not recovered as a monophyletic group; *S. lacteus* and *S. dorisae* form a well-supported clade (jackknife support = 100%; GB = 31) nested among species of the Atlantic Forest.

The PD parsimony analysis resulted in 14 MPTs of 751 steps. Similar to the TE and MD analyses, this result recovered *Sphaenorhynchus* as a well-supported monophyletic taxon, *S. pauloalvini* as the sister taxon of all other species in the genus, and *S. carneus* as the sister taxon of the remaining *Sphaenorhynchus* (see Fig. S1). The interspecific relationships of *Sphaenorhynchus* are similar in the MD and TE analyses, differing solely in that the MD analysis does not include *S. bromelicola* and *S. palustris* (for which there are no DNA sequences; see Fig. S2). Nevertheless, all conflict between the 14 MPTs in the PD analysis is restricted to the internal relationship of the sister group of *S. carneus*, which involves the positions of *S. bromelicola*, *S. cammaeus*, *S. canga* and *S. platycephalus* with respect to the remaining species inside that clade (see Fig. S1). The interspecific relationships are poorly supported in general (jackknife support < 66%; GB = 2–3) in the PD analysis; exceptions are the position of *S. carneus* in relation to the other species, the sister taxon of *S. carneus*, and *S. mirim* + *S. planicola* that are well supported (jackknife support > 85%; GB = 6–7); and *S. botocudo* + *S. palustris* and *S. caramaschii* + *S. surdus*, which are moderately supported (jackknife support = 68% and 73%; GB = 2–3). Also, in contrast with the TE analysis, *S. lacteus* and *S. dorisae* do not form a clade in the PD analysis.

## Discussion

### *Topological effects of including terminals with missing data*

The main concern about including terminals with a large amount of missing data in total evidence analyses is that those terminals might exhibit wildcard behaviour (Nixon and Wheeler, 1992). However, the amount of missing data *per se* is not enough for the terminals to behave as wildcards. Unpredictability of the relationship between amount of evidence and wildcard behaviour was demonstrated by previous studies (e.g. Kearney, 2002; Grant and Kluge, 2003; Kearney and Clark, 2003; Grant et al., 2017).

Our TE dataset included 55 terminals, with two terminals that lack molecular data—*S. bromelicola* and *S. palustris*—and therefore the effect of putative wildcard behaviour focuses on these terminals. The inclusion of *S. bromelicola* in the TE analyses appears to be responsible for the incongruence among primary topologies, because it could be sister taxon of *S. canga*, *S. platycephalus*, or *S. botocudo* + *S. palustris*. This terminal contributed to the corresponding polytomies and low support within the clade including *S. botocudo*, *S. canga*, *S. palustris*, *S. platycephalus* and *S. surdus*. The exclusion of *S. bromelicola* results in moderately to well-supported (jackknife support > 77%) resolved interspecific relationships within this clade in the strict consensus. By contrast, the position of *S. palustris* was consistent among the optimal topologies. This terminal is sister taxon of *S. botocudo* with 76% jackknife support in the TE analysis.

As mentioned before, the interspecific relationships of *Sphaenorhynchus* are similar in the MD and TE analyses, differing solely in that the MD analysis does not include *S. bromelicola* and *S. palustris* (Fig. S2). In the PD analysis, the internal relationships of the sister group of *S. carneus* are different from those in the TE analyses; exceptions are the position of *S. botocudo* as sister taxon of *S. palustris*, and *S. mirim* as sister taxon of *S. planicola*, which are consistent in both analyses. The position of *S. palustris* is moderately supported in the PD analysis (jackknife support = 73%, GB = 3) similar to the TE analysis (jackknife support = 76%, GB = 3). In contrast, the position of *S. bromelicola* is unresolved in both PD and TE analyses, but in the TE analysis it is nested inside a well-supported group (jackknife support = 98%, GB = 11) with all other morphologically similar species of the Atlantic Forest, a relationship that was not supported in the PD analysis (compare Fig. 1 with Fig. S1). Therefore, our results indicate that only one of the terminals with missing data behaved as a wildcard, but its impact on our inference

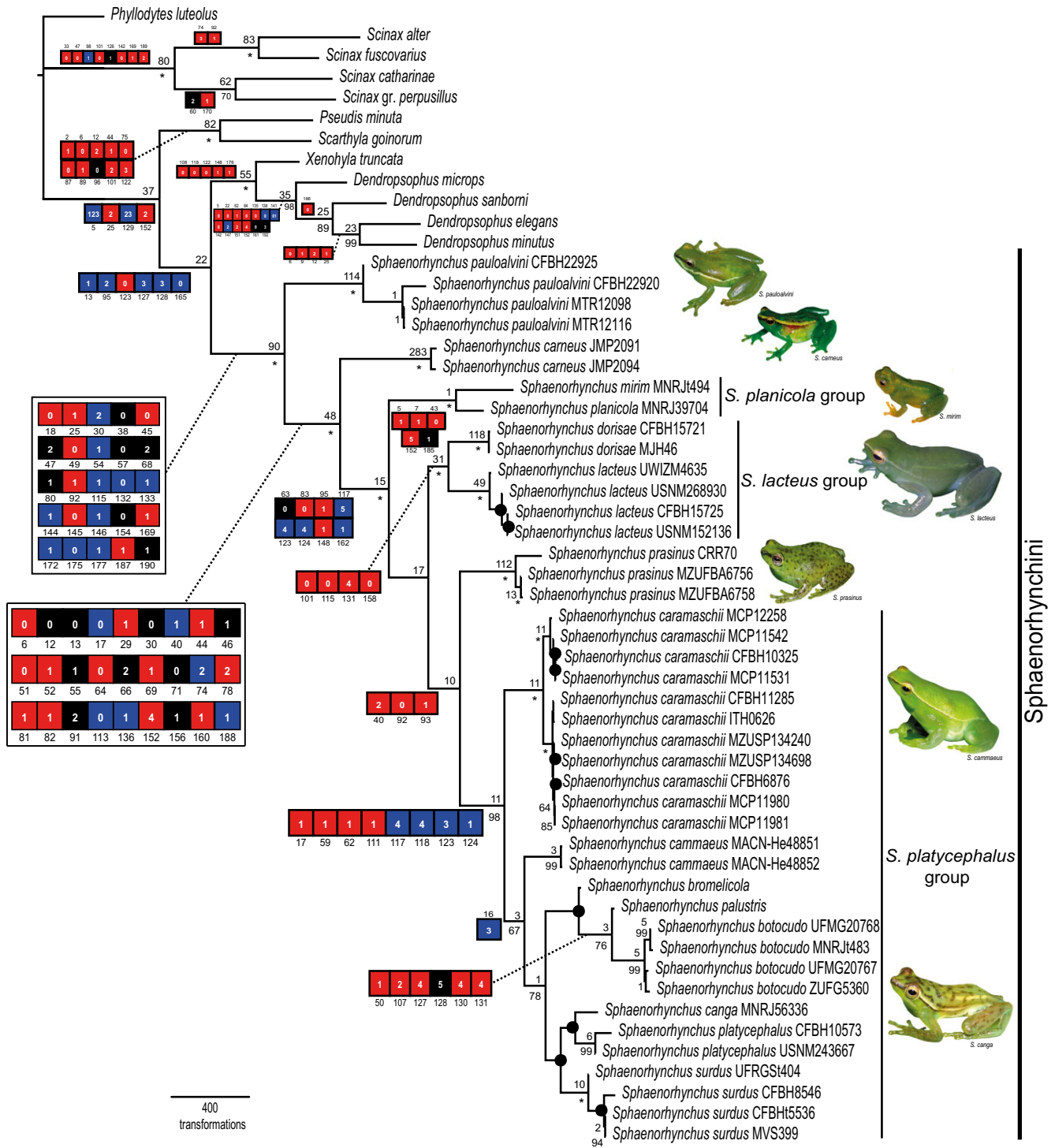


Fig. 1. Phylogenetic relationships of *Sphaenorhynchus* as recovered in one of the nine most parsimonious trees obtained from the analysis of total evidence (TE) with direct optimization (length 9557 steps) under equal weights for all transformations. Black circles indicate nodes that collapse in the strict consensus. Values above nodes are Goodman–Bremer support. Values below nodes are parsimony jackknife support absolute frequencies estimated for the static alignment analysed with parsimony in TNT with gaps as fifth state. An asterisk (\*) indicates groups with 100% for parsimony jackknife frequencies. Nodes lacking values have < 50% jackknife support. Nodes are labelled with unambiguously optimized phenotypic synapomorphies (black square = unique, nonhomoplastic; red square = unique, homoplastic; blue square = nonunique, homoplastic; character number below or above squares; derived character-states inside squares). Photos of I.J. Roberto (*S. cammaeus* and *S. prasinus*), F.S.F. Leite (*S. canga*), C.E. Costa-Campos (*S. carneus*), T. Grant (*S. lacteus*), J.L. Gasparini (*S. mirim*), and M.T. Rodrigues (*S. pauloalvini*).



is restricted to few interspecific relationships inside the sister group of *S. cammaeus*.

#### *Sphaenorhynchus monophyly and outgroup relationships*

The main goal of our analysis was to provide a rigorous test of the monophyly of *Sphaenorhynchus* and its internal relationships, and not the relationships between *Sphaenorhynchus* and other hylids, given that previous studies have performed stronger tests of those relationships (Faivovich et al., 2005; Wiens et al., 2006; Duellman et al., 2016). However, some putatively shared morphological synapomorphies proposed for *Sphaenorhynchus* and outgroups deserve comment (Duellman and Wiens, 1992; Izecksohn, 1998; Faivovich et al., 2005). Contrary to Duellman and Wiens's (1992) hypothesis, the monophyly of *Scarthyla*, *Scinax* and *Sphaenorhynchus* is rejected in our results (see also Faivovich et al., 2005; Wiens et al., 2005, 2006; Duellman et al., 2016). However, Duellman and Wiens (1992) proposed three putative morphological synapomorphies for this group: (i) narrow sacral diapophyses (rounded, not strongly dilated), (ii) anteriorly inclined alary processes of the premaxillae and (iii) tadpole with large, laterally positioned eyes. The character-states of the sacral diapophyses were redefined by Faivovich (2002), who suggested that rounded or weakly expanded sacral diapophyses are a synapomorphy of *Scinax*. Subsequently, in a more comprehensive phylogenetic context, Faivovich et al. (2005) suggested that this character-state might be a synapomorphy of a more inclusive clade.

The optimization of sacral diapophysis expansion (our Ch. 95) and orientation of the premaxilla (our Ch. 19; orientation of the alary processes of the premaxilla sensu Duellman and Wiens, 1992) indicates that moderately expanded diapophyses (our Ch. 95.1) optimize as a synapomorphy of the sister taxon of *S. carneus*, with a transformation to unexpanded diapophyses in *S. mirim* (Ch. 95.0). The anteriorly directed premaxilla (our Ch. 19.0) optimizes ambiguously on the common ancestor of *Sphaenorhynchus* + (*Xenohyla* + *Dendropsophus*), a character-state shared with *Scarthyla goinorum*, *Scinax alter* and *Sci. perpusillus*. The size and the degree of lateralization of eyes did not present informative variation, because the eyes are ventrally visible (sensu Faivovich, 2002) in all larvae of *Sphaenorhynchus* examined and we were unable to objectively delimit character-states to characterize the size of eyes.

Izecksohn (1998) suggested that *Xenohyla* and *Sphaenorhynchus* share (i) reduced number of teeth in the jaw, (ii) relatively short urostyle, (iii) elongate and posteriorly directed transverse process of presacral vertebra IV, and (iv) the quadratojugal without contact with the maxilla. We did not score the relative length of the urostyle, but we have noticed that in *S. carneus*

the urostyle is shorter than in other species of *Sphaenorhynchus* (see Appendix S7). *Xenohyla truncata* shares a 35–40% edentate maxilla (our Ch. 16.2) with *S. caramaschii*, *S. lacteus*, *S. prasinus* and *S. surdus*. However, the optimization of this character indicates that this character-state evolved independently in *Xenohyla* and these species of *Sphaenorhynchus*.

We considered the elongate and posteriorly directed transverse process of presacral vertebra IV as two independent characters, scored as (i) orientation and (ii) length of the transverse processes. In our observations, only the length of this process was variable (Ch. 91). As a result of our analyses, the elongate transverse process of presacral IV (Ch. 91.2; Fig. S12d) is a unique synapomorphy for the sister taxon of *S. pauloalvini*. *Xenohyla truncata*, in turn, presents a moderately long transverse process (Ch. 91.1), the plesiomorphic condition.

A quadratojugal without contact with the maxilla, according to our observations, is the result of two independent transformations: the posterior reduction of the maxilla (Ch. 13) and the anterior reduction of the quadratojugal (Ch. 22). For example, in *S. pauloalvini* both the maxilla (Ch. 13.1) and quadratojugal (Ch. 22.1) are moderately developed, whereas in *S. carneus* both the maxilla (Ch. 13.0) and quadratojugal (Ch. 22.0) are extremely reduced. Furthermore, these bones are not in contact due to the extreme (Ch. 13.0) and moderate (13.1) posterior reduction only the maxilla in other *Sphaenorhynchus* and *X. truncata*, respectively.

According to Barrio-Amorós et al. (2006), *Sphaenorhynchus*, *Scarthyla* and *Pseudis* share mineralized intercalary elements. In our analyses, the completely mineralized intercalary element (Ch. 101.2) is a synapomorphy of *Scarthyla* + *Pseudis*, with instances of homoplasy in *Dendropsophus minutus*, *D. sanborni*, *Sphaenorhynchus botocudo*, *S. caramaschii*, *S. mirim* and *S. pauloalvini*.

#### *Sphaenorhynchus internal relationships*

The monophyly of *Sphaenorhynchus* is well supported (jackknife support = 100%; GB = 90; Fig. 1) by molecular evidence and 25 phenotypic synapomorphies in the TE analysis (see Appendix A for the complete list of synapomorphies of *Sphaenorhynchus*), with *S. pauloalvini* being the sister taxon of all other species of the genus.

Our observations corroborate Faivovich et al. (2005) and Araujo-Vieira et al.'s (2015a) suggestions that the anteriorly directed larval nostril (Ch. 132.0) and larval nostril with fleshy flanges (Ch. 133.1) are synapomorphies of *Sphaenorhynchus*. Similarly, we corroborated Faivovich et al.'s (2005) suggestions that the presence of a differentiated m. *intermandibularis* with a well-



developed apical supplementary element (our Ch. 146.1; see Fig. S14) and the white parietal peritoneum (Ch. 190.1) are synapomorphies of *Sphaenorhynchus*. The apical element also is present in other species of hylids (e.g. *Acris crepitans* and *A. gryllus*) and Lophyohylini (e.g. *Osteopilus dominicensis* and *O. ocellatus*; Tyler, 1971; Trueb and Tyler, 1974), as is the white parietal peritoneum (e.g. *Aplastodiscus* and *Hyloscirtus bogotensis* group, *Boana punctata* group, some species in the *B. benitezi* and *B. pulchella* groups; Ruiz-Carranza and Lynch, 1982; Garcia et al., 2003; Faivovich et al., 2005, 2006), indicating that these are homoplastic in a broader phylogenetic context.

Duellman and Wiens (1992) studied six species of *Sphaenorhynchus* (*S. bromelicola*, *S. carneus*, *S. dorisae*, *S. lacteus*, *S. planicola* and *S. platycephalus*) and proposed 11 morphological synapomorphies for the genus: (i) posterior ramus of pterygoid absent; (ii) zygomatic ramus of squamosal absent or reduced to small knob; (iii) pars facialis of maxilla and alary process of premaxilla reduced; (iv) postorbital process of maxilla reduced, not in contact with quadratojugal; (v) palatine reduced to sliver or absent; (vi) pars externa plectri entering tympanic ring posteriorly (rather than dorsally); (vii) pars externa plectri round; (viii) hyale curved medially; (ix) coracoids and clavicles elongate; (x) transverse process of presacral vertebra IV elongate, oriented posteriorly; and (xi) prepollex ossified, bladlike. We divided characters (ii), (iii) and (ix) into two independent characters each (see Discussion of characters 24–25, 12 and 18, and 81–82, respectively, in Appendix S6).

Only three of Duellman and Wiens's (1992) synapomorphies are supported in our results: (ii; our Ch. 25.1), with instances of homoplasy in *Dendropsophus elegans* and *Pseudis minuta*; (iii; our Ch. 18.0), with instances of homoplasy in *D. elegans* and *D. sanborni* and (vii; our Ch. 47.2). Of the remaining character-states, (iii; our Ch.12.0), (iv; our Ch. 13.0), (viii; our Ch. 69.1) and (x; our Ch. 91.2), and modified (i; our Ch. 30.0), (v; our Ch. 40.1) and (ix; our Ch. 81.1–82.1) optimize as synapomorphies of the clade that comprises all species of *Sphaenorhynchus* except *S. pauloalvini* (Fig. 1).

There are three remaining transformations: character (ii; our Ch. 24.0), zygomatic ramus of squamosal absent optimizes as an autapomorphy of *Sphaenorhynchus carneus*, with an extremely short zygomatic ramus of squamosal (our Ch. 25.0) optimizing ambiguously for its sister taxon due to the absence of this process in *S. carneus*; character (vi; our Ch. 48.1) which optimizes ambiguously for *Sphaenorhynchus*, a character-state shared with *Pseudis minuta* and *Xenohyla truncata*; and the character (xi; our Ch. 98.0) that is plesiomorphic for *Sphaenorhynchus*.

The exceptional posterior development of the m. *interhyoideus* was suggested by Faivovich et al. (2005) to

be a putative synapomorphy of *Sphaenorhynchus*. However, the transformation in which the posterior margin of the muscle reaches the m. *pectoralis esternalis* (Ch. 152.4) is a synapomorphy of all *Sphaenorhynchus* except *S. pauloalvini*.

Furthermore, based on previous reports for six species (*S. carneus*, *S. dorisae*, *S. lacteus*, *S. planicola*, *S. prasinus*, and *S. surdus*; Duellman, 1978; Rodriguez and Duellman, 1994; Parmalee, 1999; C.F.B. Haddad, pers. obs.) Faivovich et al. (2005) proposed that myrmecophagy is a likely synapomorphy of *Sphaenorhynchus*. Our study of stomach contents of *S. pauloalvini* (MNRJ 4323) revealed ants as well, corroborating that myrmecophagy is a putative synapomorphy of *Sphaenorhynchus*.

The differences that we found regarding the synapomorphies resulting from our analysis and several of those suggested by previous studies stem from the fact that *S. pauloalvini* had not been considered in other studies. Although *S. pauloalvini* presents a number of character-states that differ from those of other species of *Sphaenorhynchus* (see Appendices S5 and S6), all of our analyses indicate that it is the sister taxon of all remaining species of the genus, and so differences in the inferred phenotypic synapomorphies result from limitations in the taxonomic sampling of earlier studies. In Appendix A we provide an updated diagnosis of *Sphaenorhynchus* including all synapomorphies inferred from our results in addition to those discussed above.

The clade including all species of *Sphaenorhynchus* except *S. pauloalvini* is well supported (jackknife support = 100%; GB = 48) by molecular evidence and 27 phenotypic synapomorphies in the TE analysis (Fig. 1). Our analysis corroborates Araujo-Vieira et al.'s (2015a, b) suggestion that the presence of few enlarged marginal papillae (Ch. 136.1: marginal papillae about twice larger than the small papillae) on the oral disc is a synapomorphy of this clade. Another of its synapomorphies, the m. *petrohyoideus anterior* with an additional layer of fibres over the hyoid plate (Ch. 156.1) is known only in this genus among hylines (see Fig. S14c). Besides the synapomorphies mentioned above, some transformations are related to the absence or reduction of bones, including the extremely short posterior ramus of pterygoid, reduced to rudimentary bumps (Ch. 30.0), and the simple proximal portion of the *pars media plectri*, with a large gap between basal plate and operculum (Ch. 51.0).

In *Sphaenorhynchus* we recover three clades including species that are quite characteristic, and three species that we do not assign to any group, the early diverging *S. pauloalvini* and *S. carneus*, and *S. prasinus*. The clades that we recover include one with the small species from coastal lowlands in southeastern Brazil that we recognize as the *S. planicola* group (*S. mirim* and *S. planicola*; combined snout-to-vent

length (SVL) in males 15.7–24.1 mm; Lutz and Lutz, 1938; Caramaschi et al., 2009); the relatively large Amazonian species that we recognize as the *S. lacteus* group (*S. dorisae* and *S. lacteus*; combined SVL in males 26.0–41.0 mm, females 36.0–46.0 mm; Rodriguez and Duellman, 1994); and the clade including the medium-sized species of the Atlantic Forest, that we recognize as the *S. platycephalus* group (*S. botocudo*, *S. bromelicola*, *S. cammaeus*, *S. canga*, *S. caramaschii*, *S. palustris*, *S. platycephalus* and *S. surdus*; combined SVL in males 22.5–36.0 mm, females 20.0–33.0 mm; Lutz and Lutz, 1938; Bokermann, 1966; Heyer et al., 1990; Toledo et al., 2007; Caramaschi et al., 2009; Araujo-Vieira et al., 2015b; Roberto et al., 2017).

Cruz and Peixoto (1980) tentatively grouped *S. planicola* with *S. prasinus* on the basis of several larval similarities including total length, colour pattern, spiracle length and marginal papillae size. However, the monophyly of this clade is rejected in our analyses. Instead, *S. planicola* is sister taxon of *S. mirim*, which we recognize as the *S. planicola* group. The monophyly of this group is supported by molecular evidence and five phenotypic synapomorphies (jackknife support = 100%; GB = 1). Some phenotypic synapomorphies are the posterior extension of the fold of the m. *interhyoideus* surpassing the m. *pectoralis externalis* (Ch. 152.5), the posterior-most extension of this muscle in *Sphaenorhynchus*, with instances of homoplasy in *Dendropsophus minutus* and *D. sanboni*, and the m. *extensor brevis superficialis digiti III* with an insertion on the third metatarsus (Ch. 185.1; Fig. S15d) as synapomorphy of this clade in our TE results (nonhomoplastic in the context of our analysis, but known to occur in several distantly related anurans such as *Pipa pipa* (Pipidae), *Chiromantis xerampelina* (Rhacophoridae), and *Phrynobatrachus kinangopensis* (Phrynobatrachidae), *Hyla meridionalis* (Hylinae), and several phyllomedusines; Dunlap, 1960; Burton, 2004).

The monophyly of the *S. lacteus* group is supported by molecular evidence and four phenotypic synapomorphies (jackknife support = 100%; GB = 31), including the light-coloured nuptial pads on Finger II in males (Ch. 115.0), with a single instance of homoplasy in *S. canga* and branch I of the m. *petrohyoideus posterior* inserted on the base of the posteromedial process of the hyoid (Ch. 158.0), with instances of homoplasy in *Dendropsophus minutus*, *Pseudis minuta* and *Scinax alter*.

The monophyly of the *S. platycephalus* group is supported by molecular evidence and eight phenotypic synapomorphies (jackknife support = 98%; GB = 11), with *S. caramaschii* as the earliest diverging taxon of this clade, followed by *S. cammaeus*. Some of these synapomorphies are as follows: maxilla overlapping the premaxilla (Ch. 17.1); dorsolateral white line present (Ch. 111.1), with instances of homoplasy in *Dendropsophus*

*sanborni*, *Scinax alter* and *S. lacteus*; subcloacal ornamentation with a weak glandular dermal fold (Ch. 117.4); poorly developed and slightly crenulated dermal folds on tarsus (Ch. 123.3); and small, rounded or flattened tubercles on heel (Ch. 124.1). A notable synapomorphy of this clade is the presence of a cartilaginous lamina that extends from the cartilaginous branch to the inferior margin of the oblique cartilage (Ch. 62.1) with instances of homoplasy in *S. lacteus*, *S. pauloalvini* and species of *Dendropsophus* (see Fig. S9). See Appendix A for a complete diagnosis and characterization of the three species groups of *Sphaenorhynchus*.

#### *Paedomorphosis and character evolution in Sphaenorhynchus*

Bokermann (1974) reported that some tadpoles of *S. bromelicola* stage 41 of Gosner (1960) possess mature oocytes and well-developed testes. Furthermore, he reported newly metamorphosed individuals and individuals close to reducing the tail having well-developed oocytes or vocal sac—with some individuals even calling—and testes in spermatogenesis. These individuals are, at least in relation to development and fertility of gonads, able to reproduce. Bokermann (1974) suggested that there is acceleration in the time of the sexual maturity (peramorphosis sensu Reilly et al., 1997) together with a delay and irregular metamorphosis (paedomorphosis sensu Reilly et al., 1997). Also, although *S. bromelicola* is associated with unstable environments (temporary ponds), the presence of individuals in the same population with regular metamorphosis suggests that this precocity is not necessarily dependent on environmental factors (Bokermann, 1974).

Among species of *Sphaenorhynchus*, sexually mature individuals with a long tail (larval somatic morphology) have been reported for *S. botocudo*, *S. bromelicola*, *S. mirim* and *S. palustris* (Haddad and Prado, 2005; Caramaschi et al., 2009). These species do not form a clade in our TE results. Instead, the presence of a long tail in sexually mature individuals optimizes as a synapomorphy of *S. botocudo* + *S. palustris*, and autapomorphies of *S. bromelicola* and *S. mirim*. This occurrence might result from a deceleration in the process of tail resorption, because the ancestral condition is absence of long tails in sexually mature individuals. Indeed, the tail is eventually resorbed entirely, but resorption is delayed, because adults of *S. bromelicola*, *S. botocudo* and *S. mirim* with tails of different lengths and lacking tails have been observed (Bokermann, 1974; Caramaschi et al., 2009). In this case, heterochrony does not affect the offset shape of adult individuals of *Sphaenorhynchus* and can, therefore, be defined as heterochronic isomorphosis (Reilly et al., 1997).

The reduction and loss of teeth in *Sphaenorhynchus* is evident, except for *S. pauloalvini* and *S. prasinus*

(Chs. 16.1 and 21.1) and might be associated with heterochronic processes. Maxillary and premaxillary teeth are absent in *S. carneus*, *S. dorisae*, *S. planicola* and *S. mirim* (Ch. 14.0), reduced in *S. botocudo*, *S. bromelicola*, *S. platycephalus* and *S. palustris* (Ch. 16.3), and inconspicuous in *S. canga* (Ch. 16.4). Other character-states that could be associated with paedomorphosis are the coexistence of both pedicellate and nonpedicellate teeth on the maxilla (Ch. 15.1: optimizes ambiguously for the sister taxon of the *S. lacteus* group); vomerine teeth nonpedicellate (Ch. 37.0: optimizes ambiguously for the sister taxon of *S. carneus*); anguloespinal and dentary without contact, in which the Meckel's cartilage is exposed (Ch. 55.1: synapomorphy of the sister taxon of *S. pauloalvini*); palatines reduced to thin ossified slivers (Ch. 40.0: *S. carneus*, *S. dorisae* and *S. mirim*); and *lamina nariochoanalis* connected to the postnasal wall (Ch. 63.0: synapomorphy of the sister taxon of *S. carneus*). Jurgens (1971) had already suggested that the latter was a neotenic condition in *Spea* (as *Scaphiopus*; Scaphiopodidae).

In addition to delayed tail resorption and dental character-states, several other character-states found in species of *Sphaenorhynchus* appear to be paedomorphic relative to the plesiomorphic states. These include: maxilla reduced posteriorly (Ch. 13.0: synapomorphy of the sister taxon of *S. pauloalvini*); dentigerous process extremely reduced (Ch. 32.0: *S. dorisae* and *S. mirim*); dentigerous process separate from the main body of the vomer (Ch. 34.0: *S. dorisae*); posterior ramus of the pterygoid extremely short, reduced to rudimentary bumps (Ch. 30.0: synapomorphy of the sister taxon of *S. pauloalvini*); maxillary and premaxillary teeth absent (Ch. 14.0: observed in *S. carneus*, *S. dorisae*, *S. planicola* and *S. mirim*), and extreme reduction of premaxillary and maxillary teeth (Ch. 16.3: maxilla edentate across 55–80% of its length in *S. botocudo*, *S. bromelicola*, *S. palustris* and *S. platycephalus*; 16.4: maxilla edentate across 95% of its length in *S. canga*; and Ch. 21.0: part of *pars dentalis* of premaxilla edentate in *S. botocudo*, *S. cammaeus* and *S. canga*, for example).

Outside *Sphaenorhynchus*, some species of *Pseudis* (*P. paradoxa* and *P. platensis*) show a shift in the timing of sexual maturity (Downie et al., 2009; Fabrezi et al., 2010). *Pseudis platensis* shows delayed metamorphosis (with a low rate of development), in which the events related to the loss of the vent tube and resorption of the tail are postdisplaced, taking place after the larval mouth structures have disappeared and the skull transformations are complete (Fabrezi and Quinzio, 2008).

#### Oviposition site

Previous studies have focused on the description of external morphology of adults and larvae of

*Sphaenorhynchus* (e.g. Lutz and Lutz, 1938; Bokermann, 1966, 1973), and limited information is available on their biology, reproduction and behaviour of adults and larvae (Bokermann, 1966; Suárez-Mayorga and Lynch, 2001).

Adults of *Sphaenorhynchus* are known to inhabit mainly open areas (temporary, permanent or semi-permanent ponds), where males vocalize while perched on the floating vegetation or partially submerged in water, or more rarely perched on bushes (e.g. Lutz and Lutz, 1938; Bokermann, 1973; Cruz and Peixoto, 1980; C.F.B. Haddad, pers. obs.). There are no records of oviposition site for *S. botocudo*, *S. bromelicola*, *S. mirim*, *S. palustris*, *S. platycephalus* and *S. prasinus* (Lutz and Lutz, 1938; Bokermann, 1966, 1973, 1974; Heyer et al., 1990; Toledo et al., 2007; Caramaschi et al., 2009).

*Sphaenorhynchus caramaschii*, *S. dorisae*, *S. lacteus*, *S. planicola* and *S. surdus*<sup>1</sup> lay their eggs in water, attached to submerged vegetation (Ch. 191.2; Cruz, 1973; Rodriguez and Duellman, 1994; Reichle and Köhler, 1998; Duellman, 2005; Izecksohn and Carvalho-Silva, 2001; K. Araujo-Vieira and T. Grant, pers. obs.); *S. pauloalvini* lays its eggs on leaves out of water (Bokermann, 1973). The oviposition in *S. carneus* has been reported to occur on leaves out of water (Bokermann, 1973; as *Sphaenorhynchus habra* [sic]) or in water, attached to submerged vegetation (Crump, 1974; W. Hödl, pers. comm.). We consider it polymorphic for coding purposes (Ch. 191.0 and 191.2); further, several studies have demonstrated that the same species can display behavioural plasticity with respect to reproductive modes (e.g. *Dendropsophus ebraccatus*, *Boana pardalis* (Hylidae), *Physalaemus spiniger* (Leptodactylidae); Haddad and Pombal, 1998; Haddad and Prado, 2005; Touchon and Warkentin, 2008; Moura et al., 2011; Toledo et al., 2012) and that the existence of alternative reproductive strategies might have evolved either due to trait selection in order to maximize fitness and avoid predation and competition or in relation to specific environmental conditions (e.g. Magnusson and Hero, 1991; Haddad and Prado, 2005; Taborsky et al., 2008; Taborsky and Brockmann, 2010). The optimization of oviposition site on our TE results indicates that oviposition in water (Ch. 191.2) is plesiomorphic in *Sphaenorhynchus*, whereas oviposition on leaves out of water (Ch. 191.0) is an autapomorphy of *S. pauloalvini*. Furthermore, our hypothesis predicts that all species for which

<sup>1</sup>K. Araujo-Vieira and T. Grant (unpubl. data) observed a single event of oviposition by *S. surdus* in a large bromeliad directly above the water of a swamp at Torres, Rio Grande do Sul, Brazil. Although this is suggestive of polymorphism, as occurs in *S. carneus*, we prefer to await other observations to ensure that the event we observed was not merely a behavioural anomaly.



oviposition is unknown will be found to oviposit in water.

## Conclusions

Our dataset for the study of the phylogenetic relationships of *Sphaenorhynchus* included 193 phenotypic characters from adult and larval morphology, osteology, myology and reproductive biology, and DNA sequences for three mitochondrial and three nuclear loci for 43 terminals of 15 ingroup species, and 12 outgroup taxa. Our results recover the monophyly of *Sphaenorhynchus* with high support, obtaining three characteristic clades that we recognize as species groups (the *S. lacteus*, *S. planicola* and *S. platycephalus* groups). Most conflict among equally parsimonious topologies is restricted to relationships inside the *S. platycephalus* group, where one of the two species for which we lack sequence data (*S. bromelicola*) exhibits wildcard behaviour. Differences in our assessment of synapomorphies of *Sphaenorhynchus* with earlier studies (Duellman and Wiens, 1992; Faivovich et al., 2005) resulted from limitations in the taxonomic sampling of those studies, which did not include *S. pauloalvini*, the sister species of the remainder of the genus.

Our study of phenotypic characters identified a number of transformations that are congruent with the occurrence of heterochronic events during the evolution of these frogs and corroborate earlier observations of precocious sexual maturity in metamorphic individuals of some species in the *S. planicola* and *S. platycephalus* groups (Bokermann, 1974; Haddad and Prado, 2005; Caramaschi et al., 2009). Our well-supported phylogenetic hypothesis will provide an evolutionary context for the study of this poorly known phenomenon and several related character systems (e.g. morphology of the larval nostril and spiracle, vocalizations; Toledo et al., 2014; Araujo-Vieira et al., 2015a).

## Acknowledgments

For access to collections, and specimen and/or tissue loans we thank José M. Padiál (AMNH), Denise C. Rossa-Feres (DZSJRP), Santiago Castroviejo-Fisher, Glaucia M.F. Pontes, and Camila Both (MCP-PUCRS), Magno V. Segalla and Julio Cesar de Moura Leite (MHNCI), José P. Pombal Jr. (MNRJ), Mirco Solé (MZUESC), Marcelo F. Napoli (MZUFBA), Renato N. Feio (MZUFV), Camila Rabello Rievers (then at PUC Minas), Miguel Trefaut Rodrigues and Vanessa K. Verdade (USP), the late Paulo E. Vanzolini and Hussam Zaher (MZUSP), Steffen Reichle (then at The Nature Conservancy, Bolivia), Igor

Joventino Roberto (UFAM), Hélio Ricardo da Silva (UFRRJ), João V. Lacerda and Paulo C.A. Garcia (UFMG), Laura Verrastro (UFRGS), Robson W. Ávila (URCA-H), Mike G. Rutherford (UWIZM), Natan Maciel (ZUFG) and Felipe Toledo (ZUEC). Walter Hödl and Steffen Reichle kindly answered our queries regarding biology of some species. Denis Jacob Machado assisted us with the use of YBYRÁ. Agustín Elias-Costa generously executed Fig. S12. Carlos Eduardo Costa-Campos, Felipe S.F. Leite, Igor Joventino Roberto, João Luiz Gasparini and Miguel Trefaut Rodrigues generously allowed us to use their photos. For support in different stages of this research, we thank: Glaucia M.F. Pontes, Roberto E. Reis, Patrick Colombo, Raquel R. Santos, Mauricio Rivera-Correa, Marco Rada, Danielle A. Fabri and Mariangeles A. Hernandez (Laboratório de Sistemática de Vertebrados-PUCRS); Bianca v. M. Berneck and Victor G. D. Orrico (Departamento de Zoologia, UNESP); and Martin O. Pereyra, Andrés Brunetti, Laura Nicoli, Sebastián Barrionuevo, Carlos Taboada, M. Celeste Luna, Agustín Elias-Costa and Daiana Ferraro (División Herpetología, MACN). Financial support and fellowships were provided by São Paulo Research Foundation (FAPESP procs. #2012/10000-5, #2013/20423-3, #2013/50741-7, and #2014/50342-8), Agencia Nacional de Promoción Científica y Tecnológica (ANPCyT, PICT 404/2013 and 820/2015), Conselho Nacional de Desenvolvimento Científico e Tecnológico (CNPq) and Organización de los Estados Americanos (OEA).

## References

- Altig, R., McDiarmid, R.W., 1999. Body plan. Development and morphology. In: Altig, R., McDiarmid, R.W. (Eds.) *Tadpoles. The Biology of Anuran Larvae*. University of Chicago Press, Chicago, IL, pp. 29–51.
- Araujo-Vieira, K., Tacioli, A., Faivovich, J., Orrico, V.G.D., Grant, T., 2015a. The tadpole of *Sphaenorhynchus caramaschii*, with comments on larval morphology of *Sphaenorhynchus* (Anura: Hylidae). *Zootaxa* 3904, 270–282.
- Araujo-Vieira, K., Lacerda, J.V.A., Pezzuti, T.L., Leite, F.S., Assis, C.L., Cruz, C.A.G., 2015b. A new species of hatchet-faced treefrog *Sphaenorhynchus Tschudi* (Anura: Hylidae) from Quadrilátero Ferrífero, Minas Gerais, southeastern Brazil. *Zootaxa* 4059, 96–114.
- Araujo-Vieira, K., Caramaschi, U., Grillitsch, H., Grant, T., Faivovich, J., 2018. On the identity of *Sphaenorhynchus platycephalus* (Werner, 1894) (Anura: Hylidae). *S. Am. J. Herpetol.* 13, 73–84.
- Barrio, A., 1965. Cloricia fisiologica en batracios anuros. *Physis*. 69, 137–142.
- Barrio-Amorós, C.L., Pascual, A.D., Mueses-Cisneros, J.J., Infante, E., Chacón, A., 2006. *Hyla vigilans* Solano, 1971, a second species for the genus *Scarthyla*, redescription and distribution in Venezuela and Colombia. *Zootaxa* 1349, 1–18.
- Benício, R.A., Silva, G.R., Fonseca, M.G., 2011. Amphibia, Anura, Hylidae, *Sphaenorhynchus lacteus* (Daudin, 1800): First record of the genus and species for the state of Piauí, Brazil. *Check List* 7, 196–197.

- Bokermann, W.C.A., 1966. Duas novas espécies de “*Sphaenorhynchus*” (Amphibia, Hylidae). *Rev. Brasil. Biol.* 26, 15–21.
- Bokermann, W.C.A., 1973. Duas novas espécies de “*Sphaenorhynchus*” da Bahia (Anura, Hylidae). *Rev. Brasil. Biol.* 33, 589–594.
- Bokermann, W.C.A., 1974. Observações sobre desenvolvimento precoce em *Sphaenorhynchus bromelicola* Bokermann, 1966 (Anura, Hylidae). *Rev. Brasil. Biol.* 36, 33–41.
- Bremer, K., 1988. The limits of amino acid sequence data in angiosperm phylogenetic reconstruction. *Evolution* 42, 795–803.
- Burton, T.C., 1996. Adaptation and evolution in the hand muscles of Australo-Papuan hylid frogs (Anura: Hylidae: Pelodyadinae). *Aust. J. Zool.* 44, 611–623.
- Burton, T.C., 1998. Variation in the hand and superficial throat musculature of neotropical leptodactylid frogs. *Herpetologica* 54, 53–72.
- Burton, T.C., 2004. Muscles of the pes of hylid frogs. *J. Morphol.* 260, 209–233.
- Caramaschi, U., 2010. Descrição do girino de *Sphaenorhynchus surdus* (Cochran, 1953) (Anura, Hylidae). *Bol. Mus. Biol. Mello Leitão, Nova Sér.* 27, 67–74.
- Caramaschi, U., Almeida, A.P., Gasparini, J.L., 2009. Description of two new species of *Sphaenorhynchus* (Anura, Hylidae). *Zootaxa* 2115, 34–46.
- Cochran, D.M., 1953. Three new Brazilian frogs. *Herpetologica* 8, 111–115.
- Crump, M.L., 1974. Reproductive strategies in a tropical anuran community. *Misc. Publ. Mus. Nat. Hist. Univ. Kans.* 61, 1–65.
- Cruz, C.A.G., 1973. Observações sobre o girino de *Sphaenorhynchus planicola* (Lutz & Lutz, 1938) (Amphibia, Anura, Hylidae). *Arq. Mus. Nac. Rio de J.* 3, 83–86.
- Cruz, C.A.G., Peixoto, O.L., 1980. Notas sobre o girino de *Sphaenorhynchus orophilus* (Lutz & Lutz, 1938) (Amphibia, Anura, Hylidae). *Rev. Brasil. Biol.* 40, 383–386.
- Daudin, F.M., 1800. *Histoire Naturelle des Quadrupèdes Ovipares*. Livraison 2. Marchant et Cie, Paris.
- Downie, J.R., Sams, K., Walsh, P.T., 2009. The paradoxical frog *Pseudis paradoxa*: Larval anatomical characteristics, including gonadal maturation. *Herpetol. J.* 19, 1–10.
- Duellman, W.E., 1974. A reassessment of the taxonomic status of some neotropical hylid frogs. *Occ. Pap. Mus. Nat. Hist. Univ. Kans.* 27, 1–27.
- Duellman, W.E., 1978. The biology of an equatorial herpetofauna in Amazonian Ecuador. *Misc. Publ. Mus. Nat. Hist. Univ. Kans.* 65, 1–352.
- Duellman, W.E., 2001. Hylid Frogs of Middle America. *Soc. Study Amphibians Rep., Contribut. Herpetol.* 18:1–1158.
- Duellman, W.E., 2005. *Cusco Amazónico. The Lives of Amphibians and Reptiles in an Amazonian Rainforest*. Cornell University Press, Ithaca, NY, xv + 433 pp.
- Duellman, W.E., Wiens, J.J., 1992. The status of the hylid frog genus *Oloolygon* and the recognition of *Scinax* Wagler, 1830. *Misc. Publ. Mus. Nat. Hist. Univ. Kans.* 15, 1–23.
- Duellman, W.E., Marion, A.M., Hedges, S.B., 2016. Phylogenetics, classification, and biogeography of the treefrogs (Amphibia: Anura: Arboranae). *Zootaxa* 4104, 1–109.
- Dunlap, D.G., 1960. The comparative myology of the pelvic appendage in the Salientia. *J. Morphol.* 106, 1–76.
- Fabrezi, M., 1992. El carpo de los anuros. *Alytes* 10, 1–29.
- Fabrezi, M., 1993. The anurans tarsus. *Alytes* 11, 46–63.
- Fabrezi, M., Quinzio, S.I., 2008. Morphological evolution in Ceratophryinae frogs (Anura, Neobatrachia): The effects of heterochronic changes during larval development and metamorphosis. *Zool. J. Linn. Soc.* 154, 752–780.
- Fabrezi, M., Quinzio, S.I., Goldberg, J., 2010. The ontogeny of *Pseudis platensis* (Anura, Hylidae): Heterochrony and the effects of larval development on postmetamorphic life. *J. Herpetol.* 271, 496–510.
- Faivovich, J., 2002. A cladistic analysis of *Scinax* (Anura: Hylidae). *Cladistics* 18, 367–393.
- Faivovich, J., Haddad, C.F.B., Garcia, P.C.A., Frost, D.R., Campbell, J.A., Wheeler, W.C., 2005. Systematic review of the frog family Hylidae, with special reference to Hylinae: Phylogenetic analysis and taxonomic revision. *Bull. Am. Mus. Nat. Hist.* 294, 240.
- Faivovich, J., Moravec, J., Cisneros-Heredia, D. F., Köhler, J., 2006. A new species of the *Hypsiboas benitezi* group (Anura: Hylidae) from the western Amazon basin (Amphibia: Anura: Hylidae). *Herpetologica* 62, 96–108.
- Faivovich, J., Haddad, C.F.B., Baeta, D., Jungfer, K.H., Álvares, G.F.R., Brandão, R.A., Sheil, C.A., Barrientos, L.S., Barrio-Amorós, C.L., Cruz, C.A.G., Wheeler, W.C., 2010. The phylogenetic relationships of the charismatic poster frogs, Phyllomedusinae (Anura, Hylidae). *Cladistics* 26, 227–261.
- Faivovich, J., Pereyra, M.O., Luna, M.C., Hertz, A., Blotto, B.L., Vásquez-Almazán, C.R., McCranie, J.R., Sánchez, D.A., Baeta, D., Araujo-Vieira, K., Köhler, G., Kubicki, B., Campbell, J.A., Frost, D.R., Wheeler, W.C., Haddad, C.F.B., 2018. On the monophyly and relationships of several genera of Hylini (Anura: Hylidae: Hylinae), with comments on recent taxonomic changes in hylids. *S. Am. J. Herpetol.* 13, 1–32.
- Farris, J.S., Albert, V.A., Källersjö, M., Lipscomb, D., Kluge, A.G., 1996. Parsimony jackknifing outperforms neighbor-joining. *Cladistics* 12, 99–124.
- Garcia, P.C.A., Vinciprova, G., Haddad, C.F.B., 2003. The taxonomic status of *Hyla pulchella joaquina* (Anura: Hylidae) with description of its tadpole and vocalization. *Herpetologica* 59, 350–363.
- Goin, C.J., 1957. Status of the frog genus *Sphoerohyla* with a synopsis of the species. *Caldasia* 8, 11–31.
- Goloboff, P.A., 1996. Methods for faster parsimony analysis. *Cladistics* 12, 199–220.
- Goloboff, P.A., 1999. Analyzing large data sets in reasonable times: solutions for composite optima. *Cladistics* 15, 415–428.
- Goloboff, P.A., Catalano, S.A., 2016. TNT version 1.5, including a full implementation of phylogenetic morphometrics. *Cladistics* 32, 221–238.
- Goloboff, P.A., Farris, J.S., Nixon, K.C., 2008. TNT, a free program for phylogenetic analysis. *Cladistics* 24, 774–786.
- Goodman, M., Olson, C.B., Beeber, J.E., Czelusniak, J., 1982. New perspectives in the molecular biological analysis of mammalian phylogeny. *Acta Zool. Fenn.* 169, 19–35.
- Gosner, K.L., 1960. A simplified table for staging anuran embryos and larvae with notes on identification. *Herpetologica* 16, 183–190.
- Grant, T., Kluge, A.G., 2003. Data exploration in phylogenetic inference: Scientific, heuristic, or neither. *Cladistics* 19, 379–418.
- Grant, T., Kluge, A.G., 2008. Credit where credit is due: The Goodman-Bremer support metric. *Mol. Phylogenet. Evol.* 49, 405–406.
- Grant, T., Kluge, A.G., 2009. Perspective Parsimony, explanatory power, and dynamic homology testing. *Syst. Biodivers.* 7, 357–363.
- Grant, T., Frost, D.R., Caldwell, J.P., Gagliardo, J.P.R., Haddad, C.F.B., Kok, P.J.R., Means, B.D., Noonan, B.P., Schargel, W., Wheeler, W.C., 2006. Phylogenetic systematics of dart-poison frogs and their relatives (Anura: Athesphatanura: Dendrobatidae). *Bull. Am. Mus. Nat. Hist.* 299, 1–262.
- Grant, T., Rada, M., Anganoy-Criollo, M., Batista, A., Dias, P.H., Jeckel, A.M., Machado, D.J., Rueda-Almonacid, J.V., 2017. Phylogenetic systematics of dart-poison frogs and their relatives revisited (Anura: Dendrobatoidea). *S. Am. J. Herpetol.* 12, S1–S90.
- Haddad, C.F.B., Pombal, J.P. Jr., 1998. Redescription of *Physalaemus spiniger* (Anura: Leptodactylidae) and description of two new reproductive modes. *J. Herpetol.* 32, 557–565.
- Haddad, C.F.B., Prado, C.P.A., 2005. Reproductive modes in frogs and their unexpected diversity in the Atlantic forest of Brazil. *Bioscience* 55, 207–217.
- Hall, T.A., 1999. BioEdit: a user-friendly biological sequence alignment editor and analysis program for Windows 95/98/NT. *Nucl. Acids. Symp. Ser.* 41, 95–98.

- Hawkins, J.A., Hughes, C.E., Scotland, R.W., 1997. Primary homology assessment, characters and character states. *Cladistics* 13, 275–283.
- Heyer, W.R., Rand, A.S., Cruz, C.A., Peixoto, G.O.L., Nelson, C.E., 1990. Frogs of Boracéia. *Arq. Zool.* 31, 231–410.
- Horton, P., 1982. Diversity and systematic significance of anuran tongue musculature. *Copeia* 1982, 595–602.
- Izecksohn, E., 1998. Novo gênero de Hylidae brasileiro (Amphibia, Anura). *Rev. Univ. Rural, Serie Ciências da Vida* 18, 47–52.
- Izecksohn, E., Carvalho-e-Silva, S.P., 2001. Anfíbios do município do Rio de Janeiro. Editora UFRJ, Rio de Janeiro, 158 pp.
- Jungfer, K.H., Faivovich, J., Padiál, J.M., Castroviejo-Fisher, S., Lyra, M.M., Berneck, B.V.M., Iglesias, P.P., Kok, P.J.R., MacCulloch, R.D., Rodrigues, M.T., Verdade, V.K., Gastello, C.P.T., Chaparro, J.C., Valdujo, P.H., Reichle, S., Moravec, J., Gvoždík, V., Gagliardi-Urrutia, G., Ernst, R., De la Riva, I., Means, D.B., Lima, A.P., Señaris, J.C., Wheeler, W.C., Haddad, C.F.B., 2013. Systematics of spiny-backed treefrogs (Hylidae: *Osteocephalus*): an Amazonian puzzle. *Zool. Scr.* 42, 351–380.
- Jurgens, J.D., 1971. The morphology of the nasal region of amphibia and its bearing on the phylogeny of the group. *Ann. Univ. Van Stellenbosch* 46, 1–146.
- Katoh, K., Standley, D.M., 2013. MAFFT multiple sequence alignment software version 7: improvements in performance utility. *Mol. Biol. Evol.* 30, 772–780.
- Kearney, M., 2002. Fragmentary taxa, missing data, and ambiguity: mistaken assumptions and conclusions. *Syst. Biol.* 51, 369–381.
- Kearney, M., Clark, J.M., 2003. Problems due to missing data in phylogenetic analyses including fossils: a critical review. *J. Vertebr. Paleontol.* 23, 263–274.
- Kenny, J.S., 1969. The Amphibia of Trinidad. *Studies Fauna Curaçao Other Caribbean Islands* 108, 1–78.
- Kluge, A.G., 1989. A concern for evidence and a phylogenetic hypothesis of relationships among *Epicrates* (Boidae, Serpentes). *Syst. Zool.* 38, 7–25.
- Kluge, A.G., Grant, T., 2006. From conviction to anti-superfluity: old and new justifications for parsimony in phylogenetic inference. *Cladistics* 22, 276–288.
- La Marca, E., Azevedo-Ramos, C., Coloma, L.A., Ron, S., Hardy, J., 2010. *Sphaenorhynchus lacteus*. The IUCN red list of threatened species.
- Lacerda, J.V.A., Moura, M.R., 2013. Vocal repertoire of *Sphaenorhynchus palustris* (Anura, Hylidae), with notes on *S. botocudo*. *Salamandra* 49, 105–108.
- Luna, M.C., McDiarmid, R.W., Faivovich, J., 2018. From erotic excrescences to pheromone shots: structure and diversity of nuptial pads in anurans. *Biol. J. Linn. Soc.* 124, 403–446.
- Lutz, A., Lutz, B., 1938. I. On *Hyla aurantiaca* Daudin and *Sphaenorhynchus* Tschudi and on two allied Hylae from southeastern Brasil. *An. Acad. Bras. Cienc.* 10, 175–194.
- Machado, D.J., 2015. YBYRA facilitates comparison of large phylogenetic trees. *BMC Bioinformatics* 16, 204.
- Maddison, W., Maddison, D., 2015. Mesquite: a modular system for evolutionary analysis. Version 3.03 (7 May 2015). Accessible at <http://mesquiteproject.org>.
- Magnusson, W.E., Hero, J.M., 1991. Predation and the evolution of complex oviposition behavior in Amazon rainforest frogs. *Oecologia* 86, 310–318.
- Moura, M.R., Motta, A.P., Feio, R.N., 2011. An unusual reproductive mode in *Hypsiboas* (Anura: Hylidae). *Zoologia* 28, 142–144.
- Nixon, K.C., 1999. The parsimony ratchet, a new method for rapid parsimony analysis. *Cladistics* 15, 407–414.
- Nixon, K.C., Wheeler, Q.D., 1992. Extinction and the origin of species. In: Novacek, M.J., Wheeler, Q.D. (Eds.), *Extinction and Phylogeny*. Columbia University Press, New York, NY, pp. 119–143.
- Padiál, J.M., Grant, T., Frost, D.R., 2014. Molecular systematics of terraranas (Anura: Brachycephaloidea) with an assessment of the effects of alignment and optimality criteria. *Zootaxa* 3825, 1–132.
- Parmalee, J.R., 1999. Trophic ecology of a tropical anuran assemblage. *Sci. Pap. Nat. Hist. Mus. Univ. Kans.* 11, 1–59.
- Pinheiro, P.D.P., Kok, P.J.R., Noonan, B.P., Means, D.B., Haddad, C.F.B., Faivovich, J., 2019. A new genus of Cophomantini, with comments on the taxonomic status of *Boana liliae* (Anura, Hylidae). *Zool. J. Linn. Soc.* 185, 226–245.
- Pyron, R.A., 2014. Biogeographic analysis reveals ancient continental vicariance and recent oceanic dispersal in amphibians. *Syst. Biol.* 63, 779–797.
- Pyron, R.A., Wiens, J.J., 2011. A large-scale phylogeny of Amphibia including over 2,800 species, and a revised classification of extant frogs, salamanders, and caecilians. *Mol. Phylogenet. Evol.* 61, 543–583.
- Reichle, S., Köhler, J., 1998. Saisonale und wasserstandsabhängige Rufplatzverteilung von Froschlurchen der südlichen Beni-Savannen, Bolivien. *Salamandra* 34, 43–54.
- Reilly, S.M., Wiley, E.O., Meinhardt, D.J., 1997. An integrative approach to heterochrony: the distinction between interspecific and intraspecific phenomena. *Biol. J. Linn. Soc.* 60, 119–143.
- Roberto, I.J., Araujo-Vieira, K., Carvalho-e-Silva, S.P., Avila, R.W., 2017. A new species of *Sphaenorhynchus* (Anura: Hylidae) from northeastern Brazil. *Herpetologica* 73, 148–161.
- Rodriguez, L.O., Duellman, W.E., 1994. Guide to the frogs of the Iquitos region, Amazonian Peru. *Sci. Pap. Nat. Hist. Mus. Univ. Kans.* 22, i–ii. 1–80.
- Ruiz-Carranza, P.M., Lynch, J.D., 1982. Dos nuevas especies de Hyla (Amphibia: Anura) de Colombia, con aportes al conocimiento de *Hyla bogotensis*. *Caldasia* 13, 647–671.
- Sabaj, M.H., 2016. *Standard Symbolic Codes for Institutional Resource Collections in Herpetology and Ichthyology: An Online Reference*. Version 6.5 (16 August 2016). American Society of Ichthyologists and Herpetologists, Washington, DC. Available at <http://www.asih.org/>.
- Sankoff, D., 1975. Minimal mutation trees of sequences. *SIAM J. Appl. Math.* 28, 35–42.
- Strong, E.E., Lipscomb, D.L., 1999. Character coding and inapplicable data. *Cladistics* 15, 363–371.
- Suaréz, P., Cardozo, D., Baldo, D., Pereyra, M.O., Faivovich, J., Orrico, V.G.D., Catroli, G.F., Grabile, M., Bernarde, P.S., Nagamachi, C.Y., Haddad, C.F.B., Pieczarka, J.C., 2013. Chromosome evolution in Dendropsophini (Amphibia: Anura: Hylinae). *Cytogenet. Genome Res.* 141, 295–308.
- Suárez-Mayorga, A.M., Lynch, J.D., 2001. Los renacuajos colombianos de *Sphaenorhynchus* (Hylidae), descripciones, anotaciones sistemáticas y ecológicas. *Rev. Acad. Colomb. Cienc. Exactas Fis. Nat.* 25, 411–420.
- Taboada, C., Brunetti, A.E., Alexandre, C., Lagorio, M.G., Faivovich, J., 2017. Fluorescent frogs: A herpetological perspective. *S. Am. J. Herpetol.* 12, 1–13.
- Taborsky, M., Brockmann, H.J., 2010. Alternative reproductive tactics and life history phenotypes. In: Kappeler, P. (Ed.), *Animal Behaviour: Evolution and Mechanisms*. Springer, Heidelberg, pp. 537–586.
- Taborsky, M., Oliveira, R.F., Brockmann, H.J., 2008. The evolution of alternative reproductive tactics: concepts and questions. In: Oliveira, R.F., Taborsky, M., Brockmann, H.J. (Eds.), *Alternative Reproductive Tactics: An Integrative Approach*. Cambridge University Press, Cambridge, UK, pp. 1–21.
- Taylor, W.R., Van Dyke, G.C., 1985. Revised procedures for staining and clearing small fishes and other vertebrates for bone and cartilage study. *Cybio* 9, 107–119.
- Toledo, L.F., Garcia, P.C.A., Lingnau, R., Haddad, C.F.B., 2007. A new species of *Sphaenorhynchus* (Anura: Hylidae) from Brazil. *Zootaxa* 1658, 57–68.
- Toledo, L.F., Garey, M.V., Costa, T.R.N., Lourenço-de-Moraes, R., Hartmann, M., Haddad, C.F.B., 2012. Alternative reproductive modes of Atlantic Forest frogs. *J. Ethol.* 30, 331–336.
- Toledo, L.F., Llusia, D., Vieira, C.A., Corbo, M., Márquez, M., 2014. Neither convergence nor divergence in the advertisement call of sympatric congeneric Neotropical frogs. *Bioacoustics* 2014, 1–17.



- Touchon, J.C., Warkentin, K.M., 2008. Reproductive mode plasticity: aquatic and terrestrial oviposition in a treefrog. *Proc. Natl Acad. Sci. USA* 105, 7495–7499.
- Trewavas, E., 1933. The hyoid and larynx of the anura. *Phil. Trans. R. Soc. Lond., Ser. B.* 222, 401–527.
- Trueb, L., 1973. Bones, frogs, and evolution. In: Vial, J.L. (Ed.), *Evolutionary Biology of the Anurans: Contemporary Research on Major Problems*. University of Missouri Press, Columbia, MO, pp. 65–132.
- Trueb, L., 1993. Patterns of cranial diversification among the Lissamphibia. In: Hanken, J., Hall, B.K. (Eds.), *The Skull*. University of Chicago Press, Chicago, IL, pp. 255–343.
- Trueb, L., Tyler, M.J., 1974. Systematics and evolution of the Greater Antillean hyliid frogs. *Occ. Pap. Mus. Nat. Hist. Univ. Kans.* 24, 1–60.
- Tyler, M.J., 1971. The phylogenetic significance of vocal sac structure in hyliid frogs. *Occ. Pap. Mus. Nat. Hist. Univ. Kans.* 19, 319–360.
- Varón, A., Wheeler, W.C., 2012. The tree alignment problem. *BMC Bioinformatics* 13, 293.
- Varón, A., Wheeler, W.C., 2013. Local search for the generalized tree alignment. *BMC Bioinformatics* 14, 66.
- Werner, F., 1894. Über einige Novitäten der herpetologischen Sammlung des Wiener zoolog. vergl. anatom. Instituts. *Zool. Anz.* 17, 155–157.
- Wheeler, W.C., 1996. Optimization alignment: the end of multiple sequence alignment in phylogenetics?. *Cladistics* 12, 1–9.
- Wheeler, W.C., 2003a. Iterative pass optimization of sequence data. *Cladistics* 19, 254–260.
- Wheeler, W.C., 2003b. Implied alignment: a synapomorphy-based multiple sequence alignment method. *Cladistics* 19, 261–268.
- Wheeler, W.C., Aagesen, L., Arango, C.P., Faivovich, J., Grant, T., D'haese, C., Janies, D.A., Smith, W.L., Varon, A., Giribet, G., 2006. *Dynamic Homology and Phylogenetic Systematics: A Unified Approach Using POY*. American Museum of Natural History, New York, NY. ISBN 0-913424-58-7.
- Wheeler, W.C., Lucaroni, N., Hong, L., Crowley, L.M., Varón, A., 2015. POY version 5: phylogenetic analysis using dynamic homologies under multiple optimality criteria. *Cladistics* 31, 189–196.
- Wiens, J.J., Fetzner, J.W., Parkinson, C.L., Reeder, T.W., 2005. Hyliid frog phylogeny and sampling strategies for speciose clades. *Syst. Biol.* 54, 719–748.
- Wiens, J.J., Graham, C.H., Moen, D.S., Smith, S.A., Reeder, T.W., 2006. Evolutionary and ecological causes of the latitudinal diversity gradient in hyliid frogs: treefrog trees unearth the roots of high tropical diversity. *Am. Naturalist* 168, 579–596.
- Wiens, J.J., Kuczynski, C.A., Hua, X., Moen, D.S., 2010. An expanded phylogeny of treefrogs (Hylidae) based on nuclear and mitochondrial sequence data. *Mol. Phylogenet. Evol.* 55, 871–882.

## Supporting Information

Additional supporting information may be found online in the Supporting Information section at the end of the article.

**Figure S1.** Phylogenetic relationships of *Sphaenorhynchus* as recovered in one of the 14 most-parsimonious trees (length 751 steps) obtained from the analysis of the phenotypic dataset (PD).

**Figure S2.** Phylogenetic relationships of *Sphaenorhynchus* as recovered in one of the four most-parsimonious trees (length 8769 steps) obtained from the analysis of the molecular-only dataset (MD).

**Figure S3.** Dorsal views of the frontoparietals of (a) *Scinax alter* (MCP 1670), (b) *Sci. catharinae* (MCP

3427), (c) *Sphaenorhynchus planicola* (MNRJ 54808), (d) *S. palustris* (MNRJ 42656), (e) *S. pauloalvini* (MNRJ 4323) and (f) *Pseudis minuta* (MACN-He 43532) showing some states of characters 4, 5 and 6 (character number is followed by the state number). Scale bars = 2 mm.

**Figure S4.** Quadratojugal–squamosal relationship.

**Figure S5.** Lateral view of quadratojugal and squamosal showing states of characters 22 and 24–27 related to these bones (character number is followed by the state number).

**Figure S6.** Ventral view of pterygoid showing states of characters 29 and 30 related to the medial and posterior rami of this bone (character number is followed by the state number).

**Figure S7.** Ventral view of vomers showing states of characters 32, 34, and 39 related to this bone (character number is followed by the state number).

**Figure S8.** Plectral apparatus of (a) *Scinax alter* (MCP 1670), (b) *Scarthyla goinorum* (MCP 12962), (c) *Sphaenorhynchus caramaschii* (CFBH 6937), (d) *S. carneus* (ZUEC 5555) and (e) *S. pauloalvini* (MNRJ 4323).

**Figure S9.** Nasal cartilages of (a) *Sphaenorhynchus prasinus* (MZUESC 6861) and (b) *S. surdus* (MCP 8324). Character number is followed by the state number. Scale bars = 1 mm.

**Figure S10.** Ventral views of the anterior part of the larynx showing some states of character 74.

**Figure S11.** Ventral views of the larynx (character number is followed by the state number).

**Figure S12.** Lateral view of scapulae (left), and dorsal view of presacral and sacral diapophyses (right; character number is followed by the state number).

**Figure S13.** Subcloacal ornamentations.

**Figure S14.** Submandibular musculature of hyoid.

**Figure S15.** (a) Dorsal view of the right hand of *Sphaenorhynchus planicola* (MNRJ 54355); note two insertions of the EDCL on digit V, one on the metacarpal V (present in all taxa), and an additional one on the fascia of the medial slip of the EBP V, reaching proximally the proximal phalanx V (Ch. 171.1); also note the presence of the m-EBD IV (Ch. 174.1).

**Appendix S1.** Voucher specimens, collection numbers, localities and GenBank accession numbers of mitochondrial and nuclear genes sequences employed in this study.

**Appendix S2.** Voucher specimens examined for phenotypic characters.

**Appendix S3.** Uncorrected p-distances between 16S (AR-BR/Wilk fragment; ~570 bp) sequences of species of *Sphaenorhynchus*.

**Appendix S4.** Primers used to amplify and sequence DNA in this study.

**Appendix S5.** Phenotypic dataset employed in the cladistic analysis of *Sphaenorhynchus*.

**Appendix S6.** Description and analysis of phenotypic characters.

**Appendix S7.** List of potentially informative morphological variation in *Sphaenorhynchus*.

## Appendix A

### Diagnosis of *Sphaenorhynchini* and its internal clades

#### *Sphaenorhynchini* Faivovich et al., 2018

**Diagnosis.** This tribe includes only the genus *Sphaenorhynchus*; therefore, the synapomorphies that diagnose this tribe are redundant with those diagnosing that genus. The monophyly of *Sphaenorhynchini* is supported by molecular evidence and 25 phenotypic synapomorphies (jackknife support = 100%; GB = 90). These include narrow alary process of the premaxilla (Ch. 18.0, with instances of homoplasy in *Dendropsophus elegans* and *D. sanborni*); short zygomatic ramus of squamosal (Ch. 25.1, with instances of homoplasy in *D. elegans* and *Pseudis minuta*); moderately long posterior ramus of the pterygoid (Ch. 30.2); presence of medial portion of the anterior process of vomers (Ch. 38.0); absence of posterolateral process of the crista parotica (Ch. 45.0, with one instance of homoplasy in *P. minuta*); completely expanded *pars externa plectri* (Ch. 47.2); *pars externa plectri* directed ventrally with respect to the transversal axis of skull (Ch. 49.0, with instances of homoplasy in *D. microps*); coronoid process forming a small projection (Ch. 54.1); rectangular, anteroposteriorly expanded alary cartilage (Ch. 57.0); rectangular shape hyoglossal sinus (Ch. 68.2); presence of cartilaginous process of arytenoid supporting the frenulum in the larynx (Ch. 80.1); transverse process of presacral vertebra VI perpendicular to body axis; (Ch. 92.1, with instances of homoplasy in *D. elegans* and *D. sanborni*, *P. minuta* and *Scinax alter* + *Sci. fuscovarius* clade); dark coloured nuptial pad on finger II in males (Ch. 115.1); anteriorly directed larval nostril (Ch. 132.0); larval nostril with fleshy flanges (Ch. 133.1); presence of dark pigmentation on the ventral surface of the vent tube (Ch. 144.1); medial vent tube (Ch. 145.0, with one instance of homoplasy in *Pseudis minuta*); apical supplementary element of m. *intermandibularis* (Ch. 146.1); m. *geniohyoideus lateralis* with a single slip (Ch. 154.0); presence of Burton's ligament (Ch. 169.1, with one instance of homoplasy in species of *Scinax*); presence of m. *extensor brevis distalis digiti II* medial (Ch. 172.1); absence of supplementary slip from the Metacarpal IV of the medial slip of the m. *extensor brevis profundus digiti V* (Ch. 175.0); presence of m. *flexor ossis metatarsi II* (FM II) with origin from distal tarsal 2–3 (Ch. 177.1); presence of lateral slip of the foot m. *extensor brevis distalis digiti V* (Ch. 187.1, with one instance of homoplasy in *Sci. catharinae*); and white parietal peritoneum (Ch. 190.1).

**Characterization.** Small to medium-sized treefrogs (combined SVL in males 15.1–41.0 mm, females 36.0–46.0 mm) with a greenish dorsal background, translucent skin, green bones and white parietal peritoneum; pointed, rounded or protruding snout in lateral view; single, subgular vocal sac, notably distended while males calling, ventrally not reaching the pectoral region (in *Sphaenorhynchus pauloalvini* and *S. prasinus*) or enlarged reaching the pectoral fold (in the remaining species of the genus); dark or light coloured nuptial pads on finger II in males; absence or presence of tympanic membrane (present in *S. lacteus* and *S. pauloalvini*); absence or presence of dermal ornamentation (tubercles, folds and/or calcar appendages) on forearm, tarsus, elbow, heel and subcloacal region in adult males and females; absence or presence of premaxillary, maxillary and vomerine teeth; adults generally inhabit ponds in open areas and

forest edges; males vocalize while perched on floating vegetation or partially submerged in the water and, more rarely, on bushes and trees; advertisement call with pulsed notes; tadpoles with subterminal oral disc; uniform or irregular size marginal papillae; labial tooth row formula 1/2–3(1), 2/3(1) or 2(2)/3(1); eyes visible ventrally; short, medium-sized or extreme long spiracle; and medial vent tube posteroventrally directed, short, entirely fused to the ventral fin and positioned under the inferior margin of the ventral fin.

**Comments.** Most species of *Sphaenorhynchus* have been described as being green, very likely as a result of the impregnation of a high concentration of biliverdin on their tissues (Barrio, 1965; Taboada et al., 2017). Furthermore, green bones occur in juveniles and adults of most, if not all, species of *Sphaenorhynchus* (*S. canga*, *S. caramaschii*, *S. carneus*, *S. dorisae*, *S. lacteus* and *S. platycephalus*; Lutz and Lutz, 1938; Goin, 1957; Duellman, 1974; Araujo-Vieira et al., 2015a,b). We observed that *S. surdus* also has green bones. A green coloration also has been reported in eggs of *S. carneus* before being preserved (Suárez-Mayorga and Lynch, 2001). However, a spawn of *S. lacteus* photographed by Reichle and Köhler (1998) has creamy white animal poles, as did a spawn of *S. surdus* (K. Araujo-Vieira and T. Grant, pers. obs.). Suárez et al. (2013) reported on the chromosome morphology and some cytogenetic markers of *Sphaenorhynchus caramaschii*, *S. carneus*, *S. dorisae*, and *S. lacteus*. They noticed that *S. carneus* has an increment from the plesiomorphic 24 to 26 chromosomes. They also noticed that in *S. lacteus* there is a large euchromatic telomeric band that comprises nearly the distal half of pair 2p, which they considered as the possible origin of heterochromatic b chromosomes in *S. dorisae*. The sister taxon relation of these two species supported by our results is congruent with this explanation. Our optimal topology, however, indicates that in order to better understand chromosome evolution in *Sphaenorhynchus*, it is necessary to study karyotypes of at least *S. pauloalvini*, and of some of the other unstudied species that are important for any inference due to its phylogenetic position (e.g., *S. prasinus*, at least one species of the *S. planicola* group, and at least an additional species of the *S. platycephalus* group).

**Content.** One genus. *Sphaenorhynchus*, which includes 15 species, of which 12 are placed in three species groups, and three are unassigned to any group (*S. carneus*, *S. pauloalvini* and *S. prasinus*).

**Distribution.** Amazon and Orinoco basins of Bolivia, Brazil, Colombia, Ecuador, Peru, and Venezuela; Trinidad, Guyana, Surinam, French Guyana. Atlantic Forest of southeastern Brazil, from Pernambuco in the north to northern Rio Grande do Sul in the south.

#### The *Sphaenorhynchus planicola* group

**Sister taxon.** The poorly supported clade including *Sphaenorhynchus prasinus*, and the *S. lacteus* and *S. platycephalus* groups.

**Diagnosis.** The monophyly of the *S. planicola* group is supported by molecular evidence and five phenotypic synapomorphies (jackknife support = 100%; GB = 1). These include posterior portion of the internal margins of frontoparietals widely separated at the level of the *tectum synoticum* (Ch. 5.1, with one instance of homoplasy in *Xenohyla truncata*); presence of medial projection of the posterior margin of the exoccipitalis (Ch. 7.1, with one instance of homoplasy in *Scinax perpusillus*); extremely reduced posteromedial process of the parasphenoid (Ch. 43.0, with one instance of homoplasy in *Sphaenorhynchus canga*); the posterior extension of the fold of the m. *interhyoideus* surpassing the m. *pectoralis externalis* (Ch. 152.5, with instances of homoplasy in *Dendropsophus minutus* and *D. sanborni*); and the m. *extensor brevis superficialis digiti III* with an insertion on the third metatarsus (Ch. 185.1). Further, the combination of small SVL in males (combined SVL 15.7–24.1 mm); snout rounded in lateral view; well-developed vocal sacs, extending

laterally and toward the posterior of the pectoral region, with lateral longitudinal folds; presence of dermal fold on elbow and round calcar appendages; subcloacal ornamentation with white dermal flap with rounded lateral margins; absence of premaxillary and maxillary teeth; and absence of dorsolateral black and white lines differentiates species of this group from other species of *Sphaenorhynchus*.

**Characterization.** Small greenish treefrogs (combined SVL in males 15.7–24.1 mm; Lutz and Lutz, 1938; Caramaschi et al., 2009) with large vocal sac extending laterally and reaching the level of the pectoral fold, with longitudinal folds; rounded snout in lateral view; dark coloured nuptial pads on Finger II in males; absence of tympanic membrane; dermal folds on forearm, tarsus and elbow; round calcar appendage; round subcloacal dermal flap; absence of premaxillary, maxillary and vomerine teeth; absence of dorsolateral black and white lines; presence of black canthal line in some specimens of *S. planicola*; advertisement call of *S. mirim* consists of a single pulsed note with 9–25 pulses and duration of 0.034–0.101 s; known tadpoles of *S. planicola* with subterminal oral disc; marginal papillae composed of alternating large and small papillae (large papillae about twice as large as the small ones); labial tooth row formula 2(2)/3(1); third tooth posterior row inside the oral disc; and medium-sized spiracle (spiracle length 16–24% of body length).

**Content.** Two species. *Sphaenorhynchus mirim* Caramaschi et al., 2009; *S. planicola* (Lutz and Lutz, 1938).

**Distribution.** Coastal lowlands of the State of Rio de Janeiro and State of Espírito Santo, southeastern Brazil.

### The *Sphaenorhynchus lacteus* group

**Sister taxon.** The poorly supported clade including *Sphaenorhynchus prasinus* and the *S. platycephalus* group.

**Diagnosis.** The monophyly of the *S. lacteus* group is supported by molecular evidence and four phenotypic synapomorphies (jackknife support = 100%; GB = 31). These include nonmineralized intercalary elements between ultimate and penultimate phalanges (Ch. 101.0, with some instances of homoplasy in *Dendropsophus elegans*, *Scinax*, *S. platycephalus* and *Xenohyla truncata*); the light coloured nuptial pads on finger II in males (Ch. 115.0, with several instances of homoplasy in the outgroup taxa and in *S. canga*); the postaxial webbing reaches the midlength of the second phalanx of toe IV (Ch. 131.4, with instances of homoplasy in *S. botocudo*, *S. palustris* and *S. planicola*); the branch I of the m. *petrohyoideus posterior* inserted on the base of the posteromedial process of the hyoid (Ch. 158.0, with instances of homoplasy in *D. minutus*, *Pseudis minuta* and *Sci. alter*). Further, the combination of the larger SVL in males and females (combined SVL, males 26.0–41.0 mm, females 36.0–46.0 mm); pointed or rounded snout in lateral view; moderately developed vocal sac extending to the middle of the pectoral region; presence of dermal fold on elbow and round or triangular calcar appendages; subcloacal ornamentation with white dermal flap with triangular or rounded lateral margins; and absence of dorsolateral black lines differentiates these species from other species of *Sphaenorhynchus*.

**Characterization.** Relatively large greenish treefrogs (combined SVL in males 26.0–41.0 mm, females 36.0–46.0 mm; Rodriguez and Duellman, 1994) with large vocal sac reaching the level of the pectoral fold, with longitudinal folds in *S. lacteus*; rounded snout in lateral view; light coloured nuptial pads on finger II in males; absence or presence of tympanic membrane (present in *S. lacteus*); dermal folds on forearm, tarsus and elbow; round (as in *S. lacteus*) or triangular (as in *S. dorisae*) calcar appendage; round (as in *S. lacteus*) or triangular (as in *S. dorisae*) subcloacal dermal flap; absence or presence of premaxillary, maxillary, and vomerine teeth (present in *S. lacteus*); absence of dorsolateral black lines; presence of black

canthal and white dorsolateral lines in *S. lacteus*; advertisement calls composed of 2–26 pulsed note with duration of 0.02–0.42 s; tadpoles with subterminal oral disc; uniform size marginal papillae (as in *S. dorisae*) or composed of alternating large and small papillae (large papillae about twice as large as the small ones; as in *S. lacteus*); labial tooth row formula 2(2)/3(1) (as in *S. dorisae*) or 2/3(1) (as in *S. lacteus*); third tooth posterior row placed on the posterior labium of the oral disc (as in *S. dorisae*) or inside the oral disc (as in *S. lacteus*); and short spiracle (spiracle length 3–11% of body length).

**Content.** Two species. *Sphaenorhynchus dorisae* (Goin, 1957); *Sphaenorhynchus lacteus* (Daudin, 1800).

**Distribution.** Amazon and Orinoco basins of Bolivia, Brazil, Colombia, Ecuador, Peru, and Venezuela; Trinidad, Guyana, Surinam, French Guyana, and states of Maranhão and Piauí, northeastern Brazil.

### The *Sphaenorhynchus platycephalus* group

**Sister taxon.** *Sphaenorhynchus prasinus*, but its sister taxon relation with the *S. platycephalus* group is poorly supported.

**Diagnosis.** The monophyly of the *S. platycephalus* group is supported by molecular evidence and eight phenotypic synapomorphies (jackknife support = 98%; GB = 11). These are as follows: maxilla overlapping the premaxilla (Ch. 17.1, with some instances of homoplasy in *S. lacteus*, *S. pauloalvini*, and outgroup taxa); the inferior prenasal cartilage laterally oriented (Ch. 59.1, with instances of homoplasy in *S. carneus* and *S. lacteus*); presence of a cartilaginous lamina that extends from the cartilaginous branch to the inferior margin of the oblique cartilage (Ch. 62.1, with instances of homoplasy in *S. lacteus*, *S. pauloalvini* and species of *Dendropsophus*); dorsolateral white line present (Ch. 111.1, with instances of homoplasy in *D. sanborni*, *Sci. alter* and *S. lacteus*); subcloacal ornamentation with a weak glandular dermal fold (Ch. 117.4); presence of two lateral thick and flat dermal pads on the ventral surface below de cloaca (Ch. 118.4); poorly developed and slightly crenulated dermal folds on tarsus (Ch. 123.3); and small, rounded or flattened tubercles on heel (Ch. 124.1, with instances of homoplasy in *D. microps* and *Phyllodytes luteolus*). Besides these synapomorphies, the species included in this group can be differentiated from other species of *Sphaenorhynchus* by the combination of a protruding snout in lateral view; a moderately developed vocal sac extending to the middle of the pectoral region, with lateral longitudinal folds; and the presence of canthal and dorsolateral white lines delimited below by a dorsolateral black line.

**Characterization.** Medium-sized greenish treefrogs (combined SVL in males 22.5–36.0 mm, females 20.0–33.0 mm; Lutz and Lutz, 1938; Bokermann, 1966; Heyer et al., 1990; Toledo et al., 2007; Caramaschi et al., 2009; Araujo-Vieira et al., 2015b; Roberto et al., 2017), with large vocal sac reaching the level of the pectoral fold, with longitudinal folds; protruding snout in lateral view; dark or light coloured nuptial pads on finger II in males; absence of tympanic membrane; presence or absence of tubercles or crenulated dermal folds on forearm, tarsus, elbow and heel; presence of many enlarged tubercles (as in *S. platycephalus*) or white, glandular subcloacal dermal fold; presence of premaxillary, maxillary and vomerine teeth; presence of canthal and dorsolateral white lines delimited below by a canthal and dorsolateral black lines; advertisement calls composed of 1–43 pulsed notes with duration of 0.008–10.21 s; tadpoles with uniform size marginal papillae (as in *S. bromelicola*, *S. platycephalus* and *S. surdus*) or composed of alternating large and small papillae (large papillae about twice as large as the small ones; as in *S. caramaschii*, *S. canga* and *S. palustris*); labial tooth row formula 2(2)/3(1); third posterior tooth row inside the oral disc; short (as in



*S. caramaschii*), medium-sized (as in *S. bromelicola*, *S. canga*, *S. platycephalus* and *S. surdus*) or large-sized spiracle (as in *S. palustris*).

**Content.** Eight species. *Sphaenorhynchus botocudo* Caramaschi et al., 2009; *S. bromelicola* Bokermann, 1966; *S. cammaeus* Roberto

et al., 2017; *S. canga* Araujo-Vieira et al., 2015b; *S. caramaschii* Toledo et al., 2007; *S. palustris* Bokermann, 1966; *S. platycephalus* (Werner, 1894); *S. surdus* (Cochran, 1953).

**Distribution.** Atlantic Forest of southeastern Brazil, from Pernambuco in the north to northern Rio Grande do Sul in the south.

**Appendix S1.** Voucher specimens, collection numbers, localities, and GenBank accession numbers of mitochondrial and nuclear sequences employed in this study. Abbreviations: *12S*-tRNA valine-*16S* (*12S*, the intervening tRNA<sup>Val</sup>, and *16S*), *ND1* (*16S*, tRNA<sup>Leu</sup>, NADH dehydrogenase subunit 1, and tRNA<sup>Ile</sup>), and *RAG1* (recombination activating gene 1). Institutional abbreviations follow Sabaj (2016). CRR = Camila R. Rievers field number. JMP = José M. Padial field number. MVS = Magno V. Segalla field number. MTR and ITH = Miguel T. Rodrigues field number. SR = Steffen Reichle field number.

Voucher	Species	<i>12S</i> -tRNA valine- <i>16S</i>	<i>cytochrome b</i>	<i>ND1</i>	<i>RAG1</i>	rhodopsin	tyrosinase	Locality
<b>Outgroup</b>								
CFBH	<i>Phyllodytes luteolus</i> *	AY843721	AY843966	GQ366314	AY844494	AY844708	AY844150	Brazil: State of Espírito Santo, Municipality of Guarapari
CFBH 6287	<i>Dendropsophus elegans</i>	-	-	-	-	-	MK266667	Brazil: State of São Paulo, Municipality of Pinda
CFBH 14964	<i>D. elegans</i>	MK266719	MK266582	-	-	MK266642	-	Brazil: State of Espírito Santo, Municipality of Sooretama
CFBH 14568	<i>D. microps</i>	-	-	-	-	-	MK266668	Brazil: State of São Paulo, Municipality of Iporanga
CFBH 22025	<i>D. microps</i>	MK266720	MK266583	-	-	-	-	Brazil: State of Rio de Janeiro, Municipality of Teresópolis, Vale da Revolta
CFBH 6532	<i>D. minutus</i>	-	-	-	MK266641	MK266665	-	Brazil: State of São Paulo, Municipality of Itirapina
CFBH 18567	<i>D. minutus</i>	MK266721	MK266584	-	-	-	-	Brazil: State of Alagoas, Municipality of Campo Alegre, Barragem de Manibu
CFBH 19176	<i>D. minutus</i>	-	-	-	-	-	MK266669	Brazil: State of Manaus, Municipality of Alcantara
MACN-He 38638	<i>D. sanborni</i> *	AY843663	AY843906	-	AY844450	AY844653	AY844106	Argentina: Entre Rios, Depto. Islas Del Ibicuy, Ruta 12 Vieja, between Brazo Largo and Arroyo Luciano
MACN-He 37786	<i>Pseudis minuta</i> *	AY843739	AY843985	GQ366339	AY844505	-	-	Argentina: Entre Rios, Depto. Islas Del Ibicuy, Ruta 12 Vieja

Voucher	Species	12S-tRNA valine-16S	cytochrome b	NDI	RAG1	rhodopsin	tyrosinase	Locality
QULC 2340	<i>Scarthyia goinorum</i> *	AY843752	AY843997	AY819521	AY844514	AY844738	-	Brazil: State of Amazonas, Igarapé Nova Empresa
CFBH 13321	<i>Scinax alter</i>	-	-	-	-	-	MK266696	Brazil: State of Espírito Santo, Municipality of Anchieta
CFBH 15936	<i>S. alter</i>	-	-	MK266716	-	-	-	Brazil: State of São Paulo, Municipality of Cananéia, Ilha de Cananéia
MNRJ 38384	<i>S. alter</i>	MK266759	MK266611	-	MK266639	MK266663	-	Brazil: State of Espírito Santo, Municipality of Santa Teresa
CFBH 10319	<i>S. catharinae</i>	-	-	MK266717	-	-	-	Brazil: State of Santa Catarina: Municipality of Treviso
MCP 3734	<i>S. catharinae</i> *	AY844742	AY844001	-	AY844517	AY844742	-	Brazil: State of Rio Grande do Sul, Pró-Mata
SR 87	<i>S. fuscovarius</i>	MK266760	MK266612	-	MK266640	MK266664	MK266695	Bolivia: Tarija
CFBH 10799	<i>S. perpusillus</i>	-	-	-	-	MK266666	MK266697	Brazil: State of São Paulo, Municipality of São Luis do Paraitinga
CFBH 27384	<i>S. v-signatus</i>	MK266761	MK266613	MK266718	-	-	-	Brazil: State of Rio de Janeiro, Campos dos Goytacazes
CFBH 7600	<i>Xenohyla truncata</i> *	AY843775	AY844018	-	-	-	-	Brazil: State of Rio de Janeiro, Restinga de Maricá
<b>Ingroup</b>								
<b><i>Sphaenorhynchus</i></b>								
MNRJt 483	<i>S. botocudo</i>	MK266724	MK266587	MK266700	MK266614	-	MK266670	Brazil: State of Espírito Santo, Municipality of Mucurici, Lagoa Nova
UFMG 20767	<i>S. botocudo</i>	MK266723	MK266586	MK266699	-	-	-	Brazil: State of Bahia, Municipality of Mucuri
UFMG 20768	<i>S. botocudo</i>	MK266722	MK266585	MK266698	-	-	-	Brazil: State of Bahia, Municipality of Mucuri
ZUFG 5360	<i>S. botocudo</i>	MK266725	MK266588	MK266701	-	-	-	Brazil: State of Bahia, Municipality of Porto Seguro
MACN-He 48851	<i>S. cammaeus</i>	MK266727	MK266590	MK266703	MK266616	MK266644	MK266672	Brazil: State of Alagoas, Municipality of Quebrangulo, Rebio Pedra Talhada
MACN-He 48852	<i>S. cammaeus</i>	MK266726	MK266589	MK266702	MK266615	MK266643	MK266671	Brazil: State of Alagoas, Municipality of Quebrangulo, Rebio Pedra Talhada



Voucher	Species	12S-tRNA valine-16S	cytochrome b	ND1	RAG1	rhodopsin	tyrosinase	Locality
MNRJ 56336	<i>S. canga</i>	MK266728	MK266591	MK266704	MK266617	MK266645	MK266673	Brazil: State of Minas Gerais, Municipality of Mariana
CFBH 6876	<i>S. caramaschii</i>	MK266734	MK266594	MK266707	MK266621	MK266648	-	Brazil: State of São Paulo, Municipality of Ribeirão Branco
CFBH 10325	<i>S. caramaschii</i>	MK266732	MK266592	MK266706	MK266619	MK266646	MK266675	Brazil: State of Santa Catarina, Municipality of Treviso
CFBH 11285	<i>S. caramaschii</i>	MK266733	MK266593	-	MK266620	MK266647	MK266676	Brazil: State of São Paulo, Municipality of Ribeirão Branco
ITH 0626	<i>S. caramaschii</i>	MK266737	MK266596	MK266708	MK266623	MK266650	MK266678	Brazil: State of São Paulo, Municipality of Buri
MCP 11531	<i>S. caramaschii</i>	MK266739	-	-	MK266625	MK266652	MK266680	Brazil: State of Rio Grande do Sul, Municipality of Torres
MCP 11542	<i>S. caramaschii</i>	MK266738	-	-	MK266624	MK266651	MK266679	Brazil: State of Rio Grande do Sul, Municipality of Torres
MCP 11980	<i>S. caramaschii</i>	MK266729	-	-	-	-	-	Brazil: State of Santa Catarina, Municipality of São Bento do Sul
MCP 11981	<i>S. caramaschii</i>	MK266730	-	-	-	-	-	Brazil: State of Santa Catarina, Municipality of São Bento do Sul
MCP 12558 (written as 12258 on Fig. 1)	<i>S. caramaschii</i>	MK266731	-	MK266705	MK266618	-	MK266674	Brazil: State of Santa Catarina, Municipality of Blumenau, Nova Rússia
MZUSP 134240	<i>S. caramaschii</i>	MK266735	-	-	-	-	-	Brazil: State of São Paulo, Municipality of Embu das Artes
MZUSP 134698	<i>S. caramaschii</i>	MK266736	MK266595	-	MK266622	MK266649	MK266677	Brazil: State of São Paulo, Municipality of Jujuitiba
JMP 2091	<i>S. carneus</i>	MK266740	MK266597	MK266709	MK266626	MK266653	MK266681	Colômbia: Departamento Amazonas, Los Lagos, Bosque de Várzea
JMP 2094	<i>S. carneus</i>	MK266741	MK266598	MK266710	MK266627	-	MK266682	Colômbia: Departamento Amazonas, Los Lagos, Bosque de Várzea
CFBH 15721	<i>S. dorisae</i>	MK266742	MK266599	-	MK266628	MK266654	MK266683	Brazil: State of Acre, Municipality of Rodrigues Alves
MJH 46	<i>S. dorisae*</i>	AY843766	AY844011	-	AY844526	AY844753	AY844187	Brazil: State of Amazonas, Municipality of Manaus, Lago Janauari
CFBH 15725	<i>S. lacteus</i>	MK266743	MK266600	-	MK266629	MK266655	MK266684	Brazil: State of Acre, Municipality of Rodrigues Alves
USNM 152136	<i>S. lacteus*</i>	-	AY844012	-	AY844527	AY844754	AY844188	Peru: Madre de Dios, 30 km SSW Puerto

Voucher	Species	12S-tRNA valine-16S	cytochrome b	NDI	RAG1	rhodopsin	tyrosinase	Locality
USNM 268930	<i>S. lacteus</i> *	AY549367	-	-	-	-	-	Peru: Madre de Dios, Tambopata Reserve
UWIZM 4635	<i>S. lacteus</i>	MK266744	-	-	-	-	-	Trinidad and Tobago: Trinidad, Icaos
MNRJt 494	<i>S. mirim</i>	MK266745	MK266601	MK266711	MK266630	MK266656	MK266685	Brazil: State of Espírito Santo, Municipality of Mucurici, Fazenda Matutina
CFBH 22920	<i>S. pauloalvini</i>	MK266747	MK266603	MK266713	MK266632	-	MK266687	Brazil: State of Espírito Santo, Municipality of Linhares, Floresta Nacional de Goytacazes
CFBH 22925	<i>S. pauloalvini</i>	MK266748	-	-	-	-	-	Brazil: State of Espírito Santo, Municipality of Linhares, Floresta Nacional de Goytacazes
MTR 12098	<i>S. pauloalvini</i>	MK266749	MK266604	-	MK266633	MK266658	MK266688	Brazil: State of Espírito Santo, Municipality of Linhares, Floresta Nacional de Goytacazes
MTR 12116	<i>S. pauloalvini</i>	MK266750	MK266605	-	MK266634	MK266659	MK266689	Brazil: State of Espírito Santo, Municipality of Linhares, Floresta Nacional de Goytacazes
MNRJ 39704	<i>S. planicola</i>	MK266751	MK266606	-	-	-	MK266690	Brazil: State of Rio de Janeiro, Municipality of Maricá
CFBH 10573	<i>S. platycephalus</i>	MK266746	MK266602	MK266712	MK266631	MK266657	MK266686	Brazil: State of São Paulo, Municipality of Bairro Alto
USNM 243667	<i>S. platycephalus</i> **	DQ380388	-	-	-	-	-	Brazil: State of São Paulo, Municipality of Salesópolis, near Estação Biológica de Boracéia, Serra do Mar
CRR 70	<i>S. prasinus</i>	MK266754	MK266608	MK266714	MK266636	MK266661	MK266693	Brazil: State of Minas Gerais, Municipality of Marliéria, Parque Estadual do Rio Doce
MZUFBA 6756	<i>S. prasinus</i>	MK266752	-	-	-	-	MK266691	Brazil: State of Bahia, Municipality of Mata de São João, Fazenda Camurujipe
MZUFBA 6758	<i>S. prasinus</i>	MK266753	MK266607	-	MK266635	MK266660	MK266692	Brazil: State of Bahia, Municipality of Mata de São João, Fazenda Camurujipe
CFBHt 5536	<i>S. surdus</i>	MK266756	MK266610	-	MK266638	MK266662	-	Brazil: State of Santa Catarina, Municipality of Lebon Regis

<b>Voucher</b>	<b>Species</b>	<b><i>12S</i>-tRNA valine- <i>16S</i></b>	<b><i>cytochrome b</i></b>	<b><i>ND1</i></b>	<b><i>RAG1</i></b>	<b>rhodopsin</b>	<b>tyrosinase</b>	<b>Locality</b>
CFBH 8546	<i>S. surdus</i>	MK266755	MK266609	MK266715	MK266637	-	MK266694	Brazil: State of Santa Catarina, Municipality of Lages
MVS 399	<i>S. surdus</i>	MK266757	-	-	-	-	-	Brazil: State of Santa Catarina, Municipality of Santa Cecilia
UFRGSt 404	<i>S. surdus</i>	MK266758	-	-	-	-	-	Brazil: State of Santa Catarina, Municipality of Campo Belo

\*Sequences produced by Faivovich et al. (2005). \*\*Sequence produced by Wiens et al. (2006).

**Appendix S2.** Voucher specimens examined for phenotypic characters. Abbreviations: MM: Specimen studied for musculature. AA: Cleared and double stained specimen. Institutional abbreviations follow Sabaj (2016).

*Phyllodytes luteolus*: BRAZIL: Bahia: Nova Viçosa, MNRJ 23272–23274 (MM), 23275 (AA, male), 23277, 23280, 23288, 23290, 23292, 23297; Espírito Santo: Guarapari, Restinga de Setiba, CFBH 890 (MM), 6624 (larvae). *Dendropsophus elegans*: BRAZIL: Espírito Santo: Linhares, CFBH 22666 (MM); Rio de Janeiro: Santa Maria Madalena, Rancho da Lelê, MNRJ 53262–53263, 53264 (AA, male), 53265 (MM), 53266–53269; São Paulo: Ubatuba, Picinguaba CFBH 6614 (larvae). *Dendropsophus microps*: BRAZIL: Rio Grande do Sul: Itati, MCP 7220; São Francisco de Paula, Potreiro Novo, MCP 2475 (AA, MM, female), 2476–2479 (MM), 2480, 3429, 3432, 3438, 3483–3484, 3742–3743 (MM), 4497, 4506–4508; Santa Catarina: Córrego Grande MCP6339; São Paulo: Ribeirão Branco, Fazenda São Luiz, CFBH 1783 (MM). *Dendropsophus minutus*: ARGENTINA: Misiones: San Pedro, Entrada al Parque Provincial Cruce Caballero, MACN-He 41973 (MM); Guaraní, San Vicente, INTA, Cuartel Rio Victoria, MACN-He 43286 (MM), MACN-He 45097 (MM). BRAZIL: Rio Grande do Sul: Candiota, MCP 5270–5273, 5276–5277, 5282, 5284, 5288 (AA, MM, female), 5289, 5326, 5340, 5344, 5347, 5350, 5387 (MM), 5462, 5798, 5802, 5826 (MM), 5870, 5979; Cerro Largo, CFBH 22721 (larvae). *Dendropsophus sanborni*: BRAZIL: Rio Grande do Sul: Candiota, MCP 3922 (MM), 4321 (AA, MM, female), 4677–4684, 4689–4693, 4695, 4744–4746, 4789, 5452, 5631; Pelotas, Bacia Santa Bárbara, MCP 8019; Santa Cruz do Sul, MCP 7575. *Pseudis minuta*: ARGENTINA: Buenos Aires: Isla Talabera, MACN-He 43532 (AA, male); Entre Ríos: Islas Del Ibicuy, Ruta 12 vieja and Arroyo Luciano, MACN-He 39253 (MM), 40042 (AA, male), 40417 (MM), 40418 (MM). BRAZIL: Rio Grande do Sul: Candiota, MCP 5814, 5825–5826 (MM), 5830, 5833, 5846, 5848; Caçapava do Sul, MCP 3440, 3369; Porto Alegre, MCP 8355.

*Scarthyla goinorum*: BRAZIL: Acre: Cruzeiro do Sul, MCP 10566–10569, 12962 (AA, female), TG 2512 (MM; TG: Taran Grant field number deposited in MCP). *Scinax alter*: BRAZIL: Espírito Santo: Linhares, CFBH 26284 (MM); Santa Catarina: Córrego Grande, MCP 6347, 6349 (MM), 6353; Florianópolis, Lagoa do Peri, MCP 6324–6325, Praia da Joaquina, MCP 6327–6330, 6333, 6335, Praia dos Naufragados, MCP 6384; Rio Grande do Sul: Terra de Areia, Serra do Pinto, MCP 1670 (AA, male). *Scinax catharinae*: BRAZIL: Rio Grande do Sul: São Francisco de Paula, Proteiro Novo, MCP 3427 (AA, female), 3449, 3470 (MM), 3733–3734, 3772–3773. *Scinax fuscovarius*: ARGENTINA: Misiones: Guaraní, Km 1272, Cuartel Rio Victoria, INTA, MACN-He 34998 (MM) 35004 (MM). BRAZIL: Paraná: Jaguariaíva, Parque Estadual do Cerrado, CFBH 21028 (MM); Pinhão, Reservatório Rio Jordão, MCP 2013–2015, 2019–2021 (MM), 2029–2030 (AA, female), 2032 (MM), 2033, 2036–2039. *Scinax perpusillus*: BRAZIL: Rio de Janeiro: Rio de Janeiro, Urca, Morro Pão de Açúcar, MNRJ 40644–40645 (AA, male), 40646–40647, 40649 (MM), 40652, 40655, 40656, 40658, 40659. *Xenohyla truncata*: BRAZIL: Rio de Janeiro: Maricá, Restinga de Maricá, CFBH 20807 (larvae), MNRJ 33266–33267, 33268 (MM), 33270–33271, 33273, 33274, 33276 (AA, male), 33278. *Sphaenorhynchus botocudo*: BRAZIL: Espírito Santo: Mucurici, Fazenda Matutina, MACN-He 46458–46459 (AA, MM, female); MNRJ 50625–50626 (paratypes), 50629–50631 (paratypes), 50635–50636, 50639 (paratypes). *Sphaenorhynchus bromelicola*: BRAZIL: Bahia: Maracás, MZUSP 99475–99499, 101507–101515, 101518 (AA, male), 126109–126109; ZUEC 2789, Fazenda Santo Onofre, 10 km E Maracás, MZUSP 73754 (holotype), 73806–73813 (paratypes), 73831–73840 (paratypes), Fazenda Canabrava, MNRJ 4289 (MM), 4290, 4292, MZUSP 79559 (larvae). *Sphaenorhynchus cammaeus*: BRAZIL: Alagoas: Quebrangulo, Pedra Talhada Biological Reserve, Lagoa do Junco, URCA-H 9293 (holotype), URCA-H 6313–6321, 9285–9292, 9294 (paratypes), MACN-He 48852 (AA, MM, male). *Sphaenorhynchus canga*: BRAZIL: Minas Gerais: Mariana, Chapada de Canga, UFMG-A 5715 (holotype), MNRJ 56335



(AA, male), MNRJ 56337–56346 (paratypes), 5716–5717 (paratypes), UFMG 633a–b (larvae), 1.5 km W MG-129, UFMG-A 7192, 7194, 7205, 7207–7208 (paratypes), 7209 (AA, MM, male), MZUFV 11912–11915 (paratypes), 5.2 km S MG-129, UFMG-A 11732, 11738–11739 (paratypes). *Sphaenorhynchus caramaschii*: BRAZIL: São Paulo: Ribeirão Branco, Fazenda São Luiz, CFBH 2285–2293 (MM), 2294, 6933 (AA, female), 6934–6936 (MM; paratypes), 6937 (AA, male, paratypes), MNRJ 19373–19377 (MM); Iporanga, PETAR-Núcleo Ouro Grosso, CFBH 6320–6323; Pilar do Sul, CFBH 8289; Ribeirão Grande, CFBH 15581, 15583, Fazenda Intermontes. CFBH 26552 (larvae), 28652 (larvae), 35923 (larvae), 35924 (larvae); Santa Catarina: Treviso, CFBH 9854, 10325. MZUSP 84589, 134045, 134047. *Sphaenorhynchus carneus*: BRAZIL: Acre: Cruzeiro do Sul, Fazenda São Geraldo, ZUEC 3527, Porto Walter, ZUEC 8429 (MM), 8431, 11083 (MM); Tarauacá, Flooded places near the church, ZUEC 5555 (AA, male); Amazonas: Capim Flutuante-Rio Solimões, CFBH 4984–4985, Seringal América-Rio Purus, MZUSP 50408, 504010, Lago Pacatuba, MZUSP 53710, 53712, 53714–53715, Lago Amaná, MZUSP 58469, 58471–58472, 58474; Tabatinga, MZUSP 111240. COLÔMBIA: Caquetá, Alíngaros, MZUSP 99431–99432, 99436, 99440, 99446, 99448, 99453, 99456, 99458–99459, 99461–99462, 99464–99466, 99468–99469, 99471, 99472. *Sphaenorhynchus dorisae*: BRAZIL: Acre: Cruzeiro do Sul, MCP 10591–10595, MCP 12963 (AA, male), TG 2836 (MM; TG: Taran Grant field number deposited in MCP), Mâncio Lima, Lagoa da Cobra, ZUEC 5850 (MM), Porto Walter, ZUEC 8426–8427 (MM), Rio Tejo, ZUEC 11091, 11095, 11096 (AA, female), 11097–11098 (MM), 11100, 11103, 11106; Rodrigues Alves, Igarapé Croa-Alto do Juruá, CFBH 15721, 15723; Amazonas: Rio Solimões, Igarapé Belém, MZUSP 34669, 34677, 34676, 34680, 34672, 34674, Boca do Paraná do Catito, MZUSP 33190; Beruri, MZUSP 50552, Lago Janauari, MZUSP 53723, 53720, Seringal América, Rio Purus, MZUSP 50413, 50415. PERU: Loreto, Estirón, Rio Ampiyacu, MZUSP 32808, 32810. *Sphaenorhynchus lacteus*: BRAZIL: Acre: Cruzeiro do Sul, MCP 10570–10590, MCP 12960

(AA, male), 12961 (AA, female), TG 2545 (MM; TG: Taran Grant field number deposited in MCP), Humaitá do Moa, ZUEC 5429 (AA, male), Vila Militar, ZUEC 4689; Rio Branco, Mâncio Lima, Lagoa da Cobra, ZUEC 5853 (MM), Parque Zoobotânico, UFAC, ZUEC 5570 (MM), Sítio Engenheiro Ramon, ZUEC 5590, Xapuri, route to Vila Boa Vista, ZUEC 5705; Tarauacá, MZUSP 99340, 99335, 99339, 99337; Amazonas: Açaituba, Rio Purus, MZUSP 50465, Lago Janauari, MZUSP 53726, 53730, Reserva Ducke, MZUSP 75715; Beruri, MZUSP 50581; Borba, MZUSP 51196; Manaus, URCA-H 3495–3499, Lago do Castanho-Rodovia Manaus, ZUEC 3929 (MM), 7041; Humaitá, MNRJ 4284–4285 (MM), 4286–4287, Amaná, MZUSP 58500, 58494, 58497, 58490, 58491, Igarapé Belém, Rio Solimões, MZUSP 32846, 32841, 32845, 32814, 32817, 32835, 32837, 32821, Puruzinho, Rio Madeira, MZUSP 51487, 51493, 51492, Boca do Acre, MZUSP 50310, 50311; São José (Jacaré), Rio Solimões, MZUSP 40367, 40365; Tabatinga, MZUSP 11238; Pará: Belém, MZUSP 1505, 1507, Pasto de Búfalos, EMBRAPA, MNRJ 4288; Oriximiná, MZUSP 22526, Tapirapé Biological Reserve, MZUSP 140061, 140064, 140068, 140065; Tucuruí, MZUSP 76464; Rondônia: Porto Velho, MZUSP 99367, 99376, 99375, 99373, 99374, 99370, 99348, 99366, 99354, 99356, 99357, 99347, ZUEC 2707; Forte Príncipe da Beira, MZUSP 99426; Maranhão: Anajatuba, MNRJ 18270–18275, 18277–18279; São Luiz Gonzaga do Maranhão, MNRJ 36635. COLÔMBIA: Caquetá, Los Alicangaros, MZUSP 99409, 99411, 99421, 99419, 99425, 99414; Isla Santa Sofia, Amazonas, MZUSP 39168, 39170, 39169, 39172, 39175, 39174. PERU: Loreto, Estirón, Rio Ampiyacu, MZUSP 32801, 32802, 32804–32807. SURINAM: Pará, MZUSP 84625. *Sphaenorhynchus mirim*: BRAZIL: Espírito Santo: Mucurici, Fazenda Matutina, MACN-He 46460–46462 (AA, MM, female), MNRJ 50648–50650, 50652–50653 (paratypes). *Sphaenorhynchus palustris*: BRAZIL: Bahia: Porto Seguro, RPPN Estação Veracel, MZUSP 127834, 127831, 127835. MNRJ 42649 (MM), 42650–42656 (AA, female), 42657, RPPN Estação Vera Cruz, MNRJ 42616 (larvae); Espírito Santo: Conceição da Barra, Refugio Sooretama, MZUSP 73758

(holotype), 73770–73772 (paratypes), Vila de Itaúnas, MNRJ 54979, 54980, Rio Preto National Forest, MNRJ 54980 (MM), 54981–54982 (AA, male), 54983. *Sphaenorhynchus pauloalvini*: BRAZIL: Bahia: Ilhéus, CEPEC, MZUSP 73751 (holotype), 73773–73776 (paratypes), 73791–73803 (paratypes), 73841–73850 (paratypes), MZUSP 79568 (larvae), 79580 (larvae); Una, MZUFBA 7621, Fazenda Santa Izabel, MZUESC 6533 (MM); Espírito Santo: Linhares, MZUSP 101500, Estação Experimental Linhares, MNRJ 4303–4306, 4308, 4310, 4312 (MM), 4314, 4316, 4318, 4320–4323 (AA, female), 4324–4329 (MM), MTR 12256 (MM; MTR: Miguel T. Rodrigues field number deposited in MZUSP). *Sphaenorhynchus planicola*: BRAZIL: Bahia: Trancoso, MNRJ 47811, 47812, Between Barras de Caravelas and Ponta de Areia, MNRJ 4366–4368, 4370, 4372 (MM), 4373 (MM), 4374, 4377, 4378; Espírito Santo: Fundão, CFBH 1586; Linhares, CFBH 1575, MNRJ 4331 (MM), 4332, Serra, CFBH 1439, 1440; Marataízes, Distrito de Gomes, Fazenda Sr. Roberto Da Roseira, Marsh near Guarnanoi lake, MNRJ 35025–35027, Anchieta, MNRJ 25335; São Mateus, MNRJ 18417, 18418; Minas Gerais: Iperó, Fazenda Ipanema, MNRJ 32824–32827; Rio de Janeiro: Macaé, lake near the city access, ZUEC 8572; Magé, Campos dos Escoteiros, Citrolândia, MNRJ 54803–54808 (AA, male), 54809 (MM), 54810–54811, Vila das Pedrinhas, MNRJ 36265, 4361, 4364; Maricá, MNRJ 39704, Barra da Tijuca, MNRJ 26880; São João da Barra, MNRJ 6716, 6718–6722, 6723 (MM), 6724–6725, 6728 (AA, female), Recreio dos Bandeirantes, MNRJ 2084, Sernambetiba MNRJ 3520; Campos dos Goytacazes, Lagoas de Cima, Marsh near the lake, MNRJ 54353–54354, 54355 (MM), 54356 (MM), 54357–54359, Fazenda Barra Seca, MNRJ 41573–41578, 41759 (MM), 41760–41752, 41753 (MM), 41754–41583; Itaguaí, MZUSP 79552 (larvae), Old route Rio-São Paulo, Km 39, ZUEC 3808. *Sphaenorhynchus platycephalus*: BRAZIL: Rio de Janeiro: Serra do Mar, 4 km outside Petrópolis, in a canal leading to the dam at Quitandinha, AL-MN 3309 (holotype of *S. orophilus*); Petrópolis, MZUSP 680–681; Quintandinha, MNRJ 3130, AL-MN 3156–3160, 3379–3385; 3387–3389, 3391–3409, 3859–3862, 3881–3882, 3944–

3994, 4162; Teresópolis, Alto do Soberbo, MZUSP 53464, 53465 (AA, male), Açude da Granja Comary, MNRJ 4381–4382, Parque Nacional da Serra dos Órgãos, MNRJ 4359, 4387, Represa do Guinle, MNRJ 31731 (AA, male), MNRJ 31732, 31734–31735 (MM), 31737, ZUEC 4096; Nova Friburgo, Duas Pedras, AL-MN 2698, 2699 (paratypes of *S. orophilus*); Rio de Janeiro, MNRJ 126; Recreio dos Bandeirantes, MNRJ 2040; São Paulo: Bananal, MNRJ 4390; Salesópolis, Estação Biológica de Boracéia, MZUSP 60228–60230, 37668; Serra da Bocaina, Fazenda do Bonito, AL-MN 1566, 2129–2131 (paratypes of *S. orophilus*), AL-MN 956–958 MNRJ 4385; Mata do Segredinho, MNRJ 4383, 4384; São José do Barreiro, Rio Ponte Alta, MNRJ 4386; Bairro Alto: Hotel Fazenda Santa Rita, CFBH 10573; Between municipalities of São Paulo and Rio de Janeiro, Serra da Bocaina, Bonito, ALMN 4324 (larvae); Santa Catarina: between municipalities of Porto União and Concórdia, Rio Roseira, MZUSP 57915 (larvae).

***Sphaenorhynchus prasinus***: BRAZIL: Alagoas: Rio largo, MNRJ 38680–38683; Quebrangulo, Pedra Talhada Biological Reserve, URCA-H 9295; Maceió, Área de Proteção Ambiental Catolé, MUFAL 12247; Bahia: Ilhéus, CEPEC, MZUSP 73749 (holotype), 73750, 73761–73762 (paratypes), 73781–73787 (paratypes), MZUSP 79571 (larvae), 79553 (larvae), MZUESC 6533, 6534, 6861 (AA, female), 6862 (MM), 6863 (MM); Mata de São João, MZUFBA 7357 (MM), 4344 (MM), 4345–4346, 2962 (MM), 2969–2973; Itagibá, Fazenda Pedra Branca, MNRJ 4295 (MM), 4296–4297, 56348, 56349; Teixeira de Freitas, Fazenda Alcopadro, MNRJ 29664–29666 (MM), 29667–29668; Espírito Santo: Linhares, MZUSP 75641, 75643, EI 59 (AA, male; EI: Eugenio Izeckson field number deposited in UFRRJ); Minas Gerais: Aimorés, MNRJ 56347; Almenara, Fazenda Limoeiro, MZUFV, 4152, 5939, 5938; Marliéria, Rio Doce State Park, MZUFV, 2631, 2633, MNRJ 20874; Nanuque, MNRJ 4517; Teófilo Otoni, MZUSP 99512, 99513; Pernambuco: Recife, Dois Irmãos, MZUSP 99503.

***Sphaenorhynchus surdus***: BRAZIL: Paraná: Adrianópolis, Rocha Church's Dike, MHNCI 5401; Campina Grande do Sul, Cedro, MHNCI 4603–4607; Castro, Caxambú Forest Park, MHNCI 199, 221, 315–317, 319; São José



dos Pinhais, Cambuí Forest Reserve, MHNCI 852; Pirai do Sul, CFBH 8223; Piraquara, MCP 8324 (AA, male), 8325, Mananciais da Serra, MHNCI 1855, 2858, 2947, 2973, 2983, 5402, 5403; Quatro Barras, Estrada Graciosa, Corvo, MHNCI 1738–1747, Pinheiros Gralha Azul, Chácara São Francisco de Assis, MHNCI 3657, 3658, Estrada Graciosa, Alto da Serra, Rio Taquari, MNRJ 4744 (MM), 4745–4747, 4751, 5750; Telêmaco-Borba, Ribeirão Anta Brava, MHNCI 4896, Taboal da Vila Preta, MHNCI 4965, Lagoa do Gaúcho, MHNCI 4979; Tijucas do Sul, DZSJR 8656 (MM), 8788, 8789, 9049; Rio Grande do Sul: Vacaria, UFRGS 2488–2491, 2507, 2788; Bom Jesus, UFRGS 2797, 2893, 2894, 2898, 2900, 2902–2910, 3075, 3076, 3082, 3100, 3102–3104, 3108, 3109, 3112, 3121, 3135, 3136, 3138, 3139, 3145; São José dos Ausentes, MCP 4618–4622; Santa Catarina: Campo Belo do Sul, UFRGS 2787, 2895–2897, 2899, 2901, 2911, 3089, 3137, MCP 8422; Campos Novos, MCP 9324; Lages, CFBH 8546; Lébon Régis, MCP 8811; Lontras, MCP 1300–1302 (AA, male), 1305; Ponte Serrada, CFBH 15752; Rio Vermelho, MZUSP 99510; São Bento do Sul, MZUSP 99508; Near São Bento, MNRJ 4402–4404, 4406, 4407 (MM), 4410, 4412 (AA, male), 4415; São Paulo: São Paulo, Conchas, MZUSP 99521, MNRJ 4333; Apiaí, MZUSP 101466; Guapiara, MNRJ 4335, Fazenda Iperó, MNRJ 18249.

**Appendix S3.** Uncorrected p-distances between *16S* (AR-BR/Wilk fragment; ~570 bp) sequences of species of *Sphaenorhynchus*.

We calculated the uncorrected pairwise distances for (i) understanding intraspecific and interspecific levels of molecular variation in species of *Sphaenorhynchus*, (ii) addressing some taxonomic problems, and (iii) corroborating the identification of GenBank sequences when vouchers were not studied by us. Uncorrected pairwise distances were calculated in PAUP\* (Swofford, 2002) for the partial sequence AR-Wilk2/BR (~570 bp) of the mitochondrial ribosomal gene 16S rRNA of all *Sphaenorhynchus* with available tissue samples (Table S1; see also Appendix S1). In general, the intraspecific pairwise distance among *Sphaenorhynchus* varies from 0.0–1.5%, whereas the interspecific distance varies from 2.8–15%. The only exception is among sequences of *S. palustris* and *S. botocudo*.

The values obtained from comparisons of the *16S* fragment showed that specimens of *Sphaenorhynchus botocudo* (topotype MNRJt 483, Municipality of Mucurici, State of Espírito Santo, Brazil) and *S. palustris* (UFMG 20767–20768 and ZUFG 5360, municipalities of Mucuri and Porto Seguro, State of Bahia, Brazil, respectively) differ only in 0.5% (Table S2). In addition, we have been unable to differentiate the adult vouchers of *S. palustris* from topotypes of *S. botocudo* (see below). Therefore, we decided to assign the sequences of *S. palustris* from Bahia to *S. botocudo*, due this small molecular difference between those specimens.

Caramaschi et al. (2009) considered the longitudinal white blotch below the eye as an autapomorphy of *Sphaenorhynchus botocudo*. However, Lacerda and Moura (2013) have observed that white blotch is present in specimens of *S. bromelicola* and *S. palustris*. Additionally, we observed the presence of this white blotch in some specimens of *S. bromelicola* (MNRJ 4289–4290, 4292), *S. cammaeus* (URCA-H 9285–

9287, 9290, 9292, 9294), *S. canga* (MNRJ 56336), *S. palustris* (MNRJ 54979–54983; CFBH 2376–2377; MZUSP 127834–127835), and *S. surdus* (UFRGS 3364, 2897, 2893; MNHCI 1739).

Also, Caramaschi et al. (2009) differentiate *Sphaenorhynchus botocudo* from *S. palustris*, the species more morphologically similar to *S. botocudo*, by having (1) a wider dorsolateral white stripe delimited above and below by clear brown lines from the posterior corner of eye to the groin, and (2) the absence of dermal folds and appendages. We observed that the wide dorsolateral stripe delimited by brown lines is also present in some specimens of *S. palustris* (MNRJ 42652), *S. bromelicola* (MNRJ 101515), *S. canga* (MNRJ 56322–56331), *S. platycephalus* (MNRJ 31737), and *S. surdus* (MHNCI 1740–1742, 1745, 2983). Moreover, we studied some topotypes of *S. botocudo* and confirmed that a white and weak dermal fold can be present below of cloaca, and a poorly developed and slightly crenulated dermal fold or small and rounded tubercles arranged in line can be present on the ventrolateral edge of forearm and tarsus of *S. botocudo* (MACN-He 46458–46459).

Although, we have not observed morphological and osteological evidences that differentiate adults of *Sphaenorhynchus botocudo* from *S. palustris*, we decided to be conservative in respect to the taxonomic identity of *S. botocudo*, since the tadpole and the advertisement call of this species are unknown. Samples tissues of topotypes of *S. palustris* should be included in the analysis before any taxonomic decision about these species.

The values of the pairwise distances between specimens of *Sphaenorhynchus caramaschii* from the Brazilian states of São Paulo and Santa Catarina (Municipality of São Bento) are 0.2–0.7%. However, these specimens are 0.9–1.5% different from those of Treviso and Torres, State of Santa Catarina (municipalities of Blumenau and Treviso)

and Rio Grande do Sul, respectively. All specimens of *S. caramaschii* are 5.5–6.0% different from those of *S. surdus*, the species more morphologically similar to *S. caramaschii* (Table S3). Adults of *S. caramaschii* differ from *S. surdus* mainly by having the advertisement call with higher duration (2 s in *S. surdus*; Toledo et al., 2007), and also by having tadpoles with short spiracle and few large marginal papillae on the oral disc (medium-sized spiracle and small and homogenous papillae in *S. surdus*; Caramaschi, 2010; Araujo-Vieira et al., 2015a).

*Sphaenorhynchus lacteus* is the most widely distributed species of *Sphaenorhynchus*. We included sequences from vouchers collected in Peru, Department of Madre de Dios; Brazil, State of Acre, Municipality of Rodrigues Alves, and from Trinidad and Tobago, Trinidad, Icacos (Table S4). Although the sampling is reduced in comparison with its wide distribution, it encompasses localities that are more than 2000 km away. The pairwise distance is 0.5% between the specimen of *S. lacteus* from Icacos, Trinidad and Tobago (UWIZM 4635) and those of Department of Madre de Dios, Peru (USNM 268930) and Municipality of Rodrigo Alves, State of Acre, Brazil (CFBH 15725).

#### *Sphaenorhynchus platycephalus*

We calculated the uncorrected pairwise distance for the partial sequence of the ribosomal *12S* gene (~700 bp) of *Sphaenorhynchus platycephalus* (referred to *S. orophilus*; USNM 243667; Wiens et al., 2006) and the equivalent fragment of the remaining species with available sample tissues of *Sphaenorhynchus*. The values obtained from these comparisons demonstrated that the voucher of *S. platycephalus* (USNM 243667; Wiens et al., 2006) from Salesópolis, a locality near the Estação Biológica de Boracéia, Serra do Mar, Brazilian State of São Paulo, is only 0.4% different from that of *S. platycephalus* (CFBH 10573) from the Municipality of Bairro



Alto, State of São Paulo, distant about 52 km WSW from Salesópolis and 250 SW from the type locality of *S. orophilus*—junior synonym of *S. platycephalus*; Araujo-Vieira et al. (2018)—(Serra do Mar, 4 km; outside Petrópolis, in canal leading to the dam at “Quitandinha”, Rio de Janeiro, Brazil; Lutz and Lutz, 1938). Also, we examined the voucher (CFBH 10573) from Municipality of Bairro Alto, and confirmed that this specimen presents the morphological characters of *S. platycephalus* (referred to *S. orophilus*) described by Lutz and Lutz (1938). Therefore, we decided to use the complete sequences of *S. platycephalus* (CFBH 10573) for the Total evidence (TE) analysis. Compared to other species of *Sphaenorhynchus* with available sequences (Table S1), *S. platycephalus* (USNM 243667 and CFBH 10573) differs 3.0–6.7% from *S. botocudo*, *S. cammaeus*, *S. canga*, *S. caramaschii*, and *S. surdus*, the species more morphologically similar to *S. platycephalus*.

**Reference not cited in the main text.**

Swofford, D.L., 2002. PAUP\*. Phylogenetic Analysis Using Parsimony (\*and other 2384 methods). Sunderland, Sinauer Associates.

**Table S1.** Uncorrected p-distances (in percentage) of *16S* fragment (AR-BR/Wilk fragment; ~570 bp) among species of *Sphaenorhynchus*. See Appendix S1 for the complete list of GenBank accession numbers; and Table S3 for the GenBank accession numbers of three sequences of *S. surdus* not included in the phylogenetic analyses.

	<b>Species</b>	<b>1</b>	<b>2</b>	<b>3</b>	<b>4</b>	<b>5</b>	<b>6</b>	<b>7</b>	<b>8</b>	<b>9</b>	<b>10</b>	<b>11</b>	<b>12</b>	<b>13</b>
<b>1</b>	<i>S. botocudo</i> (n = 4)	-												
<b>2</b>	<i>S. cammaeus</i> (n = 2)	5.3–5.5	-											
<b>3</b>	<i>S. canga</i> (n = 1)	5.3–5.5	5.0	-										
<b>4</b>	<i>S. caramaschii</i> (n = 11)	6.4–7.2	3.5–3.7	5.8–6.3	-									
<b>5</b>	<i>S. carneus</i> (n = 2)	12.8–13.0	11.8	12.8	12.3–13.2	-								
<b>6</b>	<i>S. dorisae</i> (n = 2)	11.2–11.5	11.2–11.4	10.6–10.7	11.8–12.8	13.8–14.0	-							
<b>7</b>	<i>S. lacteus</i> (n = 3)	8.9–9.2	8.2–8.7	9.0–9.4	8.3–9.2	11.6–11.8	8.0–8.5	-						
<b>8</b>	<i>S. mirim</i> (n = 1)	13.7–14.2	13.0	13.1	13.1–14.1	15.0	11.0–11.2	10.5–11.0	-					
<b>9</b>	<i>S. pauloalvini</i> (n = 4)	9.7–10.0	8.2–8.6	10.0–10.1	8.8–9.8	10.9–11.3	11.0–11.4	9.7–10.3	12.4–12.8	-				
<b>10</b>	<i>S. planicola</i> (n = 1)	11.9–12.5	12.0	10.4	11.6–12.5	13.3	10.5–10.7	10.2–10.6	5.9	11.0–11.4	-			
<b>11</b>	<i>S. platycephalus</i> (n = 1)	5.3–5.5	4.9	4.0	6.2–6.7	12.1	11.0–11.2	9.0–9.5	12.0	8.9–9.3	9.8	-		
<b>12</b>	<i>S. prasinus</i> (n = 3)	9.3–9.5	7.6	8.1	7.8–8.8	11.3–1.8	10.7–11.3	8.0–8.3	11.2–11.8	8.3–8.5	11.4–12.0	8.5–8.6	-	
<b>13</b>	<i>S. surdus</i> (n = 7)	2.8–3.2	6.3–6.8	3.0–3.0	5.5–6.0	12.0–12.2	11.0–11.4	8.5–9.2	13.2–13.4	9.0–9.6	11.6–11.8	3.0–3.2	7.8–8.2	-

**Table S2.** Uncorrected p-distances (in percentage) between *16S* (AR-BR/Wilk fragment; ~570 bp) sequences of *Sphaenorhynchus botocudo*.

<b>Species</b>	<b>Locality</b>	<b>Voucher ID</b>	<b>GenBank accession number</b>	<b>1</b>	<b>2</b>	<b>3</b>	<b>4</b>
<b>1</b> <i>S. botocudo</i>	Brazil: State of Espírito Santo, Municipality of Mucuri	UFMG 20767	MK266723	-			
<b>2</b> <i>S. botocudo</i>	Brazil: State of Espírito Santo, Municipality of Mucuri	UFMG 20768	MK266722	0.5	-		
<b>3</b> <i>S. botocudo</i>	Brazil: State of Espírito Santo, Municipality of Mucurici, Lagoa Nova	MNRJt 483	MK266724	0.5	0.0	-	
<b>4</b> <i>S. botocudo</i>	Brazil: State of Bahia, Municipality of Porto Seguro	ZUFG 5360	MK266725	0.3	0.5	0.5	-

**Table S3.** Uncorrected p-distances (in percentage) between *I6S* (AR-BR/Wilk fragment; ~570 bp) sequences of *Sphaenorhynchus caramaschii* and *S. surdus*.

	Species	Locality	Voucher ID	GenBank accession number	1	2	3	4	5	6	7	8	9	10	11	12	13	14	15	16	17	18
1	<i>S. caramaschii</i>	Brazil: State of São Paulo, Municipality of Embu das Artes	MZUSP 134240	MK266735	-																	
2	<i>S. caramaschii</i>	Brazil: State of São Paulo, Municipality of Buri	ITH 0626	MK266737	0.3	-																
3	<i>S. caramaschii</i>	Brazil: State of São Paulo, Municipality of Jquitiba	MZUSP 134698	MK266736	0.2	0.2	-															
4	<i>S. caramaschii</i>	Brazil: State of São Paulo, Municipality of Ribeirão Branco	CFBH 6876	MK266734	0.3	0.3	0.2	-														
5	<i>S. caramaschii</i>	Brazil: State of São Paulo, Municipality of Ribeirão Branco	CFBH 11285	MK266733	0.5	0.2	0.4	0.5	-													
6	<i>S. caramaschii</i>	Brazil: State of Santa Catarina, Municipality of Blumenau, Nova Rússia	MCP 12558	MK266731	1.1	1.1	0.9	1.1	1.3	-												
7	<i>S. caramaschii</i>	Brazil: State of Santa Catarina, Municipality of Treviso	CFBH 10325	MK266732	1.2	1.2	1.0	1.2	1.5	0.2	-											
8	<i>S. caramaschii</i>	Brazil: State of Santa Catarina, Municipality of São Bento	MCP 11980	MK266729	0.5	0.5	0.3	0.2	0.7	1.2	1.4	-										
9	<i>S. caramaschii</i>	Brazil: State of Santa Catarina, Municipality of São Bento	MCP 11981	MK266730	0.5	0.5	0.3	0.2	0.7	1.2	1.4	0.0	-									
10	<i>S. caramaschii</i>	Brazil: State of Rio Grande do Sul, Municipality of Torres	MCP 11542	MK266738	1.2	1.2	1.0	1.2	1.5	0.2	0.0	1.4	1.4	-								
11	<i>S. caramaschii</i>	Brazil: State of Rio Grande do Sul, Municipality of Torres	MCP 11531	MK266739	1.2	1.2	1.0	1.2	1.5	0.2	0.0	1.4	1.4	0.0	-							
12	<i>S. surdus</i>	Brazil: State of Santa Catarina, Municipality of Santa Cecília	MVS 399	MK266757	5.5	5.6	5.5	5.5	5.9	5.9	6.0	5.7	5.7	6.0	6.0	-						
13	<i>S. surdus</i>	Brazil: State of Santa Catarina, Municipality of Matos Costa	MVS 627*	MK246172	5.5	5.6	5.5	5.5	5.9	5.9	6.0	5.7	5.7	6.0	6.0	0.0	-					
14	<i>S. surdus</i>	Brazil: State of Santa Catarina, Municipality of Bom Jesus	UFRGSt 382*	MK246173	5.5	5.6	5.5	5.5	5.9	5.9	6.0	5.7	5.7	6.0	6.0	0.0	0.0	-				
15	<i>S. surdus</i>	Brazil: State of Santa Catarina, Municipality of Campo Belo	UFRGSt 404	MK266758	5.5	5.6	5.5	5.5	5.9	5.9	6.0	5.7	5.7	6.0	6.0	0.0	0.0	0.0	-			
16	<i>S. surdus</i>	Brazil: State of Santa Catarina, Municipality of Lages	CFBH 8546	MK266755	5.5	5.6	5.5	5.5	5.9	5.9	6.0	5.7	5.7	6.0	6.0	0.0	0.0	0.0	0.0	-		
17	<i>S. surdus</i>	Brazil: State of Santa Catarina, Municipality of Lebon Régis	CFBHt 5536	MK266756	5.5	5.6	5.5	5.5	5.9	5.9	6.0	5.7	5.7	6.0	6.0	0.0	0.0	0.0	0.0	0.0	-	
18	<i>S. surdus</i>	Brazil: State of Paraná, Municipality of Piraquara, Mananciais da Serra	MHNCI 2858*	MK246174	5.7	5.6	5.5	5.5	5.9	5.9	6.0	5.7	5.7	6.0	6.0	0.2	0.2	0.2	0.2	0.2	0.2	-

\*Sequences not included in the phylogenetic analyses.



**Table S4.** Uncorrected p-distances (in percentage) between *I6S* (AR-BR/Wilk fragment; ~570 bp) sequences of *Sphaenorhynchus lacteus*.

<b>Species</b>	<b>Locality</b>	<b>Voucher ID</b>	<b>GenBank accession number</b>	<b>1</b>	<b>2</b>	<b>3</b>
<b>1</b> <i>S. lacteus</i>	Peru: Madre de Dios, Tambopata Reserve	USNM 268930	AY549367	-		
<b>2</b> <i>S. lacteus</i>	Trinidad and Tobago: Trinidad, Icacos	UWIZM 4635	MK266744	0.5	-	
<b>3</b> <i>S. lacteus</i>	Brazil: State of Acre, Municipality of Rodrigues Alves	CFBH 15725	MK266743	0.5	0.5	-

**Appendix S4.** Primers used to amplify and sequence DNA in this study.

<b>Primer</b>	<b>Sequence</b>	<b>Reference</b>
MVZ15	5'-GAACTAATGGCCACACWWTACGNAA-3'	Moritz et al. (1992)
CytB2	5'-AAACTGCAGCCCCTCAGAATGATATTTGTCTCA-3'	Moritz et al. (1992)
MVZ59	5'-ATAGCACTGAAAAYGCTDAGATG-3'	Graybeal (1997)
12SL1	5'-AAAAAGCTTCAAACCTGGGATTAGATACCCCACTAT-3'	Feller and Hedges (1998)
12SM	5'-GGCAAGTCGTAACATGGTAAG-3'	Pauly et al. (2004)
MVZ50	5'-TYTCGGTGTAAGYGARAKGCTT-3'	Graybeal (1997)
12SPhe2-L	5'-AAAGCATAAACTGAAGATGTTAAGATG-3'	Wiley et al. (1998)
12SFH	5'-CTTGGCTCGTAGTTCCTGGCG-3'	Goebel et al. (1999)
12SAL	5'-AAACTGGGATTAGATACCCCACTAT	Goebel et al. (1999)
12StRNA <sub>val</sub> -H	5'-GGTGTAAAGCGARAGGCTTTKGTAAAG-3'	Goebel et al. (1999)
12SL13	5'-TTAGAAGAGGCAAGTCGTAACATGGTA-3'	Feller and Hedges (1998)
16STitus I	5'-GGTGGCTGCTTTTAGGCC-3'	Titus and Larson (1996)
16SL2A	5'-CCAAACGAGCCTAGTGATAGCTGGTT-3'	Hedges (1994)
16SH10	5'-TGATTACGCTACCTTTGCACGGT-3'	Hedges (1994)
16SAR	5'-CGCCTGTTTATCAAAAACAT-3'	Palumbi et al. (1991)
16SWilk2	5'-GACCTGGATTACTCCGGTCTGA-3'	Wilkinson et al. (1996)
16SBR	5'-CCGGTCTGAACTCAGATCACGT-3'	Palumbi et al. (1991)
16S-frog	5'-TTACCCTRGGGATAACAGCGCAA-3'	Wiens et al. (2005)
tMet-frog	5'-TTGGGGTATGGGCCCAAAGCT-3'	Wiens et al. (2005)
R1-GFF	5'-GAGAAGTCTACAAAAAVGGCAAAG-3'	Faivovich et al. (2005)
R1-GFR	5'-GAAGCGCCTGAACAGTTTATTAC-3'	Faivovich et al. (2005)
RAG1 TG1F	5'-CCAGCTGGAAATAGGAGAAGTCTA-3'	Grant et al. (2006)
RAG1 TG1R	5'-CTGAACAGTTTATTACCGGACTCG-3'	Grant et al. (2006)
Rhod1A	5'-ACCATGAACGGAACAGAAGGYCC-3'	Bossuyt and Milinkovich (2000)
Rhod1C	5'-CCAAGGGTAGCGAAGAARCTTC-3'	Bossuyt and Milinkovich (2000)
Tyr 1C	5'-GGCAGAGGAWCRTGCCAAGATGT-3'	Bossuyt and Milinkovich (2000)
Tyr 1G	5'-TGCTGGGCRTCTCTCCARTCCCA-3'	Bossuyt and Milinkovich (2000)

### References not cited in the main text.

- Bossuyt, F., Milinkovitch, M.C., 2000. Convergent adaptive radiations in Madagascan and Asian ranid frogs reveal covariation between larval and adult traits. *Proc. Natl. Acad. Sci. USA* 97, 6585–9590.
- Feller, A.E., Hedges, S.B., 1998. Molecular evidence for the early history of living amphibians. *Mol. Phylogenet. Evol.* 9, 509–516.
- Goebel, A.M., Donnelly, J.M., Atz, M.E., 1999. PCR primers and amplification methods for 12S ribosomal DNA, the control region, cytochrome oxidase I, and cytochrome b in bufonids and other frogs, and an overview of PCR primers which have amplified DNA in amphibians successfully. *Mol. Phylogenet. Evol.* 11, 163–199.
- Graybeal, A., 1997. Phylogenetic relationships of bufonid frogs and tests of alternate macroevolutionary hypotheses characterizing their radiation. *Zool. J. Linn. Soc.* 119, 297–338.
- Hedges, S.B., 1994. Molecular evidence for the origin of birds. *Proc. Natl. Acad. Sci. USA* 91, 2621–2624.
- Moritz, C., Schneider, C.J., Wake, D.B., 1992. Evolutionary relationships within the *Ensatina eschscholtzii* complex confirm the ring species interpretation. *Syst. Biol.* 41, 273–291.
- Palumbi, S.R., Martin, A., Romano, S., McMillan, W.O., Stice, L., Grabawski, G., 1991. *The Simple Fool's Guide to PCR, Version 2.0*. Privately published, compiled by S. Palumbi, University of Hawaii: Honolulu.
- Pauly, G.B., Hillis, D.M., Cannatella, D.C., 2004. The history of a nearctic colonization: molecular phylogenetics and biogeography of the nearctic toads (*Bufo*). *Evolution* 58, 2517–2535.

- Titus, T.A., Larson, A., 1996. Molecular phylogenetics of desmognathine salamanders (Caudata: Plethodontidae): A reevaluation of evolution in ecology, life history, and morphology. *Syst. Biol.* 45, 451–472
- Wilkinson, J.A., Matsui, M., Terachi, T., 1996. Geographic variation in in a Japanese tree frog (*Rhacophorus arboreus*) revealed by PCR-aided restriction site analysis of mtDNA. *J. Herpetol.* 30, 418–423.
- Wiley, E.O., Johnson, G.D., Dimmick, W.W., 1998. The phylogenetic relationships of lampridiform fishes (Teleostei: Acanthomorpha), based on a total-evidence analysis of morphological and molecular data. *Mol. Phylogenet. Evol.* 10, 417–425.

**Appendix S6.** Description and analysis of phenotypic characters.

ADULT OSTEOLOGY

**(0) Medial relationship between nasals.** There is no contact between the medial margins of nasals in the examined species. However, the degree of aperture between them is informative. The nasals are weakly separated medially in *Sphaenorhynchus*, *Dendropsophus sanborni*, *Pseudis minuta*, *Scarthyla goinorum*, and *Scinax alter* (state 0.1).

0: Nasals widely separated medially. Medial margins at level of longitudinal axes that runs through superior prenasal cartilages. 1: Slightly separated medially. Medial margins of nasals located medial to longitudinal axes that run through superior prenasal cartilages and laterally to *septum nasi*. 2: Nasals juxtaposed *septum nasi*. Medial margins of nasals juxtaposed with *septum nasi*, but not in contact. **Additive.**

**(1) Anterior angular process.** The anterior angular process of the nasals reaches the *planum terminale* and covers a small portion of the oblique cartilage posteriorly. We observed this process in *Dendropsophus elegans* and *Xenohyla truncata*. Izecksohn (1998) observed the anterior angular process previously in *X. truncata*. The shape of anterior angular process is squarer in *D. elegans* and in subtriangular in *X. truncata*.

0: Absent. 1: Present.

**(2) Relationship between maxillary process of the nasal, postnasal wall, and *planum antorbitale*.**

0: Maxillary process terminating between postnasal wall and *planum antorbitale*. 1: Maxillary process surpassing posterior limit of the *planum antorbitale*.



**(3) Relation between nasals and sphenethmoid (Heyer, 1975).** *Sphaenorhynchus caramaschii*, *S. lacteus* and *S. prasinus* are polymorphic for this character. Faivovich (2002) reported that *Scinax granulatus* (referred to as *Sci. eringiophila*), *Sci. fuscovarius*, *Sci. oreites*, *Sci. perereca*, and *Sci. squalirostris* are also polymorphic. When the nasals do not overlap the sphenethmoid (state 3.0), the degree of separation between nasals and sphenethmoid varies inter- and intraspecifically in *Sphaenorhynchus*.

0: Nasals and sphenethmoid separate, non-overlapping. 1: Internal margins of nasals overlap the sphenethmoid.

**(4) Exposure of the frontoparietal fontanelle (Faivovich, 2002; Fig. S3).** According to Faivovich (2002), the morphology of the frontoparietal anterior to the *tectum synoticum* is associated with the level of exposition of the fontanelle. The character-states 4.0 and 4.1 correspond to states 3.0 and 3.3 of Faivovich (2002), respectively. The fontanelle is almost completely concealed in *Sphaenorhynchus* due to the medial proximity of the frontoparietals (state 4.1). In this state, the level of medial proximity between the internal margins of the frontoparietal is somewhat variable, with *S. palustris* and *S. carneus* being the two extremes of a continuum. In the former, the inner margins of the frontoparietals are slightly separated, whereas in the latter and in *S. pauloalvini*, and *S. planicola* they are fused in a few points (Fig. S3e).

0: Fontanelle almost completely exposed. The frontoparietals at the level of the fontanelle are slender strips of bone, variably divergent laterally. This determines that the posterior, dorsolateral margins of the sphenethmoid are partially exposed. 1: Fontanelle exposed through a narrow space between the internal margins of the frontoparietal.

**(5) Posterior portion of the internal margins of frontoparietals (Fig. S3).** The internal margins of the frontoparietals are separate and turn abruptly parallel at their posterior end in

*Scinax fuscovarius* (state 5.2). This condition was also observed in *Sci. icterica* by Faivovich (2002, fig. 4D).

0: Widely separated at the level of the *tectum synoticum*, with roughly straight margins. 1: Widely separated at the level of the *tectum synoticum*, with margins irregularly indented. 2: Inner margins excavated forming a small keyhole-like posteromedial fenestra. 3: Juxtaposed at the level of the *tectum synoticum*, leaving a narrow space between them. 4: Fused. The inner margins of the frontoparietals are fused medially. **Additive.**

**(6) *Tectum synoticum* (Fig. S3e-f).** The frontoparietals are fused posteriorly and the *tectum synoticum* is ossified in *Sphaenorhynchus pauloalvini*, whereas they are also fused posteriorly and the *tectum synoticum* is cartilaginous in *Pseudis minuta*. It suggests that the characters 5 and 6 are independent.

0: Cartilaginous. 1: Partially ossified. 2: Entirely ossified. **Additive.**

**(7) Medial projection of the posterior margin of the exoccipitalis.**

0: Absent. 1: Present.

**(8) *Lamina perpendicularis*.**

0: Poorly developed, reaches or almost reaches the orbitonasal foramen. 1: Well-developed, surpasses the level of orbitonasal foramen forming the superior portion of the lateral wall of the skull, not reaching the optic foramen.

**(9) Degree of anterior ossification of the sphenethmoid.**

0: Not incorporating the *septum nasi*. 1: Incorporating only the base of the *septum nasi*. 2: Incorporating at least half of the *septum nasi* length. **Additive.**

**(10) Nature of the *crista supraorbitalis*.** The *crista supraorbitalis* is a laterally directed ridge that extends posteriorly from the posteromedial margin of each postnasal wall on the anterodorsal corner of the orbit, above the orbitonasal foramen (Jurgens, 1971). We observed that the *crista supraorbitalis* can be separated from the postnasal wall by a non-cartilaginous portion (transparent; alcian blue-negative).

0: Separated from postnasal wall. 1: Continuous with postnasal wall.

**(11) Relative length of the *crista supraorbitalis*.** The length of the *crista supraorbitalis* is measured with respect to the horizontal diameter of the orbit. The *crista supraorbitalis* can be absent (MACN-He 43532 and MCP 3369) or present (MACN 40042) in *Pseudis minuta*; when present it is extremely short (state 11.0).

0: Extremely short, small projection. 1: Short, reaches one third of the horizontal diameter of the orbit. 2: Moderately long, reaches one half of the horizontal diameter of the orbit. 3: Elongate, reaches two third of the horizontal diameter of the orbit. **Additive.**

**(12) Maximum height of the *pars facialis* of the maxilla.** A poorly developed *pars facialis* is one of the synapomorphies suggested for *Sphaenorhynchus* by Duellman and Wiens (1992). In general, the *pars facialis* in *Sphaenorhynchus* (except *S. pauloalvini*) is slender and antero-posteriorly reduced relative to that of outgroups studied here. However, we find informative only the height of the *pars facialis* with respect to the height of the *pars dentalis*.

0: *Pars facialis* is 1–1.2 times higher than the *pars dentalis* height. 1: *Pars facialis* is approximately 2 times higher than the *pars dentalis* height. The *pars facialis* reaches approximately the half of the distance between maxilla and *processus lingularis*. 2: *Pars facialis* is approximately 3 times higher than the *pars dentalis* height. The *par facialis* reaches or almost reaches the *processus lingularis*. **Additive.**

**(13) Posterior extension of maxilla (Duellman and Wiens, 1992).** The transformation series is defined with respect to (1) the total length of maxilla, and (2) the distance from the anterior extreme of the maxilla to the articulation between the ventral ramus of squamosal and quadratojugal, which we call X-distance. We use the edges of the tympanum to describe the character-states only for to assist in visualizing the characters-states, because the position of tympanum is dependent on inclination (angle) of the ventral ramus of squamosal. Duellman and Wiens (1992) suggested that the reduced postorbital process of maxilla not in contact with the quadratojugal is a synapomorphy of *Sphaenorhynchus*. Indeed, the maxilla is reduced posteriorly (state 13.0) in all *Sphaenorhynchus* except *S. pauloalvini*. However, both the posterior reduction of the maxilla and the anterior reduction of the quadratojugal (*Dendropsophus* species and *S. pauloalvini*) lead to the separation of the maxilla and quadratojugal (see character 22). *Sphaenorhynchus* (except *S. pauloalvini*) shares an extremely reduced maxilla with *Dendropsophus microps*, *D. minutus*, *D. sanborni*, and *Xenohyla truncata* (state 13.0).

0: Posterior extreme of maxilla reaches approximately 1/2 of the X-distance. Maxilla reaches or almost reaches half of the orbit. 1: Posterior extreme of maxilla reaches approximately 2/3 of the X-distance. Maxilla surpasses half of the orbit, not reaching the anterior margin of the tympanum. 2: Posterior extreme of maxilla reaches approximately 5/6 of the X-distance. Maxilla reaches or surpasses the anterior margin of the tympanum. 3: Posterior extreme of maxilla surpasses 5/6 of the X-distance. Maxilla almost reaches the anterior margin of the tympanum, not touching the articulation between quadratojugal and squamosal. **Additive.**

**(14) Maxillary and premaxillary teeth.** Maxillary and premaxillary teeth are absent in *Sphaenorhynchus carneus*, *S. dorisae*, *S. mirim*, and *S. planicola*.

0: Absent. 1: Present.

**(15) Structure of the maxillary and premaxillary teeth in adults.** The ontogeny of dentition implies at least two generations of teeth: (1) a first generation that does not exhibit the pedicellate condition, characterized by calcification that begins at the top of the dental germ, extends to the base, and finally fixes the tooth to the maxilla or premaxilla, and (2) a second generation (with subsequent tooth replacement) corresponding to the pedicellate condition where each dental germ has two centers of calcification that progress independently (basal pedicel and distal crown), and are kept separated by an uncalcified weakness zone (Smirnov and Vasil'eva, 1995; Vasil'eva, 1997). Thus, the absence of pedicellularity in some taxa might be the result of a decrease in the rate of development (pedomorphosis) of the second generation of teeth or an increase in development by hypercalcification (peramorphosis) of the second and subsequent generations of teeth (Smirnov and Vasil'eva, 1995). In the case of *Sphaenorhynchus*, we observed the simultaneous occurrence of pedicellate and non-pedicellate teeth on the maxilla and premaxilla of adult specimens of *Sphaenorhynchus*, except those of *S. lacteus* and *S. pauloalvini*. Since there is no evidence of hypercalcification in *Sphaenorhynchus*, the occurrence of pedicellate and non-pedicellate teeth can be interpreted by a low or incomplete development of the dentition with late appearance or absence of the second generation of teeth.

0: Pedicellate teeth only. 1: Co-occurrence of both pedicellate and non-pedicellate teeth.

**(16) Portion of the *pars dentalis* of the maxilla with teeth.** In addition to the posterior reduction of the maxilla (character 13), in *Sphaenorhynchus* the maxillary teeth are separated by small or large diastemata (varying intra and interspecifically). It suggests that the teeth were lost and/or not replaced (maybe due to a low rate of replacement). We coded the relative length of these diastemata with respect to total maxillary length, which by itself is reduced in *Sphaenorhynchus* (see character 13 above).

Izecksohn (1998) suggested that *Xenohyla truncata* shares the reduced number of teeth on maxilla with *Sphaenorhynchus*. We observed that some *Sphaenorhynchus* (e.g. *S. caramaschii* and *S. lacteus*) share a maxilla without teeth along 35–40% of its length with *Xenohyla truncata*.

0: Maxilla dentate along 95 % of its length. 1: Maxilla edentate along 10–25% of its length. 2: Maxilla edentate along 35–40% of its length. 3: Maxilla edentate along 55–80% of its length. 4: Maxilla edentate along 95% of its length. **Additive.**

**(17) Relation between maxilla and premaxilla.**

0: Maxilla and premaxilla separate, not overlapping. 1: Maxilla overlaps the premaxilla.

**(18) Width of the base of alary process of the premaxilla.** Duellman and Wiens (1992) suggested that the reduced alary process of the maxilla is a synapomorphy of *Sphaenorhynchus*. We observed that the alary process in *Sphaenorhynchus* is less developed than that of outgroups, but its reduction is apparently related to some morphological variations (e.g. shape, length, and width of this process). We scored the width of the base of alary process in relation to the length of *pars dentalis*.

0: Narrow. Width of the base is approximately one third of the length of *pars dentalis*. 1: Intermediate. Width of the base is approximately half the length of the *pars dentalis*. 2: Wider. Width of the base is approximately two thirds of the length of *pars dentalis*. **Additive.**

**(19) Orientation of the premaxilla (Duellman and Wiens, 1992).** Duellman and Wiens (1992) suggested that the anteriorly inclination of the alary process of the maxilla is a synapomorphy of *Scinax*, *Scarthyla*, and *Sphaenorhynchus*. The orientation of the alary process is determined by the orientation of the premaxilla in the specimens examined. Therefore, we code the orientation of the premaxilla. We also observed that the degree of anterior inclination of the premaxilla in *Sphaenorhynchus* is somewhat variable



intraspecifically, with some individuals of *S. caramaschii*, *S. bromelicola*, *S. platycephalus*, and *S. surdus* showing the premaxilla more anteriorly inclined than in other *Sphaenorhynchus*.

0: Directed anteriorly. 1: Directed dorsally, almost perpendicular to maxilla.

**(20) Lateral orientation of the alary process of the premaxilla.**

0: Directed laterally. 1: Directed dorsally. 2: Directed medially. **Nonadditive.**

**(21) Portion of the *pars dentalis* of the premaxilla with teeth.** In *Sphaenorhynchus*, except for *S. pauloalvini* and *S. prasinus*, the teeth on the premaxilla are separated by diastemata whose quantity (1–3) and magnitude (short/long) vary intra- and interspecifically. For example, *S. lacteus* exhibits several narrow diastemata along the premaxilla, whereas *S. palustris* exhibits only one wide diastema.

0: Teeth distinctly separated by diastemata, part of the *pars dentalis* is edentate. 1: Teeth continuously present along the entire extension of *pars dentalis*.

**(22) Degree of anterior extension of the quadratojugal.** We code the transformation series based on the relation between (1) the size of quadratojugal and (2) the X-distance. The X-distance, as mentioned in the character 13, is the distance from the articulation of the ventral ramus of squamosal with quadratojugal to the anterior extreme of the maxilla. The degree of anterior extension is somewhat variable among the species of *Sphaenorhynchus* that share character-state 22.1. For example, *S. dorisae*, *S. lacteus*, and *S. palustris* have the quadratojugal slightly longer than that of *S. bromelicola*, *S. caramaschii*, *S. planicola*, and *S. surdus*. On the other hand, *S. carneus* shares an extremely reduced quadratojugal with *Dendropsophus microps*, *D. minutus*, and *D. sanborni* (state 22.0; Fig. S5a).

0: Extremely short. The quadratojugal is knob-shaped. 1: Short. The length of the quadratojugal corresponds to approximately 1/6 of the X-distance. Anteriorly, the quadratojugal does not surpass the external edge of the tympanic ring. 2: Elongate. The length of quadratojugal corresponds to 1/5–1/3 of X-distance. Anteriorly, the quadratojugal surpasses the tympanic ring. **Additive.**

**(23) Quadratojugal-squamosal relationship (Fig. S4).** The posterior part of the quadratojugal, which corresponds to the portion that usually contacts the squamosal and palatoquadrate cartilage, is absent in most species of *Sphaenorhynchus*. Instead, the quadratojugal posteriorly contacts a peculiar, anterior extension of the unmineralized quadrate process of the palatoquadrate (Fig. S4a). *Sphaenorhynchus pauloalvini* is polymorphic for this character state (CFBH 22928: state 23.0 and MNRJ 4323: state 23.1). Ontogenetic studies of the skull in *Sphaenorhynchus* are necessary to clarify the nature of the peculiar anterior extension of the palatoquadrate that contacts the quadratojugal.

0: Separate, quadratojugal articulating posteriorly with anterior process of palatoquadrate cartilage. 1: Quadratojugal and squamosal articulate.

**(24) Zygomatic ramus of the squamosal (Duellman and Wiens, 1992; Fig. S5).** Duellman and Wiens (1992) suggested that absence or reduction of the zygomatic ramus is a synapomorphy of *Sphaenorhynchus*. We code the absence/presence and the length (reduction *sensu* Duellman and Wiens, 1992) of the zygomatic ramus as two independent characters (see character 25). The zygomatic ramus is absent in *S. carneus* (Fig. S5a).

0: Absent. 1: Present.

**(25) Relative length of the zygomatic ramus of the squamosal (Fig. S5).** The length of zygomatic ramus is measured with respect to the minimum width of the ventral ramus of

squamosal. Except for *Sphaenorhynchus pauloalvini* (state 25.1; Fig. S5c), *Sphaenorhynchus* exhibits the zygomatic ramus extremely reduced when compared with that of outgroup taxa studied here. *Sphaenorhynchus prasinus* is polymorphic for the states 25.0 and 25.1.

0: Extremely short. Zygomatic ramus is 1.0–1.5 times longer than the minimum width of the ventral ramus. 1: Short. Zygomatic ramus is 2.2–2.4 times longer than the minimum width of the ventral ramus. 2: Moderately long. Zygomatic ramus is 3.2–3.6 times longer than the minimum width of the ventral ramus. 3: Elongate. Zygomatic ramus length corresponds to 4.8–5.8 times the minimum width of the ventral ramus. **Additive**

**(26) Otic ramus of the squamosal (Fig. S5).**

0: Absent. 1: Present

**(27) Shape of the otic ramus of the squamosal in lateral view (Fig. S5).**

0: Subtriangular or cuneiform. 1: Square. 2: Rectangular. **Nonadditive.**

**(28) Relationship between otic ramus of the squamosal and ossified portion of the crista parotica (Faivovich, 2002).** According to Faivovich (2002), the relationship between the otic ramus (otic plate) of the squamosal and the ossified portion of the crista parotica is influenced by both the level of expansion of the otic plate and the level of ossification of the crista parotica. Faivovich (2002, character 4) has suggested three character-states: slight or no overlap between otic plate and ossified portion of crista parotica (state 4.0); broad overlap between otic plate and ossified portion of crista parotica, due mainly to a highly ossified crista parotica (state 4.1); and broad overlap due mainly to an expanded otic plate and a less ossified crista parotica (state 4.2). Herein, we did not observe a broad overlap between otic plate and crista parotica (states 4.1 and 4.2 from Faivovich, 2002). Nevertheless, we were able to subdivide the state 4.0 from Faivovich (2002) into two discrete states, as described below.

Species of *Sphaenorhynchus* (except *S. carneus* and *S. pauloalvini*) have a broad gap between the otic plate and the ossified crista parotica, as a result of both the otic plate being extremely reduced and the crista parotica being poorly ossified. When compared to other *Sphaenorhynchus*, *S. pauloalvini* presents a slightly smaller gap, due to a great lateral expansion of otic plate and moderate ossification of the crista parotica. In *Dendropsophus microps* and *Scinax alter* the otic plate is separated from the ossified portion of crista parotica by a very narrow gap. In some other outgroups (e.g. *Pseudis minutus*, *Scinax catharinae*, *Sci. fuscovarius*, and *Scarthyla goinorum*), the otic plate juxtaposes or slightly overlaps to the ossified portion of crista parotica. The otic plate slightly overlaps the crista parotica in *Scinax fuscovarius*, because of the posteriormost distal tip of the otic plate (Faivovich, 2002).

0: Broad gap between otic plate and ossified portion of crista parotica, due to both otic plate reduced and crista parotica poorly ossified. 1: The otic plate is juxtaposed or slightly overlaps to ossified portion of crista parotica or between otic plate and ossified portion of crista parotica there is a gap very narrow. Both conditions because of an otic plate more developed or a crista parotica more ossified than previous state.

**(29) Orientation of mediodistal portion of the medial ramus of the pterygoid (Fig. S6).**

*Sphaenorhynchus*, except for *S. pauloalvini*, has the mediodistal portion of the medial ramus of pterygoid curved posterolaterally (state 29.1; Fig. S6a–c). This character is inapplicable for *Dendropsophus sanborni* because its medial ramus is very short and does not extend beyond half of the distance between its origin and basal process.

0: Directed posteromedially. 1: Directed posterolaterally.

**(30) Length of the posterior ramus of the pterygoid (Fig. S6).** Duellman and Wiens (1992)

suggested the absence of the posterior ramus of pterygoid is a synapomorphy of *Sphaenorhynchus*. However, the posterior ramus is present in all specimens of

*Sphaenorhynchus* examined, although it is extremely reduced (Fig. 4a–d). We observed informative variation with respect to the length of the posterior ramus. In *Sphaenorhynchus* the posterior ramus is extremely short (state 30.0), the only exception being *S. pauloalvini*, whose bone is notably longer (state 30.2). In *Dendropsophus elegans* and *D. sanborni* the posterior ramus is intermediate in length (state 30.1) between *S. pauloalvini* (state 30.2) and the other species of *Sphaenorhynchus* (state 30.0). We observed intra- and interspecific variation in the extension of the posterior ramus among the *Sphaenorhynchus* species that share state 0; in some cases the length of the posterior ramus can be different for each side of skull (e.g. *S. caramaschii*: CFBH 6937), with *Sphaenorhynchus dorisae* and *S. palustris* as the two extremes of a continuum (Fig. 4a–c).

0: Extremely short, reduced to rudimentary bumps. 1: Short. Posterior ramus of pterygoid reaches approximately the half of distance between the point of origin of the posterior ramus and the distal portion of the quadrate. 2: Moderately long. Posterior ramus of pterygoid reaches slightly more than the  $\frac{3}{4}$  of the distance between the point of origin of the posterior ramus and the distal portion of quadrate. 3: Elongate. Posterior ramus of pterygoid reaches the distal portion of quadrate. **Additive.**

**(31) Dentigerous process of the vomer.** The dentigerous process is absent only in *Sphaenorhynchus carneus*. The examined specimen of *Dendropsophus sanborni* (MCP 4321) is polymorphic; when present, the dentigerous process is extremely reduced, similar to the condition observed in *Sphaenorhynchus dorisae*.

0: Absent. 1: Present.

**(32) Development of the dentigerous process of vomer (Fig. S7).** We observed extreme reduction of the dentigerous process in *Dendropsophus sanborni*, *Sphaenorhynchus dorisae*, and *S. mirim* (Fig. S7a).

0: Extremely reduced. 1: Differentiated, dentigerous process with > 3 teeth.

**(33) Relationship between dentigerous and prechoanal/postchoanal processes.**

0: The dentigerous process is located between prechoanal and postchoanal processes. 1: The dentigerous process is located medially to the postchoanal process, approximately at the level of postnasal wall. 2: the dentigerous process is located posteriorly to the postchoanal process, approximately at the level of the internal margin of *planum antorbitale*. **Nonadditive.**

**(34) Relationship between the dentigerous process and the main body of the vomer (Fig.**

**S7).** We observed that, relative to other species, *Sphaenorhynchus botocudo*, *S. bromelicola*, *S. mirim*, *S. planicola*, and *S. prasinus* present a reduction of the medial portion that connects the dentigerous process with anterior, prechoanal, and postchoanal processes (state 34.1; Fig. 7b). The extreme reduction of this portion results in a complete separation of the dentigerous process from the processes of vomer (state 34.0; Fig. S9a). The specimen *S. prasinus* (MZUEC 6861) is polymorphic for the states 34.0 and 34.1, whereas *S. planicola* (MNRJ 54808) is polymorphic for the states 34.1 and 34.2.

0: Dentigerous process is separated of the main body of vomer. 1: Dentigerous process is contiguous to the main body by a medial portion constricted. 2: Dentigerous process is continuous to the main body of vomer. **Additive.**

**(35) Medial contact between dentigerous processes.** Dentigerous processes are medially in contact in the specimen of *Scinax fuscovarius* (MCP 2030).

0: Not in contact. 1: In contact.

**(36) Vomerine teeth.** The reduction of number of teeth may be related to the reduction of dentigerous process. However, the extreme reduction of dentigerous process does not imply the absence of vomerine teeth. For example, the vomerine teeth can be present, despite its



dentigerous process extremely reduced in *Sphaenorhynchus dorisae* (ZUEC 11096: state 36.1; MCP 12963: state 36.0). We consider this character inapplicable for *S. carneus*, because the dentigerous process is absent in this species.

0: Absent. 1: Present.

**(37) Structure of the vomerine teeth.**

0: Non-pedicellate. 1: Pedicellate.

**(38) Medial portion of the anterior process of vomers that covers the *solum nasi*.** In *Sphaenorhynchus*, the medial portion of the anterior process of the vomer that covers the *solum nasi* is absent. In this condition, the medial margins of the vomers diverge from each other approximately 20° at the level of the premaxilla with respect to the main axis, whereas when the anterior process is present, they diverge approximately 45°.

0: Absent. 1: Present.

**(39) Arrangement of the vomerine teeth on the dentigerous process (Fig. S7).**

0: Irregular. 1: Arranged in a continuous row.

**(40) Relative length of the palatines.** Duellman and Wiens (1992) suggested that reduced or absent palatines are a synapomorphy of *Sphaenorhynchus*. The palatines are absent in *S. carneus*, with its occurrence being polymorphic in *S. dorisae*. We only consider the length of the palatines as an informative character

0: Palatines are reduced to thin ossified slivers. 1: Palatines overlap only  $\frac{3}{4}$  of *planum antorbitale*. 2: Palatines overlap the *planum antorbitale*. 3: Palatines reach medially the lateral portion of sphenethmoid (reach the orbitonasal foramen). 4: Palatines reach the neurocranial portion of sphenethmoid. **Additive.**

**(41) Relative length of the cultriform process (Trueb, 1970).** The length of cultriform process is measured with respect to orbitonasal foramen.

0: Anterior end of the cultriform process is at the level of orbitonasal foramen. 1: Anterior end of the cultriform process is posterior to the orbitonasal foramen.

**(42) Shape of the anterior portion of the cultriform process (Clarke, 1981).**

0: Triangular. 1: Rounded. 2: Indented. 3: Truncated. **Nonadditive.**

**(43) Relative length of the posteromedial process of the parasphenoid.**

0: Extremely reduced. 1: Shorter than the half of the distance between the posterior margin of alary process and *foramen magnum*. 2: Reaches half of the distance between the posterior margin of alary process and *foramen magnum*. **Additive.**

**(44) Relative length of the alary process of the parasphenoid.** We code the length of the alary process with respect to the condyloid fossa.

0: Extremely short, not reaching the condyloid fossa. 1: Short, at level of condyloid fossa. 2: Elongate, surpassing the condyloid fossa. **Additive.**

**(45) Posterolateral process of the crista parotica.** This slender and cartilaginous process extends posteriorly from the posterolateral margin of the crista parotica.

0: Absent. 1: Present.

**(46) Shape of the tympanic *annulus*.**

0: Shallow. 1: Deep and expanded internally, the medial surface is unusually concave.

**(47) Expansion of the *pars externa plectri* (Duellman and Wiens, 1992; Fig. S8).**

Duellman and Wiens (1992) proposed that the round *pars externa plectri* is a synapomorphy of *Sphaenorhynchus*. However, although the expansion of the *pars externa plectri* is invariably present in *Sphaenorhynchus*, its shape varies intraspecifically (Fig. S8c). Therefore, instead of coding the shape of the *pars externa plectri*, we code its expansion.

0: Not expanded, cylindrical. 1: Mediodistal portion expanded. 2: Completely expanded.

**Additive.**

**(48) Relation between *pars externa plectri* and tympanic annulus (Duellman and Wiens, 1992).** The *pars externa plectri* entering posteriorly to the tympanic annulus is another synapomorphy proposed for *Sphaenorhynchus* by Duellman and Wiens (1992). We observed that the *pars externa plectri* is entering posteriorly to the tympanic annulus in all species of *Sphaenorhynchus* examined (state 48.1). Also, this condition is observed in *Pseudis minuta* and *Xenohyla truncata*. Alternatively, the *pars externa plectri* is entering dorsally to the tympanic annulus in *Dendropsophus* and *Scinax* species, *Phyllodytes edelmoi*, and *Scarthyla goinorum* (state 48.0).

0: *Pars externa plectri* entering dorsal to the tympanic annulus. 1: *Pars externa plectri* entering posterior to the tympanic annulus.

**(49) Orientation of the *pars media plectri* with respect to the transversal skull axis.** The *pars media plectri* may be either ventrally or dorsally directed with respect to the transversal axis of skull. The distribution of states between characters 48 and 49 suggests that they are independent. For example, the *pars externa plectri* enters posteriorly to the tympanic annulus (state 48.1), but is directed dorsally in relation to the transverse axis of skull in *Pseudis minuta* (state 49.1).

0: Directed ventrally. 1: Directed dorsally.

**(50) Expansion of the distal portion of *pars media plectri* (Fig. S8).** *Sphaenorhynchus caramaschii* has a completely expanded *pars externa plectri* (state 47.2) and unexpanded distal portion of the *pars media plectri* (state 50.2), whereas *Dendropsophus sanborni* shows a *pars externa plectri* with only the mediobasal portion expanded (state 47.1) and a slightly expanded *pars media plectri* (state 50.1). It suggests that characters 47 and 50 are independent.

0: Expanded. Width of the distal portion is approximately two times larger than the minimum width of the main body of *pars media plectri*. 1: Slightly expanded. Width of the distal portion is 1.2–1.3 times larger than the minimum width of the main body of *pars media plectri*. 2: Unexpanded. Width of the distal portion is equal or less than the width of the main body of *pars media plectri*. **Additive.**

**(51) Medial end of *pars media plectri* (Fig. 6d–e).** The dilated medial end of *pars media plectri* comprises the ventral and dorsal processes (except *Dendropsophus microps*, *D. minutus*, and *D. sanborni*), which fill the rostral portion of the *fenestra ovalis* and contacts the operculum in almost all adults of the outgroup taxa studied. However, in *Sphaenorhynchus* the medial end of *pars media plectri* is markedly (as in *S. carneus*) or slightly reduced (as in the remaining species of the genus, except for *S. pauloalvini*). The degree of reduction is variable within *Sphaenorhynchus*. In *S. caramaschii*, *S. lacteus*, *S. prasinus*, and *S. surdus*, the dorsal process is longer than the ventral process, whereas in *S. dorisae* and *S. planicola* the dorsal process smaller than the ventral process, but in *S. carneus* the ventral and dorsal processes are entirely absent (Fig. 6d–e). This reduction results in a large gap between the medial end of *pars media plectri* and the operculum (state 51.0). In the outgroup taxa the dilated medial end of *pars media plectri* encloses almost completely the operculum resulting in a very narrow gap separating it from the operculum (state 51.1).

0: Reduced medial end of *pars media plectri*, large gap between basal plate and operculum. 1: Dilated medial end of *pars media plectri*, very narrow gap between basal plate and operculum.

**(52) Relationship between the *pars interna plectri* and operculum.**

0: The *pars interna plectri* occupies the dorsal portion of the operculum. 1: The *pars interna plectra* is reduced and occupies a small space in the fenestra ovalis.

**(53) Mineralization of the *pars interna plectri* (Fig. S8).**

0: Mineralized. 1: Partially mineralized. 2: Not mineralized (stained by alcian blue or not stained). **Additive.**

**(54) Coronoid process.**

0: Absent. 1: Forming a small projection. 2: Forming a prominent projection. **Additive.**

**(55) Relationship between angulosplenic and dentary.**

0: In contact or adjacent, a small space is visible between angulosplenic and dentary. Meckel's cartilage is covered by angulosplenic. 1: Not in contact, a large space is visible between angulosplenic and dentary, exposing Meckel's cartilage.

**(56) Nature of the connection between the superior prenasal and alary cartilages.** The anterior convex face of the alary cartilage is synchondrotically fused to the prenasal cartilage (e.g. *Sphaenorhynchus pauloalvini*) or separated by unchondrified tissue (e.g. *S. dorisae* and *S. prasinus*). The condition "unchondrified tissue" was defined based on the absence of Alcian blue staining. Histological studies are necessary to corroborate this observation.

0: Separated by unchondrified tissue. 1: Synchondrotically fused.

**(57) Shape of the alary cartilage.**

0: Rectangular, anteroposteriorly expanded. 1: Square, an equivalent expansion anteroposteriorly as laterolaterally.

**(58) Contact point of the inferior prenasal cartilage on the alary process of the premaxilla (Fig. S9).** The inferior prenasal cartilage extends anteroventrally from the *solum nasi* to the posterior side of the alary process of the maxilla.

0: Located on the basal portion of the posterior face of the alary process. 1: Located on the middle of the posterior face of the alary process.

**(59) Orientation of the portion of the inferior prenasal cartilage that articulates with the *solum nasi*.**

0: Oriented mediolaterally. 1: Oriented laterally.

**(60) Shape of the median prenasal process of the *septum nasi*.**

0: Subcylindrical. 1: Subtriangular. 2: Triangular 3: Rounded. **Nonadditive**

**(61) Relative length of the median prenasal process of the *septum nasi*.** We code this character with respect to the alary process of the maxilla.

0: At the level of the alary process of the premaxilla. 1: Surpassing the alary process of the premaxilla.

**(62) Cartilaginous lamina that extends from cartilaginous plate to the inferior margin of the oblique cartilage (Fig. S9).** This lamina is present in *Sphaenorhynchus bromelicola*, *S. caramaschii*, *S. lacteus*, *S. palustris*, *S. pauloalvini*, *S. platycephalus*, *S. surdus*, and *Dendropsophus* species.



0: Absent. 1: Present.

**(63) Connection between *lamina nariochoanalis* and postnasal wall (Fig. S9).** Jurgens (1971) reported that in *Spea intermontana* (referred to as *Scaphiopus intermonatanus*) the posteroventral corner of the cartilaginous plate of the *planum terminale* continues posteriorly as a strip of cartilage that fuses with the lateral aspect of the roof of the median, hollowed-out part of the postnasal wall. Jurgens (1971) also described that by forming a bridge between the *lamina nariochoanalis* and the postnasal wall, the strip of cartilage bounds the *fenestra endochoanalis* laterally and at the same time forms the ventrolateral border of the *fenestra nasolateralis*. A comparable condition exists in larval stages of *Pelobates* (Pelobatidae), but the connection is broken in the adult (Jurgens, 1971). We observed a similar condition in adult specimens of *Sphaenorhynchus*, except *S. carneus* and *S. pauloalvini*.

0: *Lamina nariochoanalis* connected to the postnasal wall. 1: *Lamina nariochoanalis* not connected to the postnasal wall.

**(64) Anterior process of hyale.** Duellman and Wiens (1992) mentioned that *Scarthyla* and *Scinax* share the presence of an anterior process of the hyale. We also observed this process in *Phyllodytes luteolus*, *Pseudis minuta*, *Sphaenorhynchus pauloalvini*, and *Xenohyla truncata*.

0: Absent. 1: Present.

**(65) Shape of the anterior process of the hyale.**

0: Slender, not expanded distally. 1: Dendriform. 2: Laminar. **Nonadditive.**

**(66) Shape of the anterolateral process.**

0: Slender, not expanded distally. 1: Slender, expanded distally. 2: Laminar. **Nonadditive.**

**(67) Relative length of the posterolateral process in males (Liem, 1970).** The length of the posterolateral process is measured relative to the total length of posteromedial process (including the cartilaginous portion). The posteromedial process of males is longer than that of females of same species. However, the length of the posteromedial process was interspecifically variable only in males.

0: Short. The length of the posterolateral process is 6–6.5 times shorter than the total length of posteromedial process. 1: Moderately long. The length of the posterolateral process is 3–3.5 times shorter than the total length of posteromedial process. 2: Elongate. The length of the posterolateral process is 2–2.5 times shorter than the total length of posteromedial process.

**Additive.**

**(68) Shape of the hyoglossal sinus (Liem, 1970; Scott, 2005).**

0: U-shaped. 1: V-shaped. 2: Rectangular. 3: Round. **Nonadditive.**

**(69) Hyale (Duellman and Wiens, 1992).** Duellman and Wiens (1992) suggested that medially curvature of the hyales is a synapomorphy of *Sphaenorhynchus*. We corroborated that the hyales are medially curved in *Sphaenorhynchus*, except for *S. pauloalvini*. We also observed continuous intraspecific variation in the degree of the medial curvature. The continuous variation goes from hyales slightly curved medially to broadly curved and overlapping medially.

0: Hyales straight. 1: Hyales curved medially.

**(70) Maximum length of the hyoid plate.** The maximum length of the hyoid plate is coded with respect to its minimum width. *Sphaenorhynchus* presents the hyoid plate shorter than *Scarthyla goinorum* and *Scinax*, and longer than *Pseudis minuta*. Among the species of *Sphaenorhynchus*, *S. planicola* presents the longest hyoid plate.

0: Length of hyoid plate corresponds to approximately 1/6 its minimum width. 1: Length of hyoid plate corresponds to 1/3–2/3 its minimum width. 2: Length of hyoid plate corresponds to 1–1.3 times its minimum width. **Additive.**

**(71) Point of attachment of the hyale to the skull (da Silva, 1998).**

0: Hyale attached to the basal process. 1: Hyale attached to the limit between basal process and otic capsule. 2: Hyale attached to the otic capsule. **Additive.**

**(72) Esophageal process in males (Faivovich, 2002, fig. 6).**

0: Absent. 1: Present.

**(73) Orientation of the esophageal process.** The esophageal process is perpendicular to the main axis of cricoid ring cartilage in the states 73.0 and 73.1.

0: Directed ventrally. 1: Directed dorsally. 2: Directed posteriorly, parallel to the main axis of cricoid ring cartilage. 3: Directed obliquely, forming an acute angle with the main axis of cricoid ring cartilage. **Nonadditive.**

**(74) Shape of the cardiac process (Faivovich, 2002, fig. 7; Fig. S10).** Herein, states 75.0, 74.3 and 74.5 correspond to the states 13.3, 13.2 and 13.0 from Faivovich (2002). *Sphaenorhynchus pauloalvini* presents the U-shaped cardiac process similar to that observed for *Aplastodiscus perviridis*, *Smilisca baudini*, and *Sm. sila* by Faivovich (2002). Only *Scinax alter* has a V-shaped cardiac process (Fig. S10d). In *Sphaenorhynchus lacteus* and *S. planicola*, which share the state 74.1, there is a small variation related to development of the medial projection of the cardiac process (Fig. S10a–b), with *S. lacteus* presenting a more developed medial projection than *S. planicola*.

0: Subcylindrical, width similar to or slightly thinner than adjacent parts of the ring. 1: Laminar, with a medial projection. 2: Laminar, width similar to or slightly thinner than adjacent parts of the ring. 3: Laminar, wider than adjacent parts of the ring. 4: V-shaped. 5: U-shaped. **Nonadditive.**

**(75) Internal buttresses of the arytenoids (Faivovich, 2002).**

0: Absent. 1: Present.

**(76) Number of internal buttresses of the arytenoids (Faivovich, 2002; Fig. S11).**

0: One, in medial position. 1: Three, one in medial position and one on each distal third.

**(77) Rod of cartilage supporting each end of the vocal cords (Fig. S11).** This structure was observed in *Scinax ruber* (referred to as *Hyla rubra*) by Trewavas (1933). Lambiris (1994) also reported "cartilaginous support rods" in the larynges of the South African bufonids that he examined; however, material of those species was not available for this study and it is not clear what his "supporting rods" are.

0: Absent. 1: Present.

**(78) Fibrous masses of the larynx.**

0: Not chondrified (absence of alcian blue and red). 1: Partially mineralized. 2: Chondrified.

**Nonadditive.**

**(79) Shape of the fibrous masses (Fig. S11).**

0: Subtriangular, occupying the medial portion of the internal space of arytenoid. 1: Elongate, occupying a slightly less than half of the internal space of arytenoid.

**(80) Cartilaginous process of arytenoid supporting the frenulum (Fig. S11).** This process is present in males of *Sphaenorhynchus*. Previously, it was observed in *Scinax ruber* (referred to as *Hyla rubra*) by Trewavas (1933).

0: Absent. 1: Present.

**(81) Relative length of coracoids (Duellman and Wiens, 1992; Fig. S12).** Duellman and Wiens (1992) suggested that elongate coracoids and clavicles are a synapomorphy of *Sphaenorhynchus*. The relative length of coracoids and clavicles is measured with respect to snout-vent length (SVL). All species of *Sphaenorhynchus* except for *S. pauloalvini* share elongate coracoids and clavicles with *Phyllodytes luteolus* (states 81.1 and 82.1). Although the distribution of their characters-states in the matrix show that the length of coracoids is dependent on the length of clavicles, we code them as two independent characters, since in others species (e.g. clavicles absent or reduced in microhylids; Trueb, 1973) these characters vary independently.

0: Short, coracoids are 0.10–0.14 times the SVL. 1: Elongate, coracoids are at least 0.17 the SVL.

**(82) Relative length of clavicles (Duellman and Wiens, 1992).**

0: Short, clavicles are 0.08–0.10 times SVL. 1: Elongate, clavicles are at least 0.15 times SVL.

**(83) Relative length of scapulae (Fig. S12).** We measured the length of scapulae with respect to the length of the lateral margin that contacts the suprascapula. In contrast to elongate coracoids and clavicles, *Sphaenorhynchus* (except for *S. carneus* and *S. pauloalvini*) presents short scapulae (state 83.0; Fig. S12a). It shares this character-state with *Phyllodytes luteolus* and *Xenohyla truncata*.

0: Short, scapulae are 1.15–1.4 times longer than the length of the margin that contacts the suprascapula. 1: Elongate, scapulae are 1.75–2.20 times longer than the length of the margin that contacts the suprascapula.

**(84) Anterior margin of scapula.**

0: Concave, with a medial constriction. 1: Oblique to body axis.

**(85) Anterior process of suprascapula (Tyson, 1987).**

0: Absent. 1: Present.

**(86) Relative width of *pars acromialis*.** *Pseudis minuta* and *Xenohyla truncata* share an expanded *pars acromialis* (state 86.0).

0: *Pars acromialis* is almost 2 times more expanded than the *pars glenoidalis*. 1: *Pars acromialis* is equal to or slightly more expanded than the *pars glenoidalis*.

**(87) Shape of the distal portion of sternum.**

0: Expanded, bilobed, the distal portion of sternum is medially divided. 1: Expanded, simple.

**(88) Distal portion of the omosternum.**

0: Not Expanded. 1: Expanded.

**(89) Relative length of the base of omosternum.** This character is coded with respect to the minimum width of the base of omosternum.

0: The length of the base of omosternum is 1.0–2.0 times the width of its base. 1: The length of the base of omosternum is at least 2.6 times the width of its base.

**(90) Orientation of the transverse process of Presacral Vertebra II (Fig. S12).**

0: Inclined anteriorly. 1: Perpendicular to body axis.

**(91) Relative length of the transverse process of Presacral Vertebra IV (Duellman and Wiens, 1992; Fig. S12).** Duellman and Wiens (1992) proposed that the elongate and posteriorly oriented transverse process of Presacral Vertebra IV is a synapomorphy of *Sphaenorhynchus*. We observed that the transverse process of Presacral IV is clearly elongate and curved posteriorly in *Sphaenorhynchus* (Fig. S12d); the only exception is for *S. pauloalvini*. According to Izecksohn (1996), *Xenohyla truncata* shares the transverse processes of Presacral Vertebra IV elongate and oriented posteriorly with *Sphaenorhynchus*. However, we observed that *X. truncata* present a moderately long transverse process (state 91.1), a condition shared with *S. pauloalvini* and other outgroups (e.g. *Dendropsophus microps*, *Scarthyia goinorum*, and *Pseudis minuta*; Fig. S12c). The cartilaginous portion of transverse process of the Presacral IV was included in the measurement of length.

0: Short. The distal end of the transverse process is at the level of the articulation of the prezygapophyses of Presacral V. 1: Moderately long. The distal end of the transverse process is at the level of the anterior margin of the base of the transverse process of Presacral V. 2: Elongate. The distal end of the transverse process aligns behind of the posterior margin of the base of the transverse process of presacral V. **Additive.**

**(92) Orientation of the transverse process of Presacral Vertebra VI.**

0: Inclined posteriorly. 1: Perpendicular to body axis.

**(93) Orientation of the transverse process of Presacral Vertebra VII.**

0: Inclined anteriorly. 1: Approximately perpendicular to body axis. 2: Inclined posteriorly.

**Additive.**



**(94) Contact between presacrals II and III.** Dorsally, the posterior margin of Presacral II contacts Presacral III medially via a cartilaginous extension in *Pseudis minuta* visible in dorsal view.

0: Not in contact. 1: In medial contact by a cartilaginous extension.

**(95) Expansion of the sacral diapophyses (Duellman and Wiens, 1992; Fig. S12).**

Duellman and Wiens (1992) suggested that narrow sacral diapophyses is a synapomorphy of *Scinax*, *Scarthyla* and *Sphaenorhynchus*. We code the expansion of the sacral diapophyses according to Faivovich (2002) and Grant et al.'s (2006) definitions. They coded the expansion of the sacral diapophyses as the ratio of the width of the tip of the diapophyses, which is the width of the associated cartilage, to the width of the base of the diapophyses. The diapophyses often have irregular fringes of cartilage at the tip, which were not included in the measurements of expansion. The variation is not continuous and the states are separated by gaps. The state diapophyses moderately expanded (state 95.1) is similar to the state rounded diapophysis (ratio between width maximum/minimum < 3.5) proposed by Faivovich (2002: ch. 21). The diapophyses are 1.5–3.0 times wider at the tip than at the base in the state 95.1; and 4.5–5.69 times in the state 95.2. *Sphaenorhynchus carneus*, *S. pauloalvini*, *Dendropsophus* species, and *Xenohyla truncata* share strongly expanded diapophyses (Fig. S12d). We describe the states based on the degree of expansion of the sacral diapophyses instead of the shape, because they are invariably elliptical in cross section (Grant et al., 2006).

0: Unexpanded. 1: Moderately expanded. Diapophyses are 1.5–3 times wider at the tip than at the base. 2: Strongly expanded. Diapophyses are at least 4.5 times wider at the tip than at the base. **Additive.**

**(96) Shape of the iliac arch.**

0: U-shaped. 1: V-shaped.

**(97) Numbers of distal prepollical elements.**

0: One. 1: Two.

**(98) Shape of the first distal prepollical element (Duellman and Wiens, 1992).** The bladelike and ossified prepollex is another synapomorphy of *Sphaenorhynchus* proposed by Duellman and Wiens (1992). We refer to the prepollex as the first distal prepollical element. All species of *Sphaenorhynchus* examined have a bladelike first distal element (state 98.0). This condition is also present in *Dendropsophus microps*, *Scarthyla goinorum*, and *Xenohyla truncata*. In contrast, the degree of mineralization of the first distal prepollical element varies intraspecifically from cartilaginous, partially mineralized, to completely mineralized. We consider that the first distal element of *Sphaenorhynchus* corresponds to the first distal element of *Scinax*, due to differences in the number of distal prepollical elements.

0: Bladelike. 1: Cylindrical. 2: Subcylindrical. **Nonadditive.**

**(99) Longitudinal axis of the terminal phalange (Manzano et al., 2007).** Among all taxa examined, only *Pseudis minuta* presents a straight longitudinal axis (state 99.1).

0: Curved. 1: Straight.

**(100) Shape of the intercalary element between ultimate and penultimate phalanges (Lynch, 1973).** According to Manzano et al. (2007), there are three morphological types of intercalary elements based on their general shape: (1) the intercalary is long and cylindrical, with planar articular surfaces (*Pseudis* in Hylidae); (2) the intercalary is a low element that could be described as a disc with variable thickness among taxa but the height is always lower than the radius, with both articular surfaces concave (most Hyloides); and (3) the intercalary is a cuboid or prismatic element, wedge-shaped in lateral view, with a proximal articular surface like a rider sitting in a saddle and a distal articular surface almost planar. The proximal

articular surface includes a well-developed posterior process. We observed the first two morphological types (states 100.0 and 100.1). *Pseudis minuta* is the only species that presents the characteristics referent to the morphological type 1 (state 100.0).

0: Elongate and cylindrical with articular surfaces planar. 1: Forming a thick disc with concave articular surfaces.

**(101) Mineralization of intercalary elements between ultimate and penultimate phalanges (Duellman and Wiens, 1992).** The intercalary elements are partially mineralized in *Dendropsophus microps*, *Phyllodytes luteolus*, *Sphaenorhynchus carneus*, *S. planicola*, *S. palustris*, and *S. surdus* (state 101.1). A similar condition was observed in species of the *Scinax catharinae* clade by Faivovich (2002).

0: Not mineralized. 1: Partially mineralized. 2: Completely mineralized. **Additive.**

**(102) Preaxial dilatation of the metacarpal IV (Tyler and Davis, 1978).** This dilatation is located dorsolaterally on the middle of the preaxial edge of metacarpal IV.

0: Absent. 1: Present.

**(103) Contact between proximal portions of the metatarsi IV and V (da Silva, 1998).** The basal portions of metatarsi IV and V may be in close contact or free. In the former condition, movement between them is not allowed. In this case, histological analyses are necessary to confirm whether they are fused or not.

0: Free, separated. 1: In close contact.

**(104) Number of distal elements in the prehallux.**

0: One. 1: Two. 2: Three. 3: Four. 4: Five. **Additive.**

**(105) Preaxial dilatation on metatarsus I.** The preaxial dilatation is located dorsolaterally on the distal third of metatarsus I.

0: Absent. 1: Present.

#### ADULT EXTERNAL MORPHOLOGY

**(106) Vocal sac structure (Liu, 1935).** The vocal sac is single and subgular in *Sphaenorhynchus*. Males of *S. pauloalvini* and *S. prasinus* present a less developed vocal sac that occupies the throat region, whereas those of *S. lacteus*, *S. palustris*, and *S. surdus*, for example, present a moderately developed vocal sac that extends to the anterior pectoral region (approximately on the insertion anterior of the arms). However, the most developed vocal sac is present in *S. mirim* and *S. planicola*, for which the vocal sac extends laterally and toward the pectoral region, reaching the postaxial region of arms. Despite of evident character-states related to the external development of the vocal sac, we decided code the anterior and posterior development of the m. *interhyoideus* (see characters 151 and 152) that shows the degree of development of the vocal sac. Furthermore, the vocal sac of *Sphaenorhynchus* can be characterized by the presence of external longitudinal lateral folds (absent in *S. botocudo*, *S. mirim*, *S. pauloalvini*, and *S. prasinus*; Caramaschi et al., 2009; Toledo et al., 2007; Lutz and Lutz, 1938). Since dissections revealed that there is no connective tissue or any other internal element that supports the occurrence of these longitudinal lateral folds, their presence might be a consequence of the development of vocal sac, especially the development of the m. *interhyoideus*. Therefore, as we already have coded the development of the external muscles of the vocal sac and the presence of these external folds might be an artifact of fixation, we did not code the presence of these folds here.

0: Median, subgular. 1: Paired, lateral.

#### **(107) Orientation of nostrils.**

0: Directed laterally. 1: Directed laterodorsally. 2: Directed dorsally. **Additive.**

**(108) Black lateral line.** The black lateral line is absent in *Sphaenorhynchus dorisae* and *S. mirim*. When present, it can be incomplete or complete. The incomplete black lateral line extends from the tip of the snout to the anterior corner of the eye (state 108.1). In contrast, the complete black lateral line runs posteriorly from the tip of snout to the groin (state 108.2). In this condition, the posterior extension of this line varies intraspecifically along the flank. The black lateral line can be absent, incomplete or complete in *S. carneus* (see Rodriguez and Duellman, 1994, plate 7H) and *S. planicola*. Therefore, we consider these species as polymorphic for states 108.0–108.2.

0: Absent. 1: Incomplete, reaching anterior corner of the eye. 2: Complete, extending beyond the eye toward the groin. **Additive.**

**(109) White lateral line.** The white lateral line is present in *Scarthyla goinorum* and *Sphaenorhynchus pauloalvini*. It is bordered above by the black lateral line and begins at the tip of snout, slightly after the tip or below the eye. Posteriorly, it extends to a point immediately anterior to the sacrum or reaches the groin region.

0: Absent. 1: Present.

**(110) White canthal line.** The white canthal line extends from the tip of snout to the anterior corner of the eye. It is bordered below by the black lateral line. According to Caramaschi et al. (2009), this line is absent in *Sphaenorhynchus botocudo*, but we observed the white canthal line in the specimen MNRJ 50639 (paratopotype). Similarly, it is absent in the examined specimens of *S. carneus*, but Rodriguez and Duellman (1994, plate 7H) reported that *S. carneus* has the white canthal line. Thus, we consider both *S. botocudo* and *S. carneus* as polymorphic. We also found *S. bromelicola*, *S. caramaschii*, *S. palustris*, *S. platycephalus*, and *S. surdus* to be polymorphic.

0: Absent. 1: Present.

**(111) White dorsolateral line.** The white dorsolateral line extends from the posterior corner of eye to the groin; its posterior extension varies extensively within species of *Sphaenorhynchus*. It is absent in the examined specimens of *S. carneus*. However, Rodriguez and Duellman (1994, plate 7H) showed that *S. carneus* presents this dorsolateral white line, which extends posteriorly to a point immediately anterior to the sacrum. Thus, we consider *S. carneus* to be polymorphic. The distribution of states between characters 110 and 111 suggests that they are independent.

0: Absent. 1: Present.

**(112) Longitudinal white line under eye.** According to Caramaschi et al. (2009), the longitudinal white line under eye is a putative autapomorphy of *Sphaenorhynchus botocudo*. However, we observed that it is also present in some specimens of *S. bromelicola* (MNRJ 4289–4290, 4292), *S. palustris* (MNRJ 54979–54983; CFBH 2376–1377; MZUSP 127834–127835), *S. surdus* (UFRGS 3364, 2897, 2893; MNHCI 1739), and *Sphaenorhynchus cammaeus* (URCA-H 9285–9287, 9290, 9292, 9294). Lacerda and Moura (2013) have also observed that the longitudinal white line can be present or absent in specimens of *S. bromelicola* and *S. palustris*. We only use the white line as a character, because it has a fixed-state in *S. botocudo*. However, a greater series of specimens of *S. botocudo* should be examined to confirm this character-state.

0: Absent. 1: Present.

**(113) Tympanic membrane (see Araujo-Vieira et al., 2015, fig. 3).**

0: Absent. 1: Present.

**(114) Nature of nuptial pad on Finger II.** We have identified two character-states related to nuptial pads: the nuptial pad can be a thick patch, white or cream, without epidermal modification, where the acini are visible within the translucent skin (state 114.0), or the nuptial pad can be a thick patch with dark or light colored epidermal projections (state 114.1). All species of *Sphaenorhynchus* present the character-state 114.1.

0: Nuptial pad without epidermal modification. 1: Nuptial pad with dark or light colored epidermal projections.

**(115) Coloration of nuptial pad with epidermal projections on Finger II.**

0: Light colored nuptial pad. 1: Dark colored nuptial pad.

**(116) Relative size of the epidermal projections of the nuptial pad on Finger II.** It is difficult to measure accurately the size of the epidermal projections by examination under a stereomicroscope. Therefore, we code this character using photos taken at the same scale and count the number of epidermal projections per 0.01 mm<sup>2</sup>.

0: Nuptial pads have 10–12 epidermal projections by quadrant. 1: Nuptial pads have 5–7 epidermal projections by quadrant.

**(117) Subcloacal ornamentation (Fig. S13).** *Sphaenorhynchus* presents extensive variation in subcloacal ornamentation that varies from single tubercles and dermal folds to well-developed dermal flaps. These structures are usually white and occur immediately below the cloaca. *Sphaenorhynchus botocudo*, *S. bromelicola*, *S. caramaschii*, *S. palustris*, *S. platycephalus*, and *S. surdus* present a weak, white dermal fold in the subcloacal region (Fig. S13a–c) that clearly differentiates those species from *S. carneus* and *S. pauloalvini* (small, discrete tubercles), *S. dorisae* (white dermal flap with triangular lateral margins; Fig. S13g–i), and *S. lacteus*, *S. mirim*, *S. planicola*, and *S. prasinus* (white dermal flap with round lateral margins; Fig. S13d–f). The degree of development and coloration of these ornamentations

varies intraspecifically in *Sphaenorhynchus*, possibly in relation to age, sex, and/or reproductive condition, and they are affected by poor preservation (Heyer, 1978, 1985; Cisneros-Heredia and McDiarmid, 2007).

0: Not subcloacal ornamentation (smooth). 1: Small, flattened or rounded tubercles. 2: Small, elevated and conical tubercles. 3: Many swelled tubercles, but not forming a dermal fold. Tubercles. 4: Weak dermal fold. 5: Dermal flap with round lateral margins. 6: Dermal flap with triangular lateral margins. **Nonadditive.**

**(118) Ornamentation on the ventral surface (Fig. S13).** In addition to the subcloacal ornamentation, some species of *Sphaenorhynchus* have dermal pads on the ventral surface immediately below the subcloacal area. In *S. botocudo*, *S. bromelicola*, *S. caramaschii*, *S. palustris*, and *S. surdus*, the weak, white dermal fold below the cloaca extends anteroventrally to form two thick and flat lateral dermal pads on the ventral surface (Fig. S13b). Otherwise, all examined species of *S. platycephalus* only present two small, round, lateral dermal pads on the ventral surface (see Araujo-Vieira et al., 2015b, fig. 5C–D). *Sphaenorhynchus bromelicola*, *S. palustris* and *S. surdus* are polymorphic for the states 118.1, 118.3 and 118.4. We considered the pair of tubercles immediately below the subcloacal region of *Phyllodytes luteolus* as homologous to the state 118.4.

0: Absent (smooth). 1: Small, flattened or rounded tubercles. 2: Small, elevated and conical tubercles. 3: Two lateral, round, and small dermal pads. 4: Two lateral thick and flat dermal pads. **Nonadditive.**

**(119) Cloacal sheath.** Duellman (2001) mentioned that the opening cloacal is covered by a moderately long or elongate cloacal sheath (reported as an "anal sheath") in some hylids (e.g. *Agalychnis dacnicolor*). Within *Sphaenorhynchus*, the cloacal sheath is present only in *S. pauloalvini*.



0: Absent. 1: Present.

**(120) Dermal ornamentation on forearm.** There is also a great variation in the dermal ornamentation on the lateral edge of the forearm in *Sphaenorhynchus*, for which we observed three conditions: small, rounded or flattened tubercles arranged in line (e.g. *S. palustris*: state 120.1); poorly developed and weakly crenulated dermal folds (e.g. *S. botocudo* and *S. palustris*: state 120.3), and well-developed and smooth dermal fold (e.g. *S. dorisae* and *S. prasinus*: state 120.4). We have observed some degree of intraspecific variation of the third character-state in some individuals of *S. palustris*, which show these folds more developed and crenulated. However, the difference between the third and fourth character-states is clearly visible. In general, these dermal ornamentations are white colored; however this coloration is usually lost after long periods of preservation.

0: Absent. 1: Small, rounded or flattened tubercles arranged in line. 2: Small, elevated and conical tubercles arranged in line. 3: Poorly developed and weakly crenulated dermal folds. 4: Well-developed and smooth dermal folds. **Nonadditive.**

**(121) Dermal ornamentation on elbow.** *Sphaenorhynchus dorisae*, *S. mirim*, *S. planicola*, and *S. prasinus* present a small, usually white, smooth dermal fold on the elbow.

0: Absent. 1: Present.

**(122) Internal dermal ornamentation on tarsus.**

0: Absent. 1: Small, rounded or flattened tubercles arranged in line. 2: Slightly crenulated dermal folds. 3: Smooth dermal folds. 4: Keel. **Nonadditive.**

**(123) External dermal ornamentation on tarsus.**

0: Absent. 1: Small, rounded or flattened tubercles arranged in line. 2: Small, elevated and conical tubercles arranged in line. 3: Poorly developed and slightly crenulated dermal fold. 4: Smooth dermal folds. **Nonadditive.**

**(124) Dermal ornamentation on heel.** We have observed the presence of tubercles, spicules, and calcar appendages on heels is independent of the presence of external ornamentation on the tarsus.

0: Absent. 1: Small, rounded or flattened tubercles. 2: Small, elevated and conical tubercles. 3: Slightly crenulated dermal fold. 4: Round calcar appendages. 5: Triangular calcar appendages. **Nonadditive.**

**(125) Supratympanic fold.**

0: Weak supratympanic fold that borders the tympanic ring dorsally. 1: Strong supratympanic fold that borders the tympanic ring superiorly and extends beyond its posterior margin.

**(126) Shape of the adhesive disc on the hands (Duellman and Wiens, 1992).**

0: Rounded. 1: Truncated (*Scinax* species). 2: Oval and/or elliptical (*Pseudis minuta*).

**(127) Degree of the preaxial webbing of Finger IV.**

0: Absent. 1: Fringe. 2: In its maximal expression, the webbing reaches the distal margin of the antepenultimate subarticular tubercle. 3: The webbing reaches the midlength of the basal phalange. 4: In its maximal expression, the webbing reaches the distal margin of the penultimate subarticular tubercle. **Additive.**

**(128) Degree of the postaxial webbing of Finger IV.**

0: Absent. 1: Fringe. 2: The webbing reaches the midlength of the basal phalange. 3: In its maximal expression, the webbing reaches the distal margin of the penultimate subarticular

tubercle. 4: The webbing reaches the midlength of the second phalange. 5: The webbing reaches the base of the adhesive disc. **Additive.**

**(129) Degree of webbing between Toes I and II (Wagler, 1830; see also Duellman and Wiens, 1992 and Faivovich, 2002).**

The extension of the webbing is expressed in relation to Toe I.

0: Absent. 1: In its maximal expression, the webbing reaches the distal margin of the subarticular tubercle. 2: The webbing reaches the midlength of the first phalange. 3: The webbing reaches the base of the adhesive disc. **Additive.**

**(130) Degree of the preaxial webbing of Toe IV.**

0: Fringe. 1: In its maximal expression, the webbing reaches the distal margin of the antepenultimate subarticular tubercle. 2: In its maximal expression, the webbing reaches the distal margin of the penultimate subarticular tubercle 3: The webbing reaches the midlength of the basal phalange. 4: The webbing reaches the base of the adhesive disc. **Additive.**

**(131) Degree of the postaxial webbing of Toe IV.**

0: Fringe. 1: In its maximal expression, the webbing reaches the distal margin of the antepenultimate subarticular tubercle. 2: The webbing reaches the midlength of the basal phalange. 3: In its maximal expression, the webbing reaches the distal margin of the penultimate subarticular tubercle. 4: The webbing reaches the midlength of the second phalanx. 5: The webbing reaches the base of the adhesive disc. **Additive.**

## LARVAL MORPHOLOGY

**(132) Position of the nostrils with respect to the main body axis (Faivovich et al., 2005; see also Araujo-Vieira et al., 2015a, fig. 3).** Nostril position was determined with respect to the main larval body axis. This character is inapplicable for species that have round nostrils, like *Scinax catharinae*.

0: The longer axis of the nostrils forms an acute angle with respect to the main body axis. 1: The longer axis of the nostrils is parallel to the main body axis.

**(133) Fleshy flanges on internal margins of the nostrils (Faivovich et al., 2005; see also Araujo-Vieira et al., 2015a, fig. 3).** Based on previous studies (e.g. Kenny 1969; Cruz 1973), Faivovich et al. (2005) suggested that the morphology of the nostrils could be considered a synapomorphy for some species of *Sphaenorhynchus*. Later, Araujo-Vieira et al. (2015a), based on their own observations of six species (*S. bromelicola*, *S. pauloalvini*, *S. palustris*, *S. planicola*, *S. prasinus*, and *S. platycephalus*), expanding the information available in literature, also suggested that the fleshy flanges present in the nostrils of *Sphaenorhynchus* larvae also could be a synapomorphy of the genus.

0: Absent. 1: Present.

**(134) Position of the oral disc (Faivovich, 2002).** We code the character-states following Faivovich (2002). He defined the position of the oral disc in reference to an imaginary line that separates the oral disc from the body. If this line is perpendicular to the main body axis, the oral disc is terminal; if the line forms an acute angle with the main body axis, the oral disc is subterminal; if the line is nearly parallel to the main body axis, the oral disc is ventral.

0: Ventral. 1: Subterminal. 2: Terminal. **Additive.**

**(135) Submarginal papillae of the oral disc.**

0: Absent. 1: Present.

**(136) Marginal papillae of the oral disc (Araujo-Vieira et al., 2015a, fig. 4).** Larvae of *Sphaenorhynchus caramaschii*, *S. carneus*, *S. lacteus*, *S. palustris*, *S. planicola*, and *S. prasinus* show few enlarged marginal papillae, about twice larger than the small ones, located mainly in the posterior portion of the oral disc and arranged next to each other or alternating with the smaller ones. *Sphaenorhynchus bromelicola*, *S. dorisae*, *S. pauloalvini*, *S. platycephalus*, and *S. surdus* present small and homogeneous marginal papillae on the oral disc.

0: Small and homogeneous marginal papillae. 1: Few enlarged marginal papillae, about two times larger than the small papillae.

**(137) Ventral gap in the row of marginal papillae of the oral disc (Faivovich, 2002).** We code the presence and absence of the ventral gap, which is independent of the presence of the oral structure known as the labial arm (McDiarmid and Altig, 1990; see also of Faivovich, 2002, character 69).

0: Absent. 1: Present.

**(138) Anterior teeth rows.**

0: Absent. 1: Present

**(139) Number of the anterior teeth rows.**

0: One. 1: Two.

**(140) Posterior teeth rows.**

0: Absent. 1: Present.

**(141) Number of the posterior teeth rows.** According to Suárez-Mayorga and Lynch (2001), larvae of *Sphaenorhynchus carneus* have three or two posterior teeth rows. Since the third

posterior teeth row can be absent independently of the stage of larval development, we considered *S. carneus* as polymorphic for character-states 141.1 and 141.2.

0: One. 1: Two. 2: Three. 3: Four. **Additive.**

**(142) Gap in the first posterior teeth rows.**

0: Absent. 1: Present.

**(143) Relative length of the spiracle (Araujo-Vieira et al., 2015a, fig. 5)** Spiracle length was measured as the distance between the origin of the external wall of the spiracle and its posterior margin. We code this character in relation to the body length (BL). A short spiracle, 3–10% of BL, fused to the body wall except at its posterior edge, occurs in *Sphaenorhynchus caramaschii*, *S. carneus*, *S. dorisae*, *S. lacteus*, *S. pauloalvini*, *S. planicola*, and *S. prasinus* (Suarez-Mayorga and Lynch 2001; Bokermann 1973, Cruz 1973). *Sphaenorhynchus bromelicola*, *S. platycephalus* and *S. surdus* share a medium-size spiracle, 16–24% of BL (Bokermann, 1966; Cruz and Peixoto, 1980; Caramaschi, 2010). The spiracle of *S. platycephalus* and *S. surdus* is somewhat shorter than in *S. bromelicola*, whereas the spiracle in *S. palustris* is notably larger, reaching at least 28% of BL. It is directed posteriorly and is entirely free except at its base. We consider *S. canga* to be polymorphic for states 143.1 and 143.2.

0: Short spiracle, 3–10% of BL. 1: Medium-size spiracle, 16–24% of BL. 2: Larger spiracle, reaching at least 28% of BL. **Additive.**

**(144) Dark pigmentation on ventral surface of the vent tube.**

0: Absent. 1: Present.

**(145) Direction of the opening of the vent tube.**

0: Medial. 1: Dextral. **Nonadditive.**

## MYOLOGY

**(146) Apical supplementary element of the m. *intermandibularis* (Tyler, 1971; Fig. S14).**

The m. *intermandibularis* differentiated to form a well-developed apical supplementary element was first reported for *Sphaenorhynchus lacteus* by Tyler (1971). Our observations demonstrated that all examined species of *Sphaenorhynchus* have an apical supplementary element with transversal fibers that cannot be separated from the m. *intermandibularis*.

0: Absent. 1: Present.

**(147) Relationship between m. *intermandibularis* and m. *submentalis* (Tyler, 1971).**

The transversal fibers of the apical supplementary element of the m. *intermandibularis* completely overlap the posterior margin of the m. *submentalis* in *Sphaenorhynchus* (state 147.0). This condition is independent of the presence of the apical element, since *Xenohyla truncata* does lack the apical element but the m. *intermandibularis* overlaps the posterior margin of the m. *submentalis*.

0: Overlaps the posterior margin of the m. *submentalis*. 1: Overlaps the posterolateral margin of the m. *submentalis*. 2: Juxtaposes the posterior margin of the m. *submentalis* medially. 3: Overlaps the posterior margin of the m. *submentalis* medially. **Nonadditive.**

**(148) Medial raphe of the m. *intermandibularis* (Tyler, 1971).**

The m. *intermandibularis* of the examined *Sphaenorhynchus* (except *S. carneus* and *S. pauloalvini*) has a small, diamond-shaped aponeurosis. However, Tyler (1971) reported that the m. *intermandibularis* of *S. lacteus* has a medial raphe. Therefore, we considered this species to be polymorphic for states 148.1 and 148.2.

0: Absent. 1: Present.

**(149) Medial aponeurosis of the m. *intermandibularis*.**

0: Absent. 1: Present.

**(150) Medial portion of the m. *interhyoideus* (Tyler, 1971).**

0: Agraphic. 1: Medial raphe present.

**(151) Relative degree of anterior development of the m. *interhyoideus*.** We code the relative degree of anterior development of the m. *interhyoideus* with respect to the maximum length of the mandibular arch.

0: Poorly developed. M. *interhyoideus* occupies approximately 1/5 of mandible length. It reaches the anterior margin of the tympanic ring. 1: Moderately developed. M. *interhyoideus* occupies approximately one third of mandible length. It reaches approximately the posterior margin of the eye. 2: Well-developed. M. *interhyoideus* occupies approximately half of mandible length. It reaches approximately the middle of the eye. **Additive.**

**(152) Posterior extension of the fold of the m. *interhyoideus*.** Tyler (1971) observed that the m. *interhyoideus* of *Sphaenorhynchus lacteus* is exceptionally well developed posteriorly and extends considerably beyond the articular portion of the mandible. We expand this observation for all examined species of *Sphaenorhynchus*. We also observed that the posterior fold of the m. *interhyoideus* of *Sphaenorhynchus* (except *S. pauloalvini*) surpasses the articular portion of the mandible, extending beyond the m. *deltoideus*, with *S. mirim* and *S. planicola* presenting the posteriormost extension (state 152.5). We code the character-states based on specimens with distended and well-fixed vocal sacs. The distribution of states between characters 151 and 152 suggests that they are independent.

0: M. *interhyoideus* barely surpasses the mandible. 1: M. *interhyoideus* surpasses the mandible and reaches from one third to half of the length of the m. *deltoideus*. 2: M. *interhyoideus* surpasses the mandible and reaches the posterior portion of the m. *deltoideus*. 3:



*M. interhyoideus* reaches the anterior margin of the *m. pectoralis esternalis*. 4: *M. interhyoideus* reaches the posterior margin of the *m. pectoralis esternalis*. 5: *M. interhyoideus* surpasses the *m. pectoralis esternalis*. **Additive.**

**(153) Origin of the *m. geniohyoideus lateralis*.** The *m. geniohyoideus lateralis* originates on the lingual surface of the mandible. Among the examined species, it is attached to the mandible by a short and broad tendon only in *Pseudis minuta*.

0: Tendon. 1: Membranous tissue or fibers or membranous tissue and fibers.

**(154) Number of slips of the *m. geniohyoideus lateralis* (Fig. S14a–b).** *M. geniohyoideus lateralis* can be arranged in one (external) or two parts (external and internal). The external part is inserted on the posterolateral process of hyoid; whereas the internal one inserts on either the posteromedial portion of the hyoid plate or the posteromedial portion of the hyoid plate and the distal end of the posteromedial process (see character 155).

0: One, external part. 1: Two, external and internal parts.

**(155) Insertion of the internal part of the *m. geniohyoideus lateralis*.**

0: Posteromedial portion of the hyoid plate and distal end of the posteromedial process. 1: Posteromedial portion of the hyoid plate.

**(156) *M. petrohyoideus anterior* (Fig. S14c–d).** The *m. petrohyoideus anterior* originates in the otic region of the skull, more precisely on the prootics, and inserts on the lateral edge of the hyoid plate. In addition to inserting on the lateral edge, the *m. petrohyoideus anterior* has a layer of fibers that covers the medial region of the hyoid plate and some fibers inserted on the on the hyale in *Sphaenorhynchus*, except for *S. pauloalvini*.

0: Inserted on the lateral margin of the plate hyoid, subjacent to the alary process of hyoid. 1: With one additional layer of fibers over the plate hyoid.

**(157) Disposition of the fibers of the m. *petrohyoideus anterior*.**

0: Separated in bundles. 1: Continuous.

**(158) Insertion of branch I of the m. *petrohyoideus posterior*.** The m. *petrohyoideus posterior* has a single origin on the skull, adjacent to the m. *petrohyoideus anterior*, but inserts via three branches: branches I and II insert on the lateral edge of the ossified portion of the posteromedial process, while branch III inserts on the cartilaginous epiphysis of the posteromedial process and/or the cricoid ring.

0: Inserted on the base of the posteromedial process of hyoid. 1: Inserted approximately on the half of the length of the posteromedial process of hyoid.

**(159) Number of insertions of the branch III of the m. *petrohyoideus posterior*.**

0: One, on the posteromedial process of hyoid. 1: Two, on the posteromedial process and cricoid ring.

**(160) Insertion of the m. *sternohyoideus* (Fig. S14e–f).**

0: Ventral and dorsal strips with continuous insertions. 1: Ventral and dorsal strips with distinct insertions (discontinuous).

**(161) *Pars dorsalis* of the m. *sternohyoideus*.** The *pars dorsalis* arises from the sternum and crosses the rest of the m. *sternohyoideus* obliquely.

0: Absent. 1: Present.

**(162) Insertions of the *pars dorsalis* of the m. *sternohyoideus*.**

0: On the hyoid plate between the posteromedial and posterolateral processes. 1: On the hyoid plate (in a position similar to previous state) and *thyroide* membrane (the space between the posterolateral and the posteromedial processes of hyoid). 2: On the lateral edge of the posteromedial process of hyoid. 3: On the thyroid membrane. **Nonadditive.**

**(163) Relationship between the main body of the m. *hyoglossus* and the posteromedial process of the hyoid.** We consider the main body of the m. *hyoglossus* excluding the medial segment, which inserts towards the midline of the tongue.

0: Subterminal. M. *hyoglossus* originates from the posterior third of the posteromedial process. 1: Terminal. M. *hyoglossus* originates from the posterior end of the posteromedial process.

**(164) Origin of the medial segment of the m. *hyoglossus* (Fig. S14g–h).** The medial segment is separated from the main body of the hyoglossus and arises on the ventral surface of the hyale, near the alary process, in all species of *Sphaenorhynchus* (state 164.1) except *S. pauloalvini*.

0: Hyoid plate. 1: On the hyale posteriorly to the alary process of hyoid. 2: Posteromedial process of hyoid. **Nonadditive.**

**(165) Inflected fibers of the m. *genioglossus*.**

0: Absent. 1: Present.

**(166) M. *lumbricalis brevis digiti IV*, lateral slip (LBB IV lateral; see also Burton, 1998).**

0: Absent. 1: Present.

**(167) Origin of the m. *lumbricalis brevis digiti V*, lateral slip (LBB V lateral).**

0: Distal carpal 5–4–3. 1: Aponeurosis palmaris.

**(168) Origin of the m. *flexor teres digiti V* (FT V).**

0: Metacarpal IV and V. 1: Metacarpal V.

**(169) Burton's ligament (Faivovich, 2002).**

0: Absent. 1: Present.

**(170) Insertion of the medial branch of the m. *extensor digitorum communis longus* (EDCL) on fascia of m. *extensor brevis superficialis digiti IV*.** The m. *extensor digitorum communis longus* originates on the distal margin of the humerus and extends over the radio-ulna up to the dorsum of the hand, where it is divided into three branches that insert on metacarpals III, IV, and V, respectively. All *Sphaenorhynchus* examined present the medial branch with a single insertion on metacarpal IV, with the exception of *S. palustris*, which presents an additional insertion of the medial branch on the fascia of the m. *extensor brevis superficialis* digiti IV (which inserts on phalanx), similar to *Scinax catharinae* and *Sci. perpusillus*.

0: Absent. 1: Present.

**(171) Insertion of the postaxial branch of the m. *extensor digitorum communis longus* (EDCL) on fascia of the medial slip of the m. *extensor brevis profundus digiti V* (EBP V; Fig. S15).** The postaxial branch can be single, inserting on the lateral region metacarpal V, or divided in two slips, inserting both lateral region metacarpal V and on the fascia of the EBP V. *Sphaenorhynchus dorisae*, *S. mirim*, *S. planicola*, *S. prasinus* share a postaxial branch of the EDCL divided with an insertion on fascia of the medial slip of the EBP V (Fig. S15a).

0: Absent. 1: Present.

**(172) M. *extensor brevis distalis digiti II*, medial slip (EBD 2 medial).**

0: Absent. 1: Present.

**(173) *M. extensor brevis profundis digiti II*, lateral slip (EBP II lateral): origin from Distal Carpal 2.**

0: Absent. 1: Present.

**(174) *M. extensor brevis distalis digiti IV*, medial slip (EBD IV medial; Fig. S15).**

0: Absent. 1: Present.

**(175) *M. extensor brevis profundis digiti V*, medial slip (EBP V medial): accessory slip from Metacarpal IV (Burton, 1998; Fig. S15).**

0: Absent. 1: Present.

**(176) *M. flexor teres hallucis* (Burton 2004).**

0: Absent. 1: Present.

**(177) *M. flexor ossis metatarsi digiti II* (FM II): origin from Distal tarsal 2–3 (or Distal Tarsal 3; Fig. S15; see also Burton, 2004).**

0: Absent. 1: Present.

**(178) *M. flexor ossis metatarsi digiti IV* and *m. transversus metatarsus IV* (FM IV and TM IV): distal end of FM IV dorsal to TM IV (see also Burton, 2004).**

0: Absent. 1: Present.

**(179) *M. flexor ossis metatarsi digiti IV* and *m. transversus metatarsus IV* (FM IV and TM IV): distal end of FM IV ventral to TM 4.**

0: Absent. 1: Present.

**(180) *M. lumbricalis brevis digiti V*, medial slip (LBB V medial): additional insertion onto Metatarsus V.**

0: Absent. 1: Present.

**(181) *M. flexor digitorum brevis superficialis* (FDB): structure of the tendon of insertion (see also Burton, 2004).**

0: Undivided. 1: Divided.

**(182) Origin of *m. transversus plantae distalis* (TVPD) from Distal tarsal 2–3.**

0: Absent. 1: Present.

**(183) *M. extensor digitorum communis longus* (EC): insertion on digiti II (pes).**

0: Absent. 1: Present.

**(184) *M. extensor brevis superficialis hallucis* (EBS I): insertion lateral fibers on medial region of basal Phalanx 2 via tendon (see also Burton, 2004).**

0: Absent. 1: Present.

**(185) *M. extensor brevis superficialis digiti III* (EBS III): insertion on Metatarsus III (see also Burton, 2004).**

0: Absent. 1: Present.

**(186) *M. extensor brevis distalis digiti II*. lateral slip (EBD II lateral) (pes; Faivovich, 2002).**

0: Absent. 1: Present.

**(187) *M. extensor brevis distalis digiti V*, lateral slip (EBD V lateral) (pes; Faivovich, 2002).**

0: Absent. 1: Present.

**(188) Length of the fibers of the m. *extensor brevis distalis digiti V*, lateral slip (EBD V lateral) (pes; Faivovich, 2002).**

0: Fibers reach the distal margin of the first phalange. 1: Fibers reach the distal margin of the second phalange.

**(189) Origin of the m. *pectoralis portio abdominalis* (da Silva, 1998).** Faivovich (2002) followed da Silva (1998) in considering three states: fibers originate at midbody; fibers originate on pelvis; tendon not evident; and fibers originate on pelvis, tendon evident.

0: Fibers originate at midbody. Fibers originate on pelvis, tendon not evident. 2: Fibers originate on pelvis, tendon evident.

#### ADULT INTERNAL ANATOMY

**(190) White parietal peritoneum.**

The peritoneum is a serous membrane, mostly transparent, covering the abdominal wall (parietal peritoneum) and the viscera (visceral peritoneum). White peritoneum is present in all *Sphaenorhynchus* species.

0: Transparent peritoneum. 1: White peritoneum.

#### NATURAL HISTORY

**(191) Oviposition site.**

*Sphaenorhynchus pauloalvini* lays its eggs out of the water, on leaves overhanging water. The situation is ambiguous in *S. carneus*, which has been reported to lay clutches on leaves overhanging water (Bokermann, 1973) or in the water (Crump, 1974; W. Hödl, pers. comm.). We score these character-states only for the species for which there is an explicit literature reference about their oviposition site. **Nonadditive.**

0: Leaves overhanging water. 1: Phytotelmata. 2: Submerged.

## CHROMOSOME

### **(192) Number of chromosomes.**

Knowledge on chromosome morphology in *Sphaenorhynchus* is limited to *S. caramaschii*, *S. carneus*, *S. dorisae*, and *S. lacteus* as described by Suárez et al. (2013) from where we took the information. Outgroup informations were taken from Suárez et al. (2013) and Cardozo et al. (2011). **Additive.**

0: 22. 1: 24. 2: 26. 3: 30.

### **References not cited in the main text.**

Cardozo, D.E., Leme, D.M., Bortoleto, J.F., Catroli, G.F., Baldo, D., Faivovich, J. Kolenc, F., Silva, A.P.Z., Borteiro, C., Haddad, C.F.B., Kasahara, S., 2011. Karyotypic data on 28 species of *Scinax* (Amphibia: Anura: Hylidae): Diversity and Informative Variation. *Copeia*, 251–263.

Clarke, B., 1981. Comparative osteology and evolutionary relationships in the African Raninae (Anura Ranidae). *Monit. zool. ital.* 15, 285–331.

da Silva, H.R., 1998. Phylogenetic relationships of the family Hylidae with emphasis on the relationships within the subfamily Hylinae (Amphibia: Anura). Ph.D. dissertation, Department of Systematics and Ecology, University of Kansas.

Heyer, W.R., 1975. A preliminary analysis of the intergeneric relationships of the frog family Leptodactylidae. *Smithson. Contr. Zool.* 199, 1–55.

Heyer, W.R., 1978. Variation in members of the *Centrolenella eurygnatha* complex (Amphibia: Centrolenidae) from Serra do Mar and Serra da Mantiqueira, Brasil. *Pap. Avulsos Zool.* 32, 15–33.



- Heyer, W.R., 1985. Taxonomic and natural history notes on frogs of the genus *Centrolenella* (Amphibia: Centrolenidae) from southeastern Brasil and adjacent Argentina. Pap. Avulsos Zool. 36, 1–21.
- Cisneros-Heredia, D.F., McDiarmid, R.W., 2007. Revision of the characters of Centrolenidae (Amphibia: Anura: Athesphatanura), with comments on its taxonomy and the description of new taxa of glassfrogs. Zootaxa 1572, 1–82.
- Liem, S.S., 1970. The morphology, systematics, and evolution of the Old World treefrogs (Rhacophoridae and Hyperoliidae). Fieldiana: Zoology 57, 1–145
- Liu, C.C., 1935. Types of vocal sac in the Salientia. Proc. Boston Soc. Nat. Hist. 41, 19–40.
- Lynch, J.D., 1973. Review "Evolution in the genus *Bufo*". Bioscience 23, 497.
- Manzano, A.S, Fabrezi, M., Vences, M., 2007. Intercalary elements, treefrogs, and the early differentiation of a complex system in the Neobatrachia. Anat. Rec. 290, 1551–1567.
- Scott, E., 2005. A phylogeny of ranid frogs (Anura: Ranoidea: Ranidae), based on a simultaneous analysis of morphological and molecular data. Cladistics 21, 507–574.
- Simirnov, S.V., Vasil'eva, A.B., 1995. Anuran dentition: development and evolution. Russian J. Hepetol. 2, 120–128.
- Trueb, L., 1970. Evolutionary relationships of casque-headed tree frogs with co-ossified skulls (family Hylidae). Univ. Kansas Publ. Mus. Nat. Hist. 18, 547–716.
- Tyson, H., 1987. The structure and development of the anuran breast shoulder apparatus, forelimb, and associated musculature. Ph.D. Dissertation, University of Alberta.
- Tyler, M.J., Davis, M. 1978. Species groups within the Australopapuan hylid frog genus *Litoria* Tschudi. Austr. J. Zool., Suppl. Ser. 63, 1–47.
- Vasil'eva, A.B., 1997. The role of pedomorphosis in the formation of the tooth system in Anura with the example of the fire-billed toads (*Bombina*, Discoglossidae). Dokl. Akad. Nauk. 354, 566–568.

Wagler, J., 1830. Natürliches System der Amphibien, mit Vorangehender Classification der Säugthiere und Vögel. Müncher, Stuttgart and Tübingen.

**Appendix S7.** List of potentially informative morphological variation in *Sphaenorhynchus*.

In this section, we mention 22 characters that show morphological variation in *Sphaenorhynchus*, but were not coded mainly due to: (i) unclear definition of the character-states, and/or (ii) unclear independence between the characters. They are as follows: (1) Length of ventral ramus of squamosal. Some species of *Sphaenorhynchus* (e.g. *S. dorisae*) have a ventral ramus of squamosal that does not reach the quadratojugal. (2) Shape of the ventral ramus of squamosal, which may be either straight, slightly curved medially or strongly curved medially. (3) Degree of inclination of the ventral ramus of squamosal is somewhat variable in *Sphaenorhynchus*. (4) Length of the *pars media plectri*: this structure is apparently longer in *Sphaenorhynchus* (except for *S. carneus* and *S. pauloalvini*) than that of the studied species of *Dendropsophus*, *Pseudis*, *Scinax*, *Scarthyla*, and *Xenohyla*. (5) Relationship between palatines and *planum antorbitale*: the palatines can be either partially (e.g. *S. caramaschii* and *S. planicola*) or completely enclosed inside the *planum antorbitale* (e.g. *S. pauloalvini*). (6) Shape or development of occipital condyles, which in *S. carneus* are smaller than those of the remaining *Sphaenorhynchus*. (7) Dorsal color pattern: the degree of dark pigmentation on dorsum varies from the absence of melanophores (e.g. *S. dorisae*) to a dorsum almost completely dark (e.g. *S. bromelicola*, *S. palustris*, *S. platycephalus*, and *S. surdus*). (8) Advertisement call parameters (e.g. note duration, dominant frequency, number of notes, and interval between notes) are apparently informative. See recent study by Toledo et al. (2014). (9) Alary process of premaxilla: the shape of the alary process varies in *Sphaenorhynchus*. (10) The degree of contact between alary process and superior prenasal cartilage are variable in *Sphaenorhynchus*. (11) Relative length of medial ramus of pterygoid with respect to basal process and optic capsule. (12) Degree of contact between medial ramus of pterygoid and basal process. (14) Presence of a thickened lateral process of the

odontophore in most species of *Sphaenorhynchus*, except for *S. carneus* and *S. dorisae*, where the odontophore is absent (*S. carneus*) or very reduced (*S. dorisae*). (15) *Sphaenorhynchus caramaschii*, *S. platycephalus*, and *S. surdus* present the distal portion of the transverse process of Presacral VII anteriorly directed and perpendicular to the longitudinal body axis; (16) Urostyle length (apparently proportionally shorter in *Sphaenorhynchus carneus* than in other species of *Sphaenorhynchus*). (17) Shape of the zygomatic ramus of the squamosal, which may be slender, curved, pointed, robust, or truncated. (18) Length of the esophageal process: this element is longer in *S. pauloalvini* than in other studied species. (19) Percentage of cultriform process with parallel margins: the margins of the cultriform process are parallel in *Sphaenorhynchus bromelicola* and *S. botocudo*, whereas they are parallel throughout 50–90% of the total length of the cultriform process in the other species studied. (20) Shape of the *sternum* (excluding its distal portion). (21) Shape of nasals in dorsal view: the shape of the nasals varies extensively and forms a series of complex morphological transformations. (22) Shape of the oblique cartilage in dorsal view, which can be rounded, pointed and concave, or truncated.

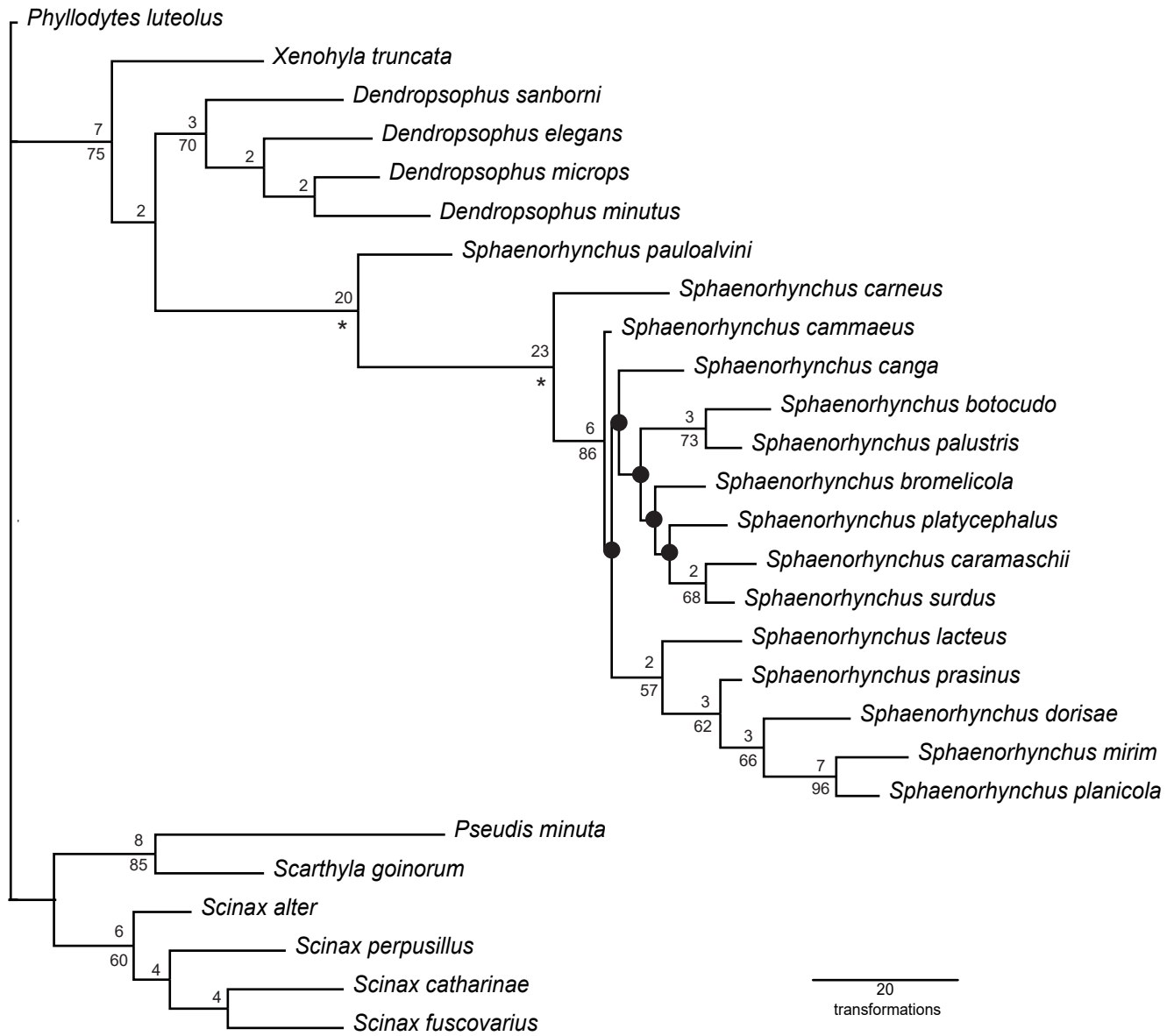


**Fig. S1.** Phylogenetic relationships of *Sphaenorhynchus* as recovered in one of the 14 most parsimonious trees (length 751 steps) obtained from the analysis of phenotypic dataset (PD). Black circles indicate nodes that collapse in the strict consensus. Values below nodes are parsimony jackknife support absolute frequencies; values above nodes are Goodman-Bremer support. An asterisk (\*) indicates groups with 100% for parsimony jackknife frequencies. Nodes lacking values have < 50% absolute jackknife frequencies.

*Phyllodytes luteolus*

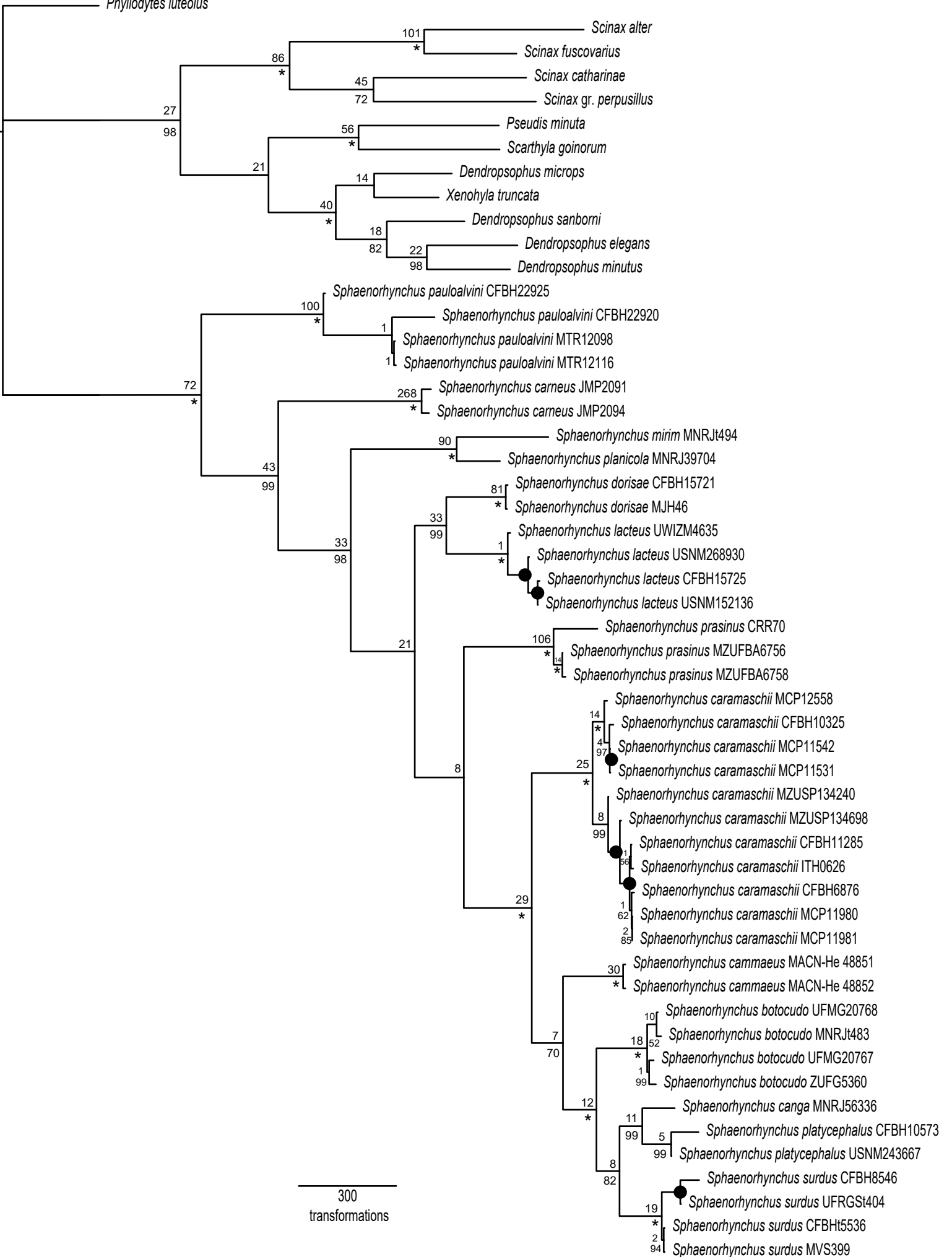


**Fig. S2.** Phylogenetic relationships of *Sphaenorhynchus* as recovered in one of the four most parsimonious trees (length 8769 steps) obtained from the analysis of molecular-only dataset (MD). Black circles indicate nodes that collapse in the strict consensus. Values below nodes are parsimony jackknife support absolute frequencies; values above nodes are Goodman-Bremer support. An asterisk (\*) indicates groups with 100% for parsimony jackknife frequencies. Nodes lacking values have < 50% absolute jackknife frequencies.



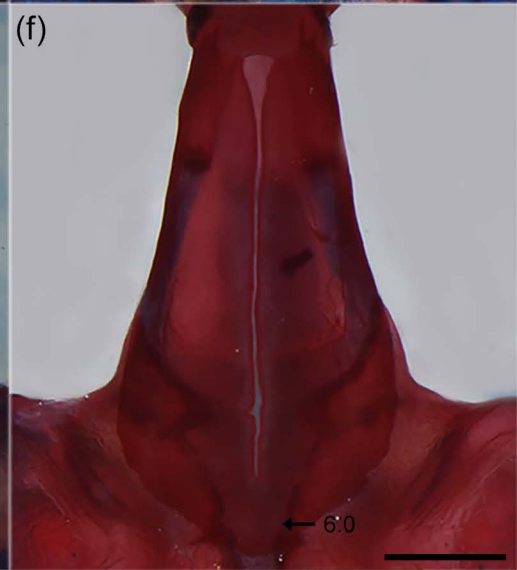
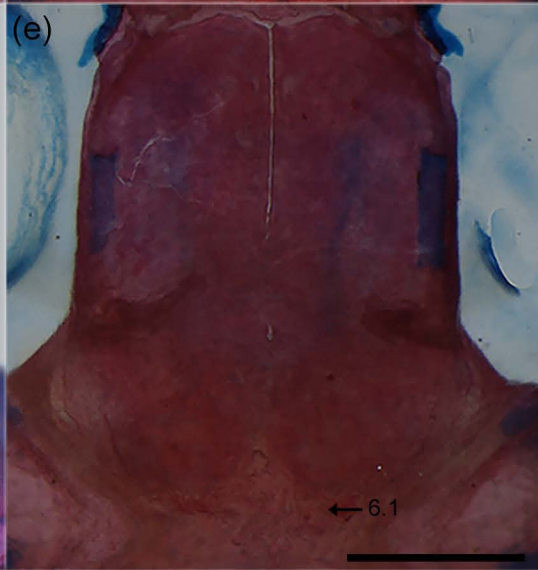
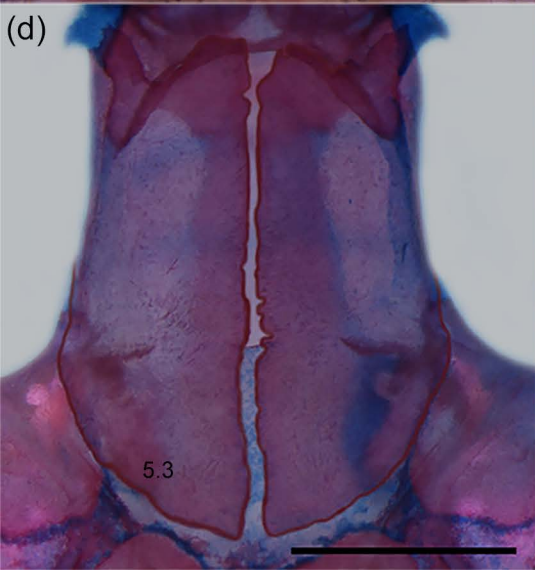
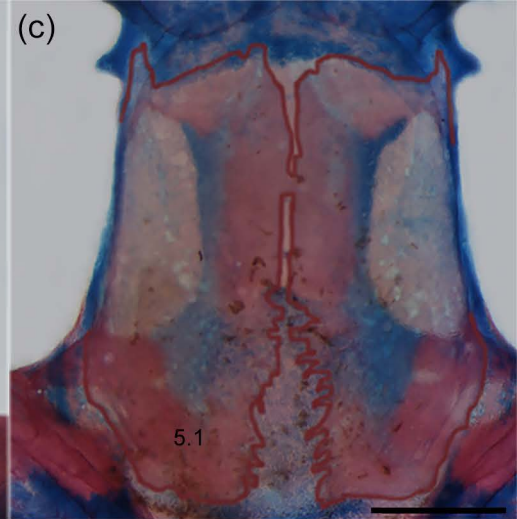
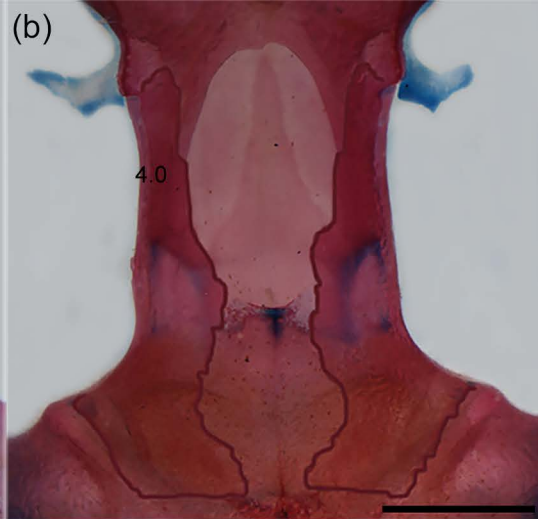
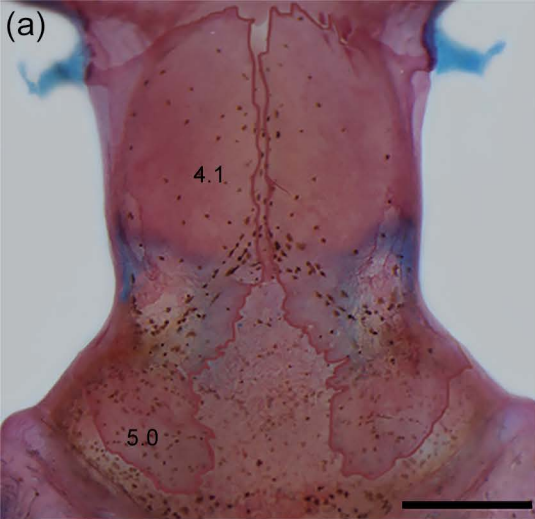
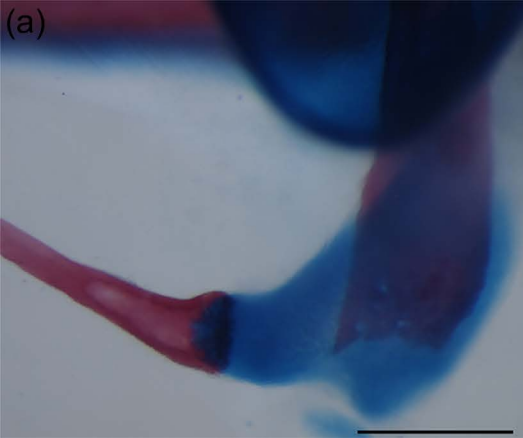
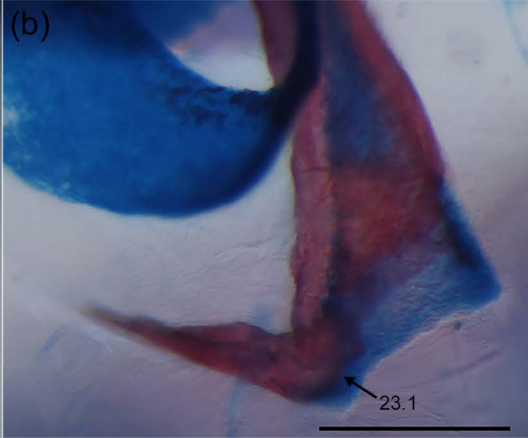


**Fig. S3.** Dorsal views of the frontoparietals of (a) *Scinax alter* (MCP 1670), (b) *S. catharinae* (MCP 3427), (c) *Sphaenorhynchus planicola* (MNRJ 54808), (d) *S. palustris* (MNRJ 42656), (e) *S. pauloalvini* (MNRJ 4323), and (f) *Pseudis minuta* (MACN-He 43532) showing some states of characters 4, 5, and 6 (character number is followed by the state number). Scale bars = 2 mm.

(a)



(b)



(c)

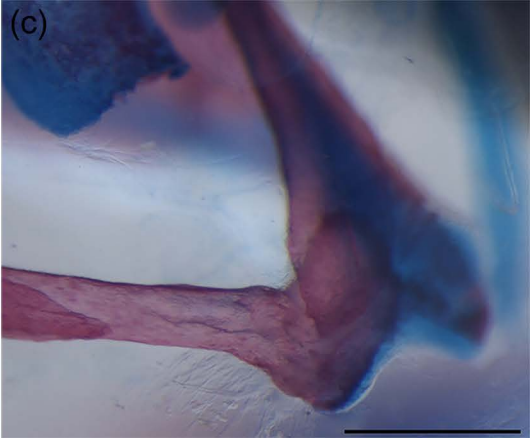


**Fig. S4.** Quadratojugal-squamosal relationship. (a) *Sphaenorhynchus prasinus* (EI 59: Ch. 23.0), (b) *S. pauloalvini* (MNRJ 4323: Ch. 23.1), and (c) *Scinax alter* (MCP 1670: Ch. 23.1). Scale bars = 0.5 mm.

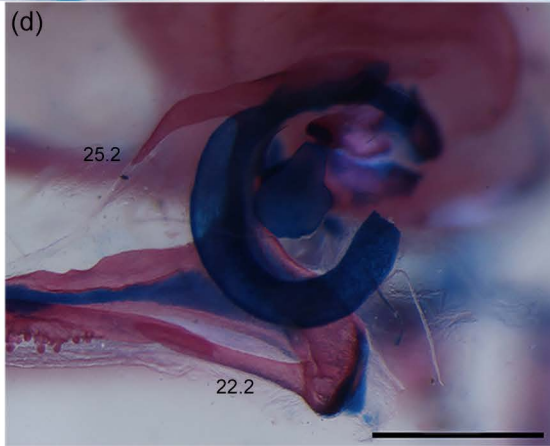
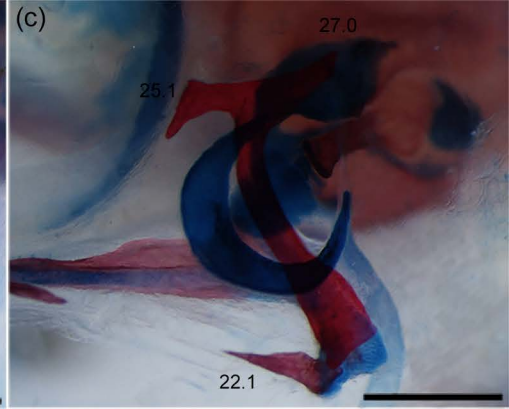
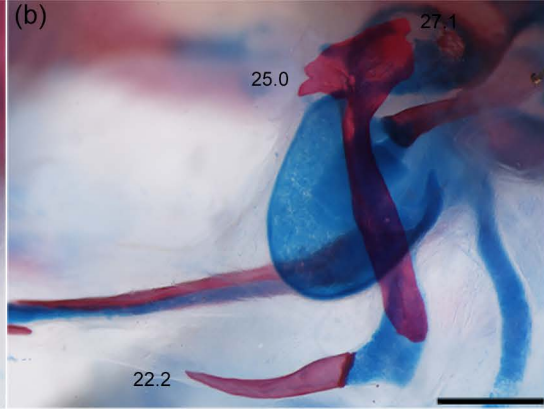
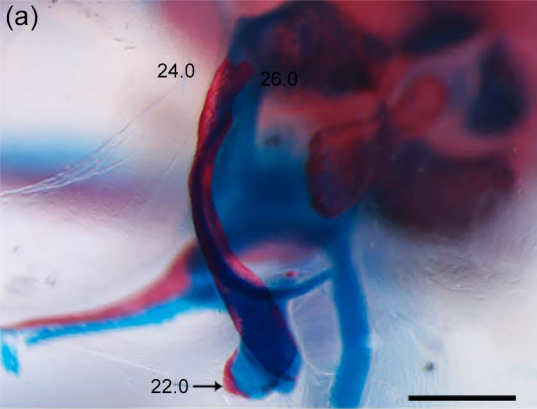
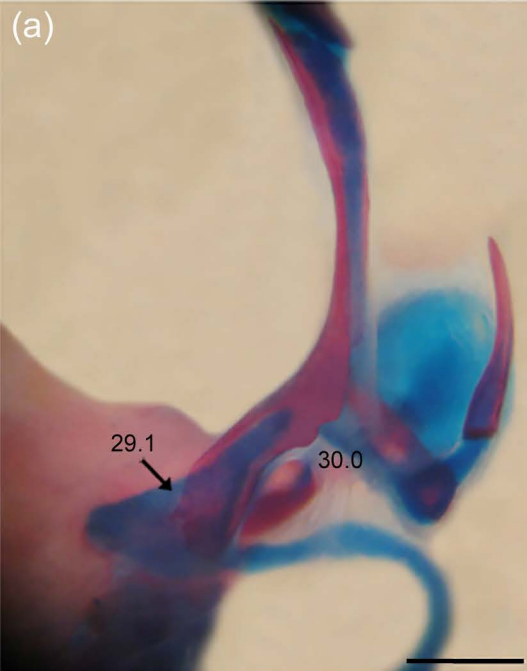
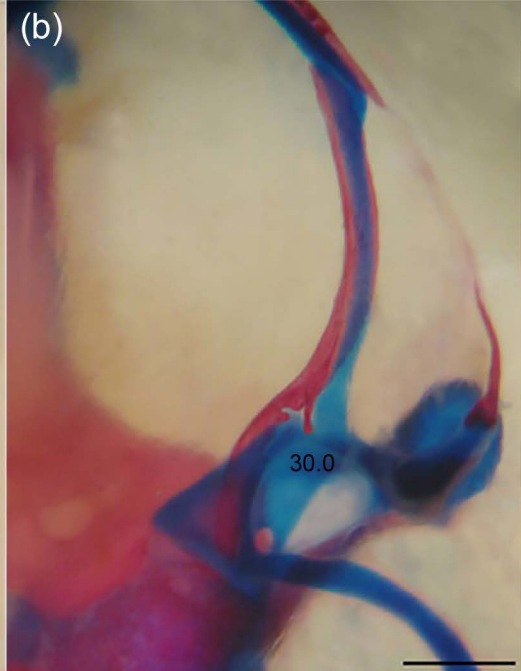


**Fig. S5.** Lateral view of quadratojugal and squamosal showing states of characters 22 and 24–27 related to these bones (character number is followed by the state number). (a) *Sphaenorhynchus carneus* (ZUEC 5555), (b) *S. dorisae* (ZUEC 11096), (c) *S. pauloalvini* (MNRJ 4323), (d) *Scarthyla goinorum* (MCP 12962), and (e) *Scinax alter* (MCP 1670). Scale bars = 0.5 mm (upper) and 1 mm (lower).

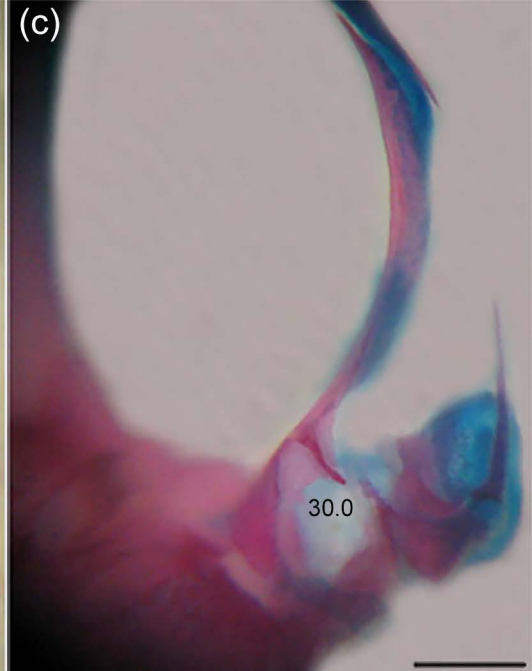
(a)



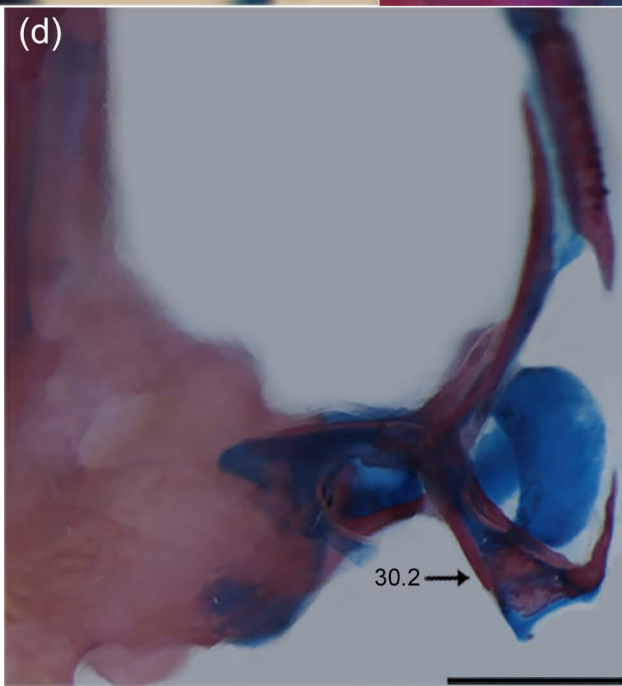
(b)



(c)



(d)



(e)

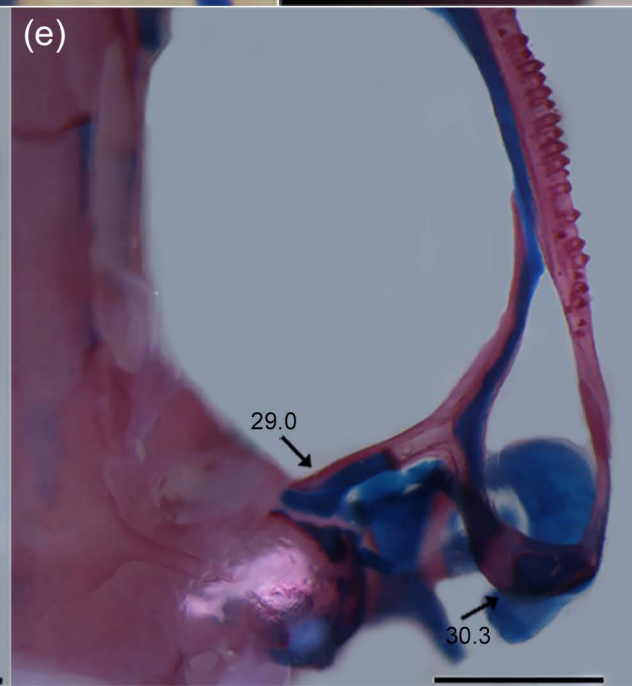
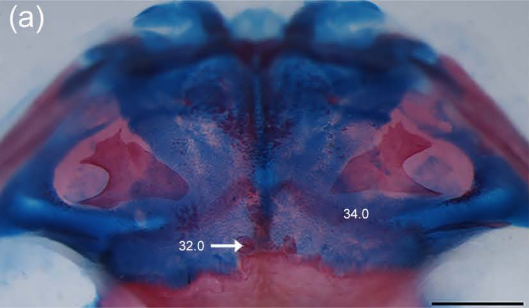




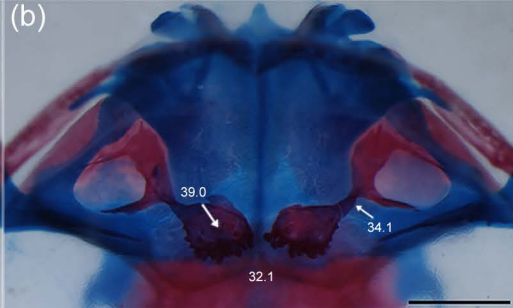
**Fig. S6.** Ventral view of pterygoid showing states of characters 29 and 30 related to the medial and posterior rami of this bone (character number is followed by the state number). (a) *Sphaenorhynchus palustris* (MNRJ 42656), (b) *S. prasinus* (MZUESC 6861), (c) *S. dorisae* (ZUEC1 1096), (d) *S. pauloalvini* (MNRJ 4323), and (e) *Scarthyla goinorum* (MCP 12962). Scale bars = 1 mm.



(a)



(b)



(c)

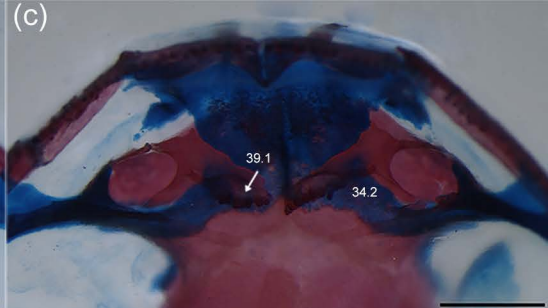


**Fig. S7.** Ventral view of vomers showing states of characters 32, 34, and 39 related to this bone (character number is followed by the state number). (a) *Sphaenorhynchus dorisae* (ZUEC 11096), (b) *S. prasinus* (EI 59), and (c) *S. pauloalvini* (MNRJ 4323). Scale bars = 1 mm.

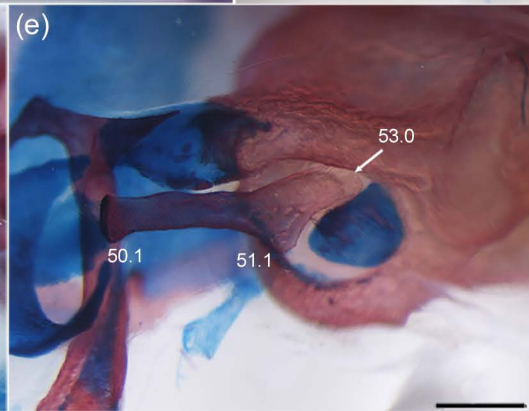
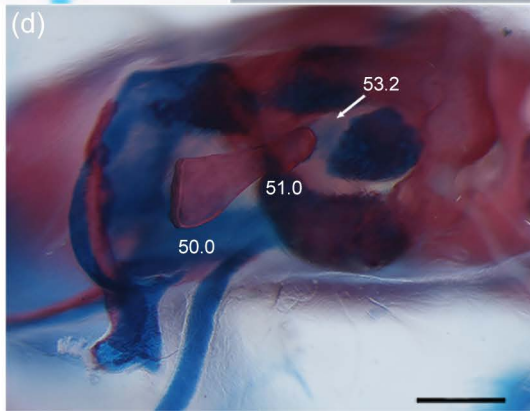
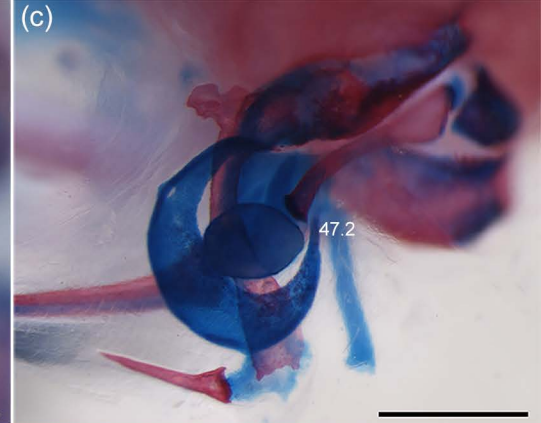
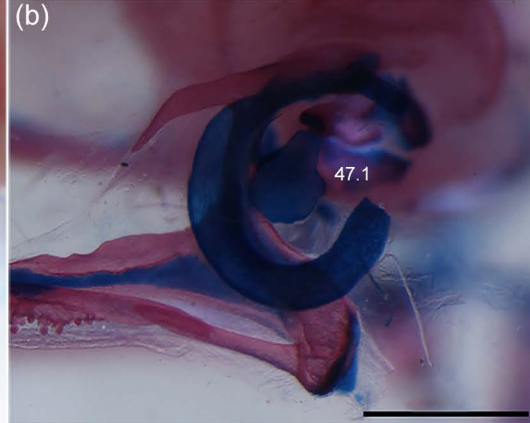
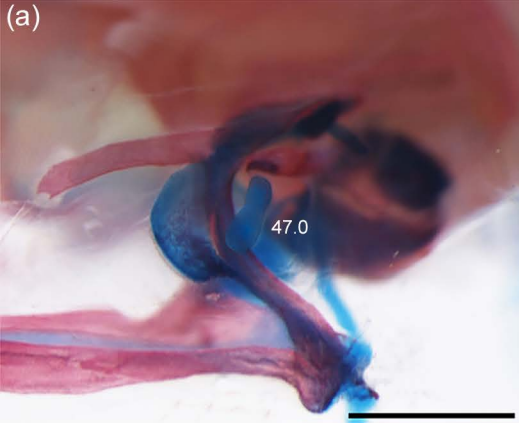
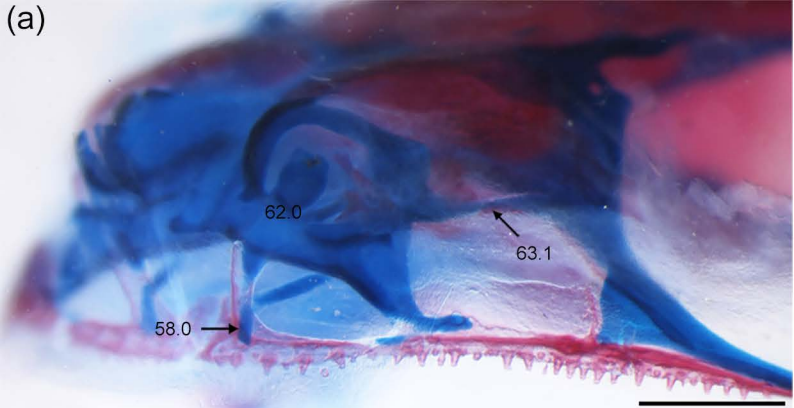


**Fig. S8.** Plectral apparatus of (a) *Scinax alter* (MCP 1670), (b) *Scarthyla goinorum* (MCP 12962), (c) *Sphaenorhynchus caramaschii* (CFBH 6937), (d) *S. carneus* (ZUEC 5555), and (e) *S. pauloalvini* (MNRJ 4323). Character number is followed by the state number. Scale bars = 1 mm (upper) and 0.5 mm (lower).

(a)



(b)

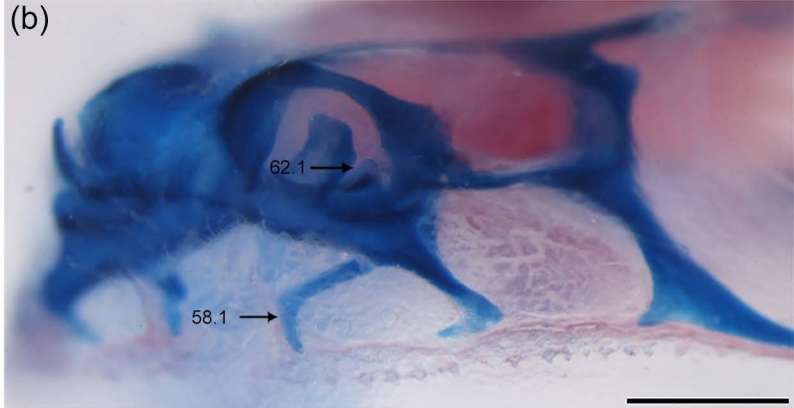


**Fig. S9.** Nasal cartilages of (a) *Sphaenorhynchus prasinus* (MZUESC 6861), (b) *S. surdus* (MCP 8324). Character number is followed by the state number. Scale bars = 1 mm.

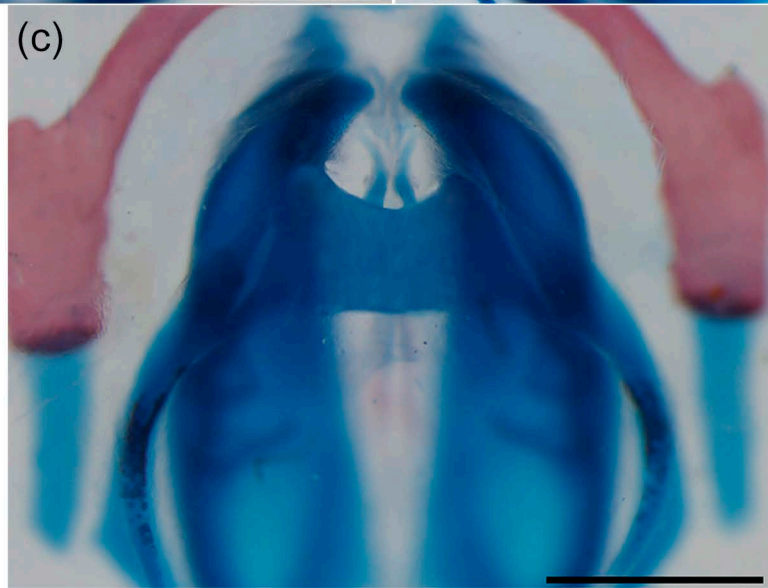
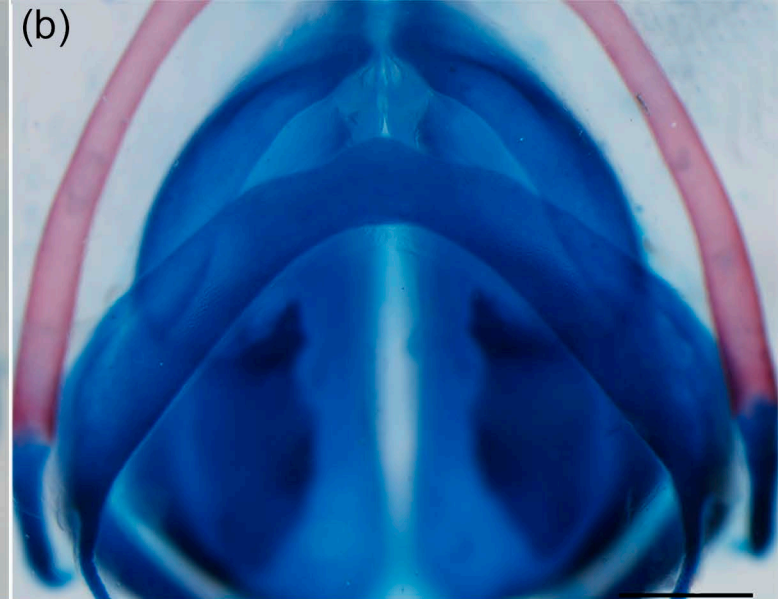


**Fig. S10.** Ventral views of the anterior part of the larynx showing some states of character 74. (a) *Sphaenorhynchus prasinus* (EI 59: Ch. 74.1), (b) *S. lacteus* (MCP 12961: Ch. 74.1), and (d) *Scinax alter* (MCP 1670: Ch. 74.4). Scale bars = 1 mm.



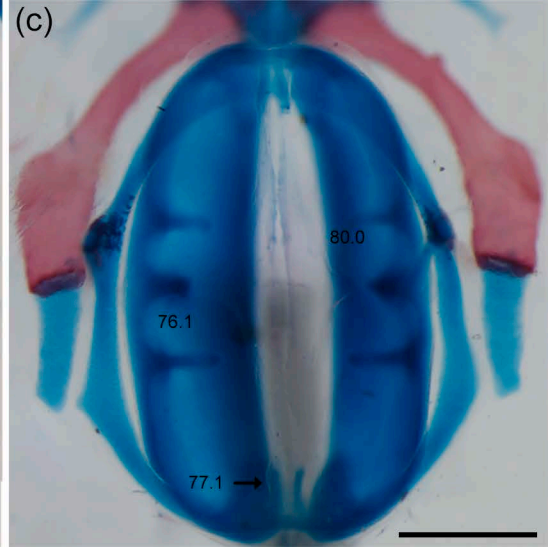
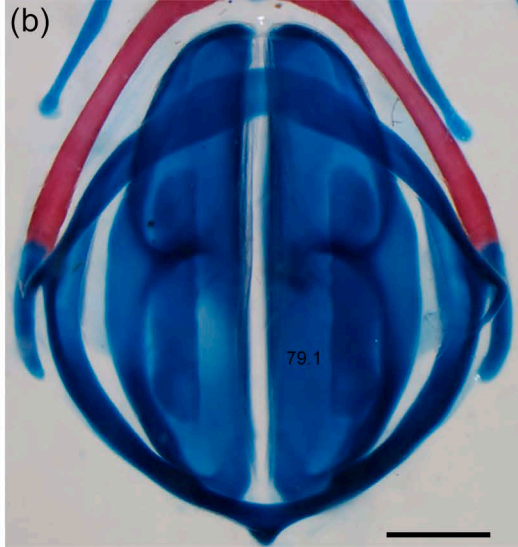
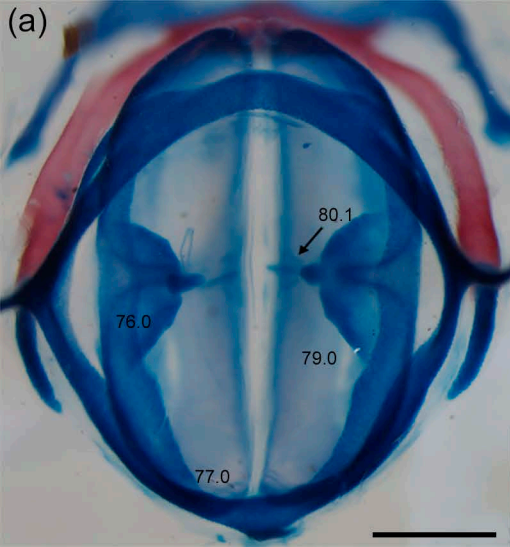


**Fig. S11.** Ventral views of the larynx (character number is followed by the state number).  
(a) *Sphaenorhynchus planicola* (MNRJ 54808); (b) *S. prasinus* (EI 59), and (c) *Scinax alter*  
(MCP 1670). Scale bars = 1 mm.

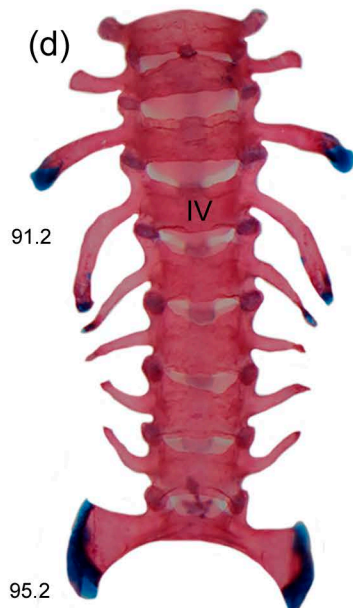
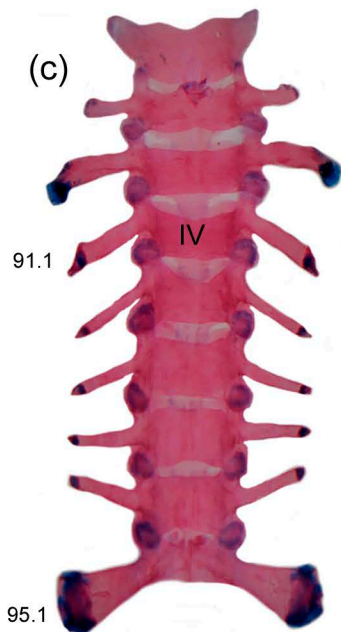
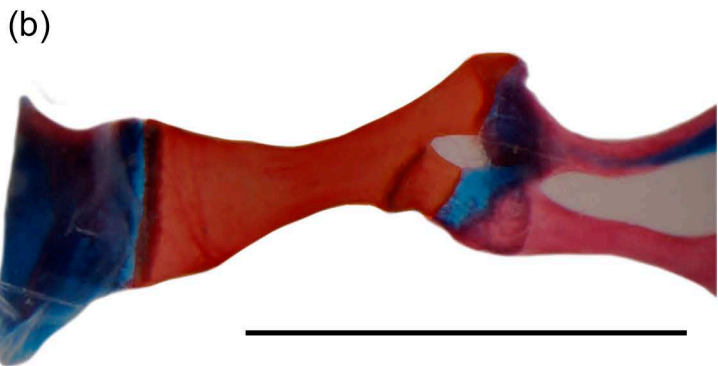
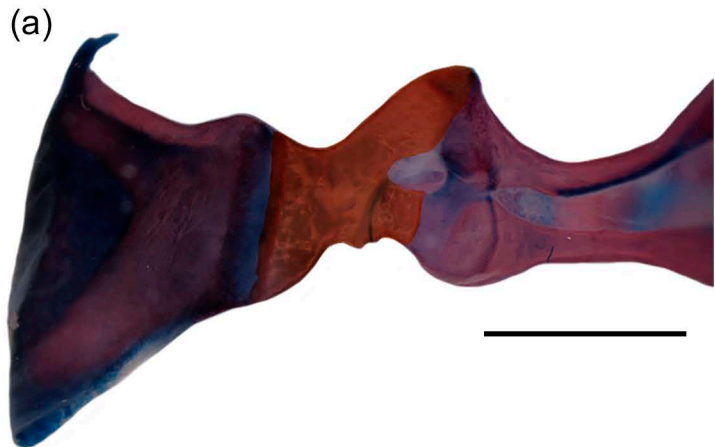


**Fig. S12.** Lateral view of scapulae (left), and dorsal view of presacral and sacral diapophyses (right; character number is followed by the state number). (a) *Sphaenorhynchus lacteus* (MCP 12961: Ch.83.0), (b) *S. carneus* (ZUEC 5555: Ch. 83.1), (c) *Scarthyla goinorum* (MCP 12962), and (d) *S. carneus* (ZUEC 5555). Scale bars = 2 mm.

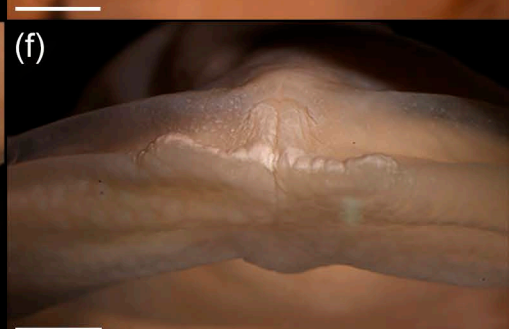


**Fig. S13.** Subcloacal ornamentations. (a) Dorsal, (b) ventral, and (c) posterior views of *Sphaenorhynchus bromelicola* (MZUSP 101515: Ch. 117.4). (d) Dorsal, (e) ventral, and (f) posterior views of *S. lacteus* (ZUEC 5570: Ch. 117.5). (g) Dorsal, (h) ventral, and (i) posterior views of *S. dorisae* (ZUEC 8426: Ch. 117.6). Scale bars = 2 mm..

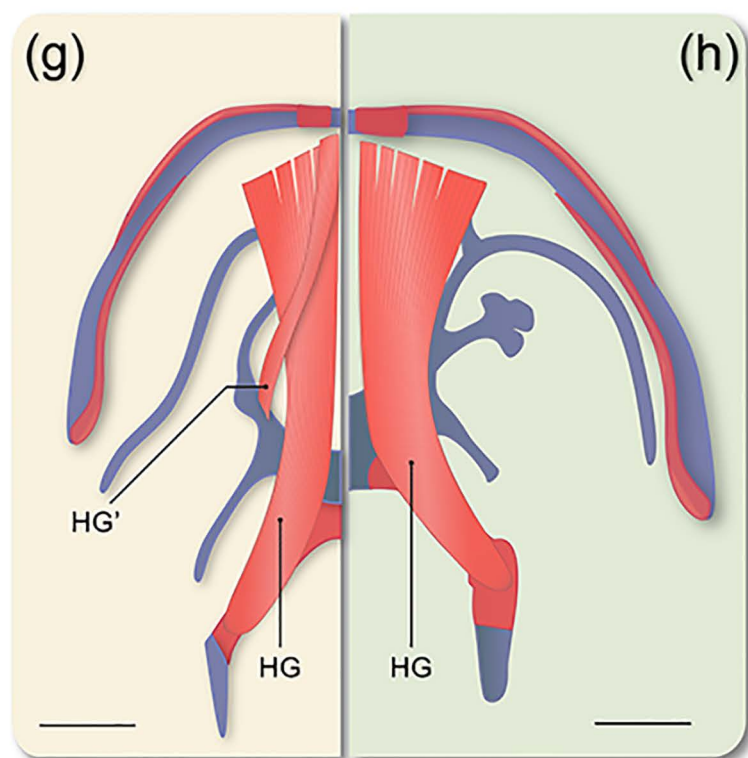
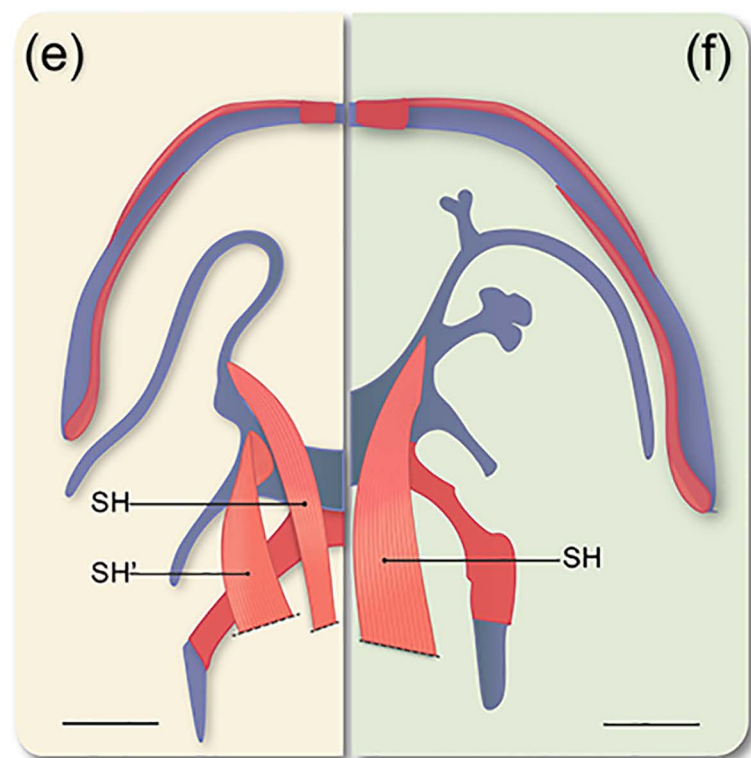
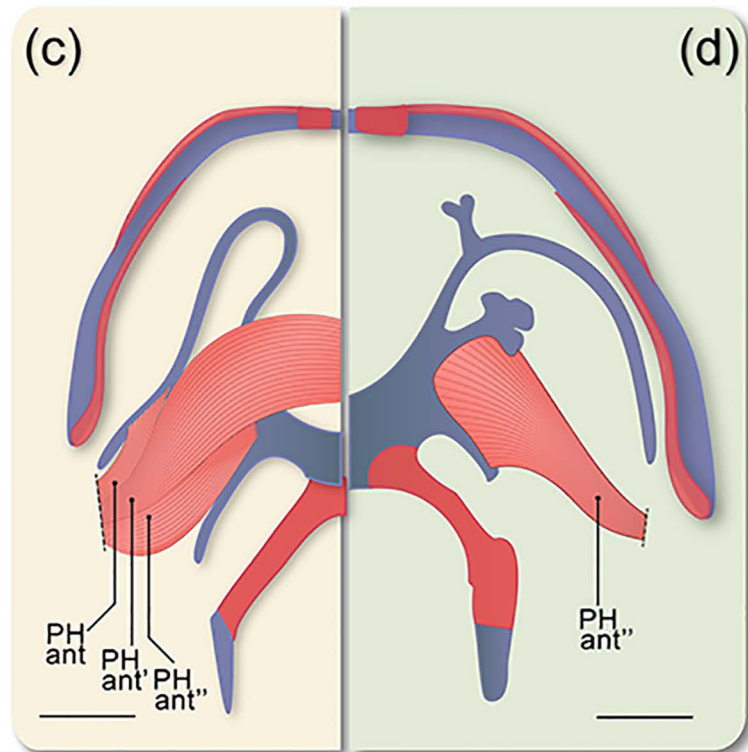
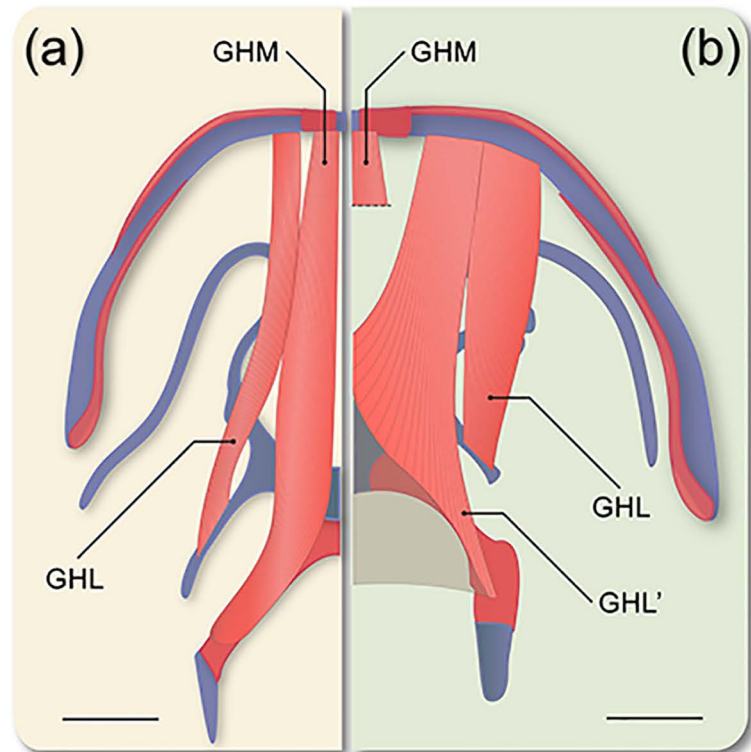




**Fig. S14.** Submandibular musculature of hyoid. (a) *Sphaenorhynchus lacteus* (TG 2545: Ch. 15.0), (b) *Scinax alter* (MCP 6349: Ch. 154.1); GHL: m. *geniohyoideus lateralis*, external slip; GHL': m. *geniohyoideus lateralis*, internal slip; GHM: m. *geniohyoideus medialis*. (c) *S. lacteus* (TG 2545: Ch. 156.1), (d) *Sci. alter* (MCP 6349: Ch. 156.0); PH ant: m. *petrohyoideus anterior*, fibers inserted on the hyale; PH ant': m. *petrohyoideus anterior*, additional layer of fibers over the plate hyoid; PH ant'': m. *petrohyoideus anterior*, fibers inserted on the lateral margin of the plate hyoid. (e) *S. lacteus* (TG 2545: Ch. 160.1), (f) *Sci. alter* (MCP 6349: Ch. 160.0); SH: m. *sternohyoideus*, ventral strip; SH: m. *sternohyoideus*, dorsal strip; in (f) the ventral slip overlaps the dorsal strip. (g) *S. lacteus* (TG 2545: Ch. 164.1), (h) *Sci. alter* (MCP 6349: Ch. 164.0); HG: m. *hyoglossus*; HG': medial segment of m. *hyoglossus* inserted on the hyale. Scale bars = 1 mm.



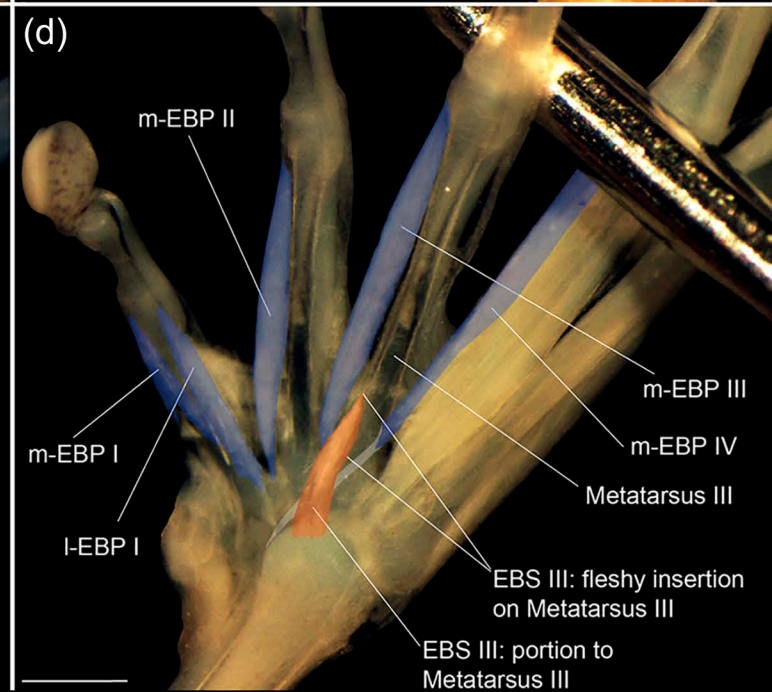
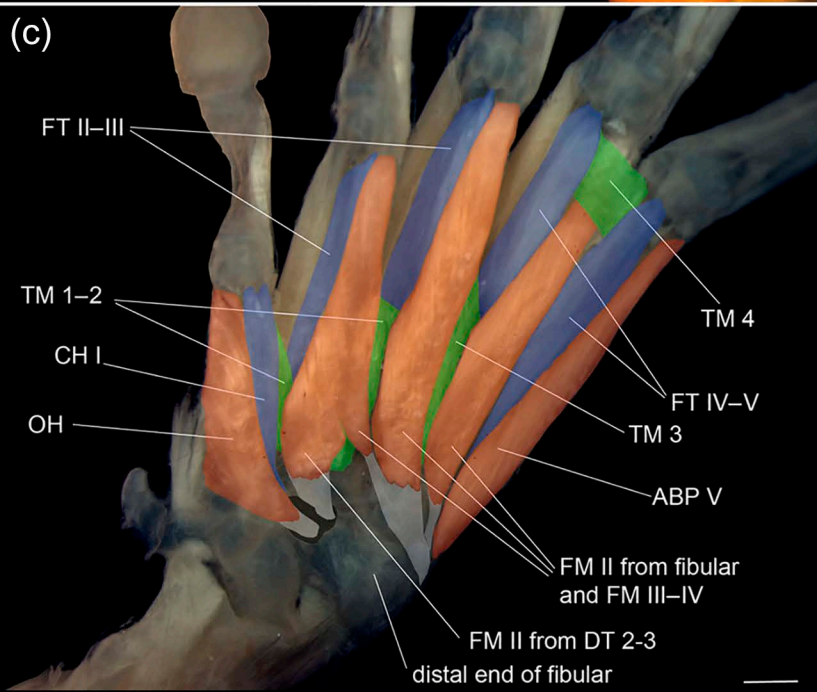
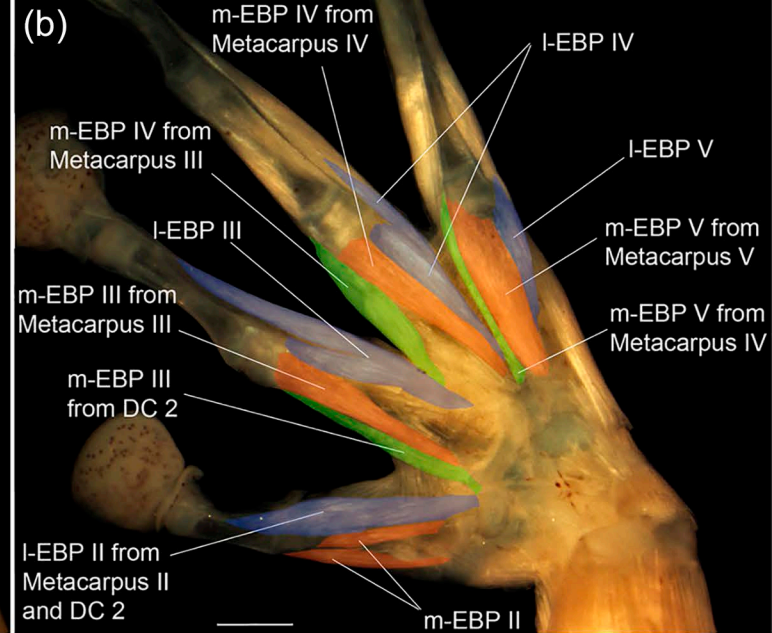
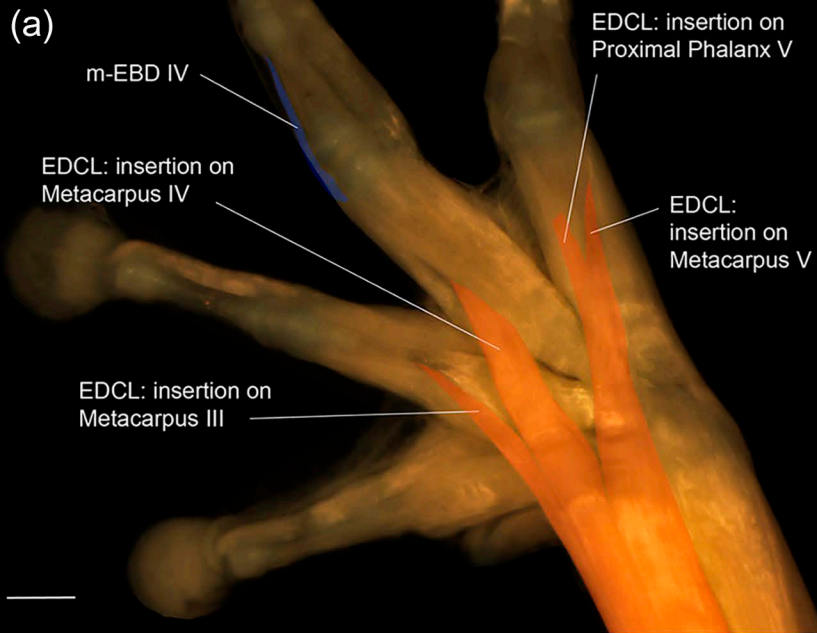


**Fig. S15.** (a) Dorsal view of the right hand of *Sphaenorhynchus planicola* (MNRJ 54355); note two insertions of the EDCL on digiti V, one on the Metacarpal V (present in all taxa), and an additional one on the fascia of the medial slip of the EBP V, reaching proximally the Proximal Phalanx V (Ch. 171.1); also note the presence of the m-EBD IV (Ch. 174.1). (b) Dorsal view of the left hand (reflected for purpose of comparison with the other figures) of *Scinax alter* (MCP 6349); note the presence of the m-EBP V with origin from the proximal end of the Metacarpal IV (Ch. 175.1). (c) Plantar view of the left foot of *Sphaenorhynchus platycephalus* (MNRJ 31735). Note the additional origin of the FM II from the DT 2–3 (Ch. 177.1); the DT 2–3 is gray shaded. (d) Dorsal view of the right foot of *S. mirim* (MACN-He 46461); note the portion of the EBS III inserting on the Metatarsus III (Ch. 185.1). Removed elements: in (a): no removals. (b): ECU, EDCL, EBS II–V, ABD II, EBM II–IV, l-EBP IV from Metacarpal V. (c): TS I–V, ABH, LBL III–V, LLG IV, LBB I–V, PC, and distal ends of FDB, PP and TVP. (d): ABD V, EDCL, EBS I–II, portion of EBS III inserting on Proximal Phalanx III. The following elements were not shaded/edited in the figures, although they are present: in (a): tendon of insertion of the EDCL proximally on Proximal Phalanx V; this is a thin, flat tendon, almost translucent. (b): tendons of insertion of EBP II–V. (d): EBS IV; EBP V; tendon of origin from the fibular of the portion of the EBS III inserting on Metatarsus III; tendons of insertion of the EBP I–IV. See Appendix S6 for abbreviations. Scale bars = 0.5 mm.